3GPP TR 37.840 V2.0.0 (2013-02)

Technical Report

3rd Generation Partnership Project; Technical Specification Group Radio Access Network; Study of AAS Base Station; (Release 12)





Keywords

LTE, UMTS, Base Station, Radio

3GPP

Postal address

3GPP support office address
650 Route des Lucioles - Sophia Antipolis
Valbonne - FRANCE

Tel.: +33 4 92 94 42 00 Fax: +33 4 93 65 47 16

Internet

http://www.3gpp.org

Copyright Notification

No part may be reproduced except as authorized by written permission. The copyright and the foregoing restriction extend to reproduction in all media.

© 2011, 3GPP Organizational Partners (ARIB, ATIS, CCSA, ETSI, TTA, TTC). All rights reserved.

UMTSTM is a Trade Mark of ETSI registered for the benefit of its members $3GPP^{TM}$ is a Trade Mark of ETSI registered for the benefit of its Members and of the 3GPP Organizational Partners LTETM is a Trade Mark of ETSI registered for the benefit of its Members and of the 3GPP Organizational Partners GSM® and the GSM logo are registered and owned by the GSM Association

Contents

Forew	vord	6
1	Scope	7
2	References	7
3	Definitions, symbols and abbreviations	۶
3.1	Definitions	
3.2	Symbols	
3.3	Abbreviations	
	General	
4.1	SI objectives	
4.1.1	The objectives	
4.1.2	Methodologies	
4.1.2.1	= · · · · · · · · · · · · · · · · · · ·	
4.2 4.3	Structure of AAS BSRegulation review	
4.3.1	ITU Radio Regulations	
4.3.2	ITU-R Recommendations	
4.3.3	ECC regulation in Europe	
4.3.4	FCC regulation in the U.S.	
4.3.5	MIC regulation in Japan	
5	Study of AAS deployment scenarios	
5.1	AAS applications	
5.1.1	Tilt and radiation pattern control	
5.1.1.1		
5.1.2	Multiple input multiple output (MIMO)	
5.1.3 5.1.4	Differentiated antenna behaviours at different carrier frequencies	
5.1.4 5.2	Deployment and coexistence scenarios	
5.2.1	Deployment and coexistence scenarios Deployment scenarios	
5.2.1	Coexistence scenarios.	
5.2.2	Classifications of AAS BS	
5.4	Simulation study	
5.4.1	Objectives	
5.4.2	Simulation scenarios	
5.4.2.1		
5.4.2.2		
5.4.3	Simulation assumptions	
5.4.3.1		
5.4.3.1	1	
5.4.3.1	1.2 Propagation model	18
5.4.3.1	Down-tilt angle setting	18
5.4.3.1	.4 General simulation parameters for the initial simulation cases	20
5.4.3.2	2 Assumptions for the other applications	21
5.4.4	Array antenna model	21
5.4.4.1	C.7	
5.4.4.1		
5.4.4.1	•	
5.4.4.1	¥ 1	
5.4.4.1	e e	
5.4.4.1		
5.4.4.2	ı	
5.4.4.2	2.1 Typical array antenna parameters	27
	Study of AAS transmitter characteristics.	
6.1	General review of transmitter characteristics	
6.2	Transmitter spatial characteristics	
6.3	Simulation results	29

6.3.1	ACLR	29
6.4	Requirements for AAS transmitters	
	Output power	
	Approach 1	
	Approach 2	
	Study Item conclusions on output power	
6.4.2 A	A CLR requirements	30
7	Study of AAS receiver characteristics	31
7.1	General review of receiver characteristics	31
7.2	Receiver spatial characteristics	31
7.2.1	Element or Sub array characteristics	31
7.2.2	AAS system characteristics	
7.3	Simulation results	
7.3.1	In-band blocking	
7.3.1.1		
7.3.1.2 7.3.1.3		
7.3.1.3		
7.3.1.4 7.4	Requirements for AAS receivers	
7.4.1	Requirement Reference Point	
7.4.2	Reference sensitivity	
	Approach 1	
	Approach 2	
	Study Item conclusions on reference sensitivity	
	·	
8	AAS test aspects	
8.1 8.2	Comparison of different test methods	
8.2.1	Conducted Test	
8.2.1.1		
8.2.2	Far Field Over-the-Air Test	
8.2.3	Coupling Test	
8.2.4	Combined Test	
8.2.4.1		
8.2.4.2	Combined Close Field Coupling and Over-the-Air Test	39
8.2.5	Rayleigh Faded Multi-path Over-the-Air test	
8.2.6	Near-Field Probe Scanner Test	39
9	Conclusions	40
Δnnes	x A: (Informative) Study Item plan and progress	42
A.1	The Study Item plan	
A.2	The Study Item progress	
A.3	The list of contributions	
Annex		
B.1	Case 1a: Downlink E-UTRA AAS interferer- legacy system victim	
B.2	Case 1b: Downlink E-UTRA AAS interferer- AAS victim with equal down-tilt angles	
B.3	Case 1b: Downlink E-UTRA AAS interferer- AAS victim with non-optimal down-tilt angles	
B.4	Case 1c: Downlink E-UTRA legacy system interferer- legacy system victim	
Annex	x C: (Informative)AAS spatial domain aspects	
C.1	Transmitter spatial characteristics	
C.1.2	Simulation assumptions	
C.1.3	Simulation results	
C.2	Receiver spatial characteristics	
C.2.1	Simulation results	
C.2.1.1 C.2.1.2	1	
C.2.1.2	2 Coupling loss	
C.3.1	Simulation results	
C.3.1	Spatial EVM characteristics	
C.5	Directivity characteristics	

C.5.1	Array Element	71
C.5.2	Scan Loss	
C.5.3	Array Gain	74
C.5.4	Relation between transceiver boundary and far-field	74
C.6	Non core requirement	
Annex 1	D: (Informative) Change history	76

Foreword

This Technical Report has been produced by the 3rd Generation Partnership Project (3GPP).

The contents of the present document are subject to continuing work within the TSG and may change following formal TSG approval. Should the TSG modify the contents of the present document, it will be re-released by the TSG with an identifying change of release date and an increase in version number as follows:

Version x.y.z

where:

- x the first digit:
 - 1 presented to TSG for information;
 - 2 presented to TSG for approval;
 - 3 or greater indicates TSG approved document under change control.
- y the second digit is incremented for all changes of substance, i.e. technical enhancements, corrections, updates, etc.
- z the third digit is incremented when editorial only changes have been incorporated in the document.

[16]

1 Scope

The present document is a Technical Report of the Study Item for RF and EMC requirements for AAS, which was approved at TSG RAN#53 [2]. The report provides definition of AAS BS, the analysis of RF and EMC requirements for the corresponding deployment scenarios, as well as the test aspects of AAS BS. The possible impacts on the BS specifications are also included.

2 References

The following documents contain provisions which, through reference in this text, constitute provisions of the present document.

- References are either specific (identified by date of publication, edition number, version number, etc.) or non-specific.
- For a specific reference, subsequent revisions do not apply.
- For a non-specific reference, the latest version applies. In the case of a reference to a 3GPP document (including a GSM document), a non-specific reference implicitly refers to the latest version of that document in the same Release as the present document.

[1]	3GPP TR 21.905: "Vocabulary for 3GPP Specifications".
[2]	RP-111349, "Study of RF and EMC Requirements for Active Antenna Array System (AAS) Base Station".
[3]	Recommendation ITU-R SM.1541, "Unwanted emissions in the out-of-band domain" (2001).
[4]	Recommendation ITU-R M.1580-1, "Generic unwanted emission characteristics of base stations using the terrestrial radio interfaces of IMT-2000" (2002-2005).
[5]	Recommendation ITU-R M.1678, "Adaptive antennas for mobile systems" (05/2004).
[6]	CEPT/ERC/Recommendation 74-01, "Unwanted Emissions in the Spurious Domain" (Cardiff 2011).
[7]	ECC Recommendation 11(06), "Block Edge Mask Compliance Measurements for Base Stations" (October 2011).
[8]	Decision 2008/477/EC, "COMMISSION DECISION of 13 June 2008 on the harmonisation of the 2 500-2 690 MHz frequency band for terrestrial systems capable of providing electronic communications services in the Community"
[9]	Decision 2010/267/EU, "COMMISSION DECISION of 6 May 2010 on harmonised technical conditions of use in the 790-862 MHz frequency band for terrestrial systems capable of providing electronic communications services in the European Union".
[10]	ECC Recommendation (02)05, "Unwanted Emissions".
[11]	"Emissions Testing of Transmitters with Multiple Outputs in the Same Band (e.g., MIMO, Smart Antenna, etc)", KDB publication no 662911 D01, FCC Office of Engineering and Technology Laboratory Division, 10/25/2011.
[12]	"MIMO with Cross-Polarized Antenna", KDB publication no 662911 D02, FCC Office of Engineering and Technology Laboratory Division, 10/25/2011.
[13]	International Telecommunications Union Radio Regulations, Edition of 2008.
[14]	Recommendation ITU-R SM.329-11, "Unwanted emissions in the spurious domain" (01/2011).
[15]	Report ITU-R M.2040, "Adaptive antennas concepts and key technical aspects" (2004).

18, 1950, "Ordinance Regulating Radio Equipment"

Ministry of Internal Affairs and Communications, Radio Regulatory Commission Regulation No.

[17]	Information and Communications Technology Subcommittee Committee for Faster Mobile Phones, "Draft Report from Committee for Faster Mobile Phones; Concerning technical requirements for mobile communications systems using 700MHz bands" (http://www.soumu.go.jp/main_content/000140943.pdf (in Japanese)).
[18]	3GPP TR 25.942, "UTRA Radio Frequency (RF) system scenarios".
[19]	3GPP TR 36.942, "E-UTRA Radio Frequency (RF) system scenarios".
[20]	3GPP TR 25.816, "UMTS 900 MHz Work Item Technical Report".

3 Definitions, symbols and abbreviations

3.1 Definitions

For the purposes of the present document, the terms and definitions given in TR 21.905 [1] and the following apply. A term defined in the present document takes precedence over the definition of the same term, if any, in TR 21.905 [1].

Active Antenna System: a BS system which combines an Antenna Array with an Active Transceiver Unit Array. An AAS may include a Radio Distribution Network.

Array Element: a subdivision of a passive antenna array, consisting of a single radiating element or a group of radiating elements, with a fixed radiation pattern.

Array Factor: the radiation pattern of an array antenna when each array element is considered to radiate isotropically.

NOTE: When the radiation pattern of individual array elements are identical, and the array elements are congruent under translation, then the product of the array factor and the element radiation pattern gives the radiation pattern of the entire array.

AAS Transceiver Unit Array: an array of transceiver units which generate radio signals in the transmit direction and accept radio signals in the receive direction.

Antenna Array: a group of antenna elements characterized by the geometry and the properties of the array elements. The geometry of the array elements can be either linear or non-linear to meet the system requirements.

Cell Partitioning: the division of coverage in a sector into multiple subsectors. The subsectors may be divided in the vertical and/or horizontal planes.

Directivity (in a given direction): the ratio of the radiation intensity in a given direction from the antenna to the radiation intensity averaged over all directions.

Down-tilt Angle: the angle between the direction of the maximum antenna gain and the horizontal plane.

Equivalent Isotropic Radiated Power: in a given direction, the gain of a transmitting antenna multiplied by the net power accepted by the antenna from the connected transmitter.

Equivalent Isotropic Received Sensitivity: in a given direction, the total power received by a receiving antenna divided by the gain of the antenna.

Far-Field Region: that region of the field of an antenna where the angular field distribution is essentially independent of the distance from a specified point in the antenna region.

Front-to-Back Ratio: the ratio of maximum directivity of an antenna to its directivity in a specified rearward direction.

Gain (in a given direction): the ratio of the radiation intensity, in a given direction, to the radiation intensity that would be obtained if the power accepted by the antenna were radiated isotropically.

NOTES: If the direction is not specified, the direction of maximum radiation intensity is implied.

Half Power Beam-width: in a radiation pattern cut containing the direction of the maximum of a lobe, the angle between two directions in which the radiation intensity is one-half the maximum value.

Near-Field Region: That part of space between the antenna and far-field region.

Radio Distribution Network: a passive network which distributes radio signals generated by the active transceiver unit array to the antenna array, and/or distributes the radio signals collected by the antenna array to the active transceiver unit array.

NOTE: In the case when the active transceiver units are physically integrated with the array elements of the antenna array, the radio distribution network is a one-to-one mapping.

Radiating Element: the basic building block of an array element characterized by its radiation properties.

Radiation Pattern: the angular distribution of the radiated electromagnetic field or power level in the far field region.

Transceiver Unit: the active unit consisting of transmitter and/or receiver which transmits and/or receives radio signals.

3.2 Symbols

For the purposes of the present document, the following symbols apply:

 A_A The array antenna pattern in dB.

 $A_{\rm F}$ The composite array element pattern in dB.

P The electric far-field pattern.

 \widetilde{W} The array factor.

 φ The azimuth angle (defined between -180° and 180°).

 θ Elevation angle of the signal direction (defined between 0° and 180° , 90° represents perpendicular

to array).

 ρ The signal correlation coefficient.

3.3 Abbreviations

For the purposes of the present document, the abbreviations given in TR 21.905 [1] and the following apply. An abbreviation defined in the present document takes precedence over the definition of the same abbre viation, if any, in TR 21.905 [1].

AA Antenna Array

AAS Active Antenna System

AE Array Element AUT Antenna Under Test

ECC Electronics Communications Committee
EIRP Equivalent Isotropical Radiated Power
EIRS Equivalent Isotropical Received Sensitivity

EMC Electro magnetic compatibility

FCC Federal Communications Commission

ISD Inter-Site Distance

ITU International Telecommunications Union

MCL Minimum Coupling Loss

MIC Ministry of Internal Affairs and Communications

OTA Over-the-Air

RDN Radio Distribution Network

RR Radio Regulations
RXU Receiver Unit
TXRU Transceiver Unit
TXRUA Transceiver Unit Array
TXU Transmitter Unit
ULA Uniform Linear Array
URA Uniform Rectangular Array

WRC

World Radio Communication Conference

4 General

The Active Antenna System (AAS) within this document refers to a Base Station equipped with an antenna array system, the radiation pattern of which may be dynamically adjustable. The main purpose of this document is to study the characteristics and minimum requirements of the AAS transmitter and receiver system considering the impacts from antenna array.

This sub-clause captures the SI objectives and establishes the reference structure as well as the methodologies to achieve the SI objectives.

4.1 SI objectives

4.1.1 The objectives

The AAS introduces an alternative antenna system from the one installed in the conventional Base Station. The interactions between the antenna array system and the transmitters and receivers within the AAS might be different from the conventional BS and the conventional antenna system. The impacts of the transmitted or received radio signals on the transmitter and receivers shall be studied.

To investigate the AAS BS, a Study Item [2] was approved in RAN plenary #53. The objectives proposed in the SID are quoted below:

This is the study item to investigate the RF and EMC requirements for an AAS BS based on macro-cell deployment scenarios for both TDD and FDD. The study will cover single-RAT UTRA and E-UTRA, as well as multi-RAT base stations. The study item particularly covers the following two main aspects:

- Feasibility of defining AAS BS requirements based on the commonality of different architecture and implementations:
 - Develop/define relevant terminology associated with AAS BS to ensure common understanding.
 - Determine the appropriate approaches for standardization, specification implementation and test methodologies
- Study the following aspects
 - Transmitter and receiver characteristics and their impact on system performance and co-existence.
 - The core RF and/or EMC requirements for the transmitter and receiver.
 - Regulatory aspects related to multiple antenna transmission and the impact on AAS BS.
 - Feasibility of OTA tests.

Based on the outcome of the above studies, the following specification-related work will be identified pending approval of the related Work Item:

- 1. The RF and/or EMC requirements for AAS BS transmitters and receivers.
- 2. The methodologies for specification implementation of all the necessary changes.

In summary, the objectives of this Study Item are to study the characteristics of the AAS transmitters and receivers, and investigate the impacts on the coexistence performance with other systems based on un-coordinated deployment scenarios.

4.1.2 Methodologies

The methodologies employed to determine the minimum requirements for AAS are similar to the methodologies used for determining those requirements for previously considered systems. These methodologies as documented in TR25.942 [18] and TR 36.942 [19] which provides assumptions for typical deployment conditions can be used as baseline.

4.1.2.1 Detailed methodologies

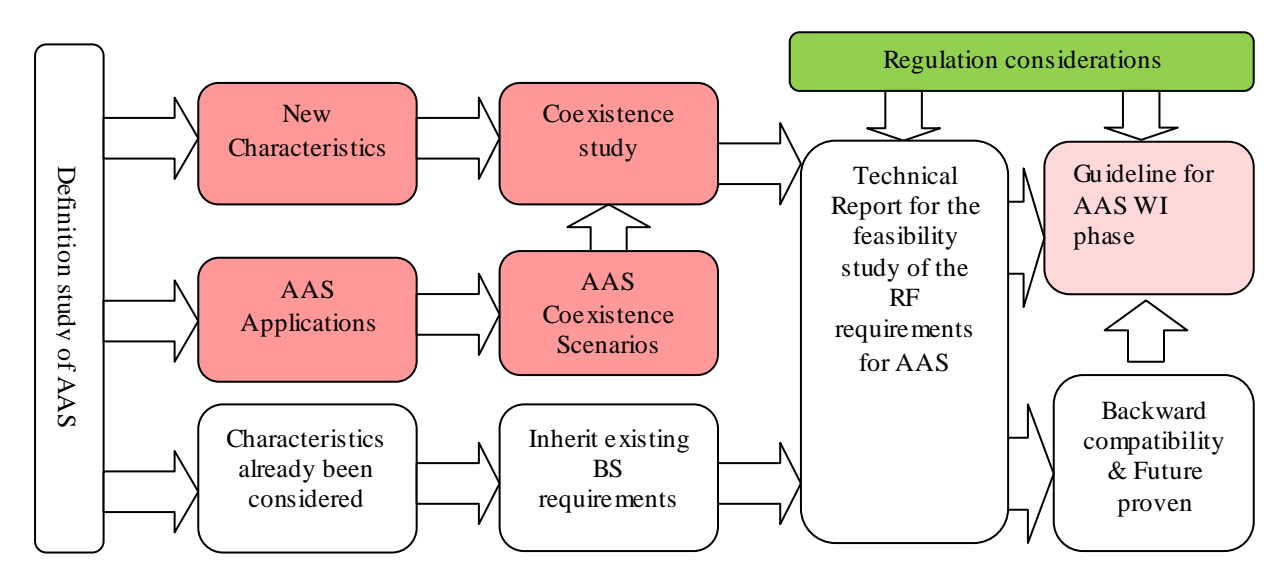


Figure 4.1.2.1-1: Procedures for AAS study

The detailed procedures for AAS study are illustrated in Figure 4.1.2.1-1. The essential part of this study is to study the new characteristics and evaluate the impacts on system coexistence and performance. The evaluation results are used to determine whether to modify existing requirements or define new requirements. The 3D coexistence simulation study requires the modelling of antenna characteristics in both horizontal and vertical domain.

4.2 Structure of AAS BS

An abstract logical representation of the AAS radio architecture is described in this section. The radio architecture is represented by three main functional blocks, the Transceiver Unit Array (TXRUA), the Radio Distribution Network, (RDN), and the Antenna Array (AA). The Transceiver Units (TXRU) interface with the base band processing within the eNodeB.

The Transceiver Unit Array consists of multiple Transmitter Units (TXU) and Receiver Units (RXU). The Transmitter Unit takes the baseband input from the AAS Base Station and provides the RFTX outputs. The RFTX outputs may be distributed to the Antenna Array via a Radio Distribution Network. The Receiver Unit performs the reverse of the Transmitter Unit operations. The Radio Distribution Network, if present, performs the distribution of the TX outputs into the corresponding antenna paths and antenna elements, and a distribution of RX inputs from antenna paths in the reverse direction. The transmitter and receiver unit can be separated and can have difference mapping towards radiating elements.

The transceiver array boundary is the point or points at which the transceiver array is connected to the RDN in figure 4.2-1. "Transceiver array boundary" may refer to the combination of all of the transceivers or may refer to an individual transceiver.

- NOTE 1: The RDN may consist of a simple one to one mapping between the TXU(s)/RXU(s) and the passive Antenna Array. In this case, the RDN would be a logical entity but not necessarily a physical entity.
- NOTE 2: The Antenna Array includes various implementations and configurations e.g. polarization, spatial separations etc.
- NOTE 3: The physical location of the Transceiver Unit Array, the Radio Distribution Network, and the Antenna Array may differ from this logical representation and is implementation dependent.
- NOTE 4: No specific mapping between TXU/RXU and antenna elements is assumed. Further the number of separate receiver and transmitter units as well as the mapping in the RDN between transceivers and radiating elements can differ between the transmit and receive directions. The AAS reference architecture allows for full asymmetry between receiver path and transmit path.

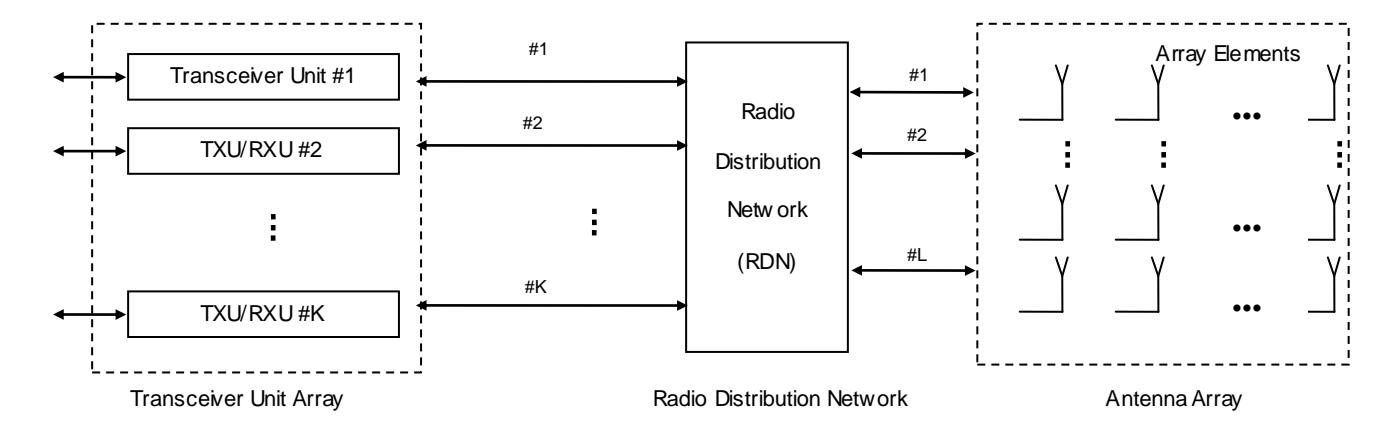


Figure 4.2-1: General AAS Radio Architecture

A BS with AAS, with general radio architecture as shown in Figure 4.2-1, is generic to all types of AAS structures including diversity, beamforming, spatial multiple xing, or any combination of the three.

4.3 Regulation review

In the work on AAS, several new concepts may be considered in terms of how to define and measure emission limits. Many limits are defined in regulation and there are also recommendations for measurements. This clause gives a brief overview of some international regulation for AAS and systems with multiple antennas.

4.3.1 ITU Radio Regulations

The Radio Regulations (RR) is the fundamental international regulatory text, containing all decisions adopted by the World Radio Congress. The most recent version is the output of WRC-07 [13]. The following passages may have some relevance for the work on AAS:

- The terms "antenna port" and "antenna transmission line" are used throughout the RR, but no explicit definition is given. RR Volume 1, chapter I sets Terminology and technical characteristics, but "antenna port" and "antenna transmission line" are not mentioned there. The terms are however always used in singular.
- RR Vol II, Appendix 3 sets limits to spurious emissions for the "antenna transmission line", which can also be found in the relevant ITU-R Recommendation SM.329 [14].
- RR Vol II, Appendix 3, Article 10bis points out that "Guidance regarding the methods of measuring spurious domain emissions is given in the most recent version of Recommendation ITU-R SM.329." and further states that "The EIRP method specified in this Recommendation should be used when it is not possible to accurately measure the power supplied to the antenna transmission line, or for specific applications where the antenna is designed to provide significant attenuation in the spurious domain. Additionally, the EIRP method may need some modification for special cases."
- RR mentions "active antennas" only in connection with unwanted emissions from satellite systems (non-GSO RNSS or MSS systems, in Annex 1 to Rec. ITU-R M.1583, which is incorporated by reference to the RR). For these cases, it is stated that in the case of an active antenna, the RF radiated power should be used instead of the unwanted emission at the input of the antenna.

4.3.2 ITU-R Recommendations

Rec. SM.329 Unwanted emissions in the spurious domain [14]

The definitions and terminology used in SM.329 [14] are very similar to the ones used in the RR. The general emission limits (category A) in SM.329 are also from the RR.

The following is noted for Space Stations in considering n):

"n) that some space stations have active antennas and the measurement of power as supplied to the antenna transmission line cannot cover emissions created within the antenna. For such space stations, the determination of field strength or pfd at a distance should be established by administrations to aid in determining when an emission is likely to cause interference to other authorized services;"

The spurious emission limits in SM.329 are qualified in the following way:

"Table 2 indicates the maximum permitted levels of spurious domain emissions, appearing in RR Appendix 3, in terms of power of any unwanted component supplied by a transmitter to the antenna transmission line..."

A general note states that "Use the EIRP method shown in Annex 2, § 3.3, when it is not practical to access the transition between the transmitter and the antenna transmission line." This note exists only for Category A limits.

Annex 2, § 3.3 of SM.329 describes an EIRP measurement method called "Method 2 – Measurement of the spurious domain emission EIRP" on a total of two pages.

Rec. SM1541 Unwanted emissions in the out-of-band domain [3]

The definitions and terminology used in SM.1541 are also very similar to the one used in the RR.

There is an Annex 12 for Fixed Services that contain a chapter on Methods of measurement. Two fundamental methods are described:

- Method 1 is the measurement of emission power supplied to the antenna port of the equipment under test (EUT). This method should be used whenever it is practical and appropriate.
- Method 2 is the measurement of the equivalent isotropic radiated power (EIRP), using a suitable test site.

The text describing Method 2 is similar to the one in SM.329 [14].

Rec. M.1580 Generic unwanted emission characteristics of base stations using the terrestrial radio interfaces of IMT-2000 [4]

This recommendation contains unwanted emission requirements for the different IMT technologies. The requirements are aligned with what is specified in 3GPP.

Rec. M.1678 Adaptive antennas for mobile systems [5]

The recommendation gives a recommendation that adaptive antenna technology should be considered in the development of new technology and used in deployments, but it does not give any recommendation regarding measurements or definitions. The ITU-R report M.2040 [15] is referenced in the recommendation.

4.3.3 ECC regulation in Europe

ERC Rec 74-01 Spurious emissions

The ERC Recommendation 74-01 [6] is the main European regulatory document giving unwanted emission limits. The recommendation is aligned with Category B emission limits in SM.329-1 [14].

In terms of terminology, ERC Rec 74-01 does not use the term antenna transmission line, but instead antenna port. Also here, no specific definitions of the terms are given.

There is a note to considering m) that explains Active antenna systems (AAS):

Note: an "Active Antenna System" (AAS) is an antenna with embedded capability for electronic amplification and/or other RF processing. The total gain of an AAS may be functionally split into an "active" gain of the electronic functions (AG) and a conventional "passive" gain/loss (directivity) due to the geometrical design performance of the antenna (PG).

Recommends 2 clearly defines where the reference points are for the emission limits:

2) that for the purpose of this Recommendation, only unwanted emissions in the spurious domain conducted to the antenna port or subsequently radiated by any integral antenna, are subject to the established limits; "

Recommends 6) is concerned with power measurements and has a note on Active antenna systems (AAS):

Note 3: When a system is coupled to an "Active Antenna System", the limits of Table 2 should be met by the combined system; therefore compliance should be verified through an EIRP measurement (either near-field or far-field) and subsequent conversion to absolute power/attenuation values delivered to the transmission line, taking into account only the conventional "passive" gain (directivity) of the antenna.

There is no explanation within the recommendation of how to conduct EIRP measurements.

ECC Rec 02(05) [10]

This is the ECC "umbrella recommendation" for unwanted emissions. It contains mostly references to other ITU-R and ECC recommendations and does not give any additional definitions in the AAS area.

ECC and EU decisions for IMT bands

There are several decisions made for IMT bands, where regulatory limits are set both for "in-block" power (intentionally trans mitted power) and "out-of-block power" in terms of "Block Edge Masks" (BEM, for unwanted emissions). Many of the base station emission limits in those decisions are defined in terms of EIRP Examples are the decision for the 2.6 GHz band [8] and the 800 MHz band [9]. There are recommendations of how to measure BEMs in ECC Rec 11(06) [7].

ECC Rec 11(06) Block Edge Mask Compliance Measurements for Base Stations [7]

The recommendation discusses both conducted and radiated measurements. The following is stated in Annex A.1.4.4 regarding measurements of absolute power limits:

"The assessment of block edge masks with absolute power limits should be done using a conducted measurement directly at the transmitter output. Although a radiated measurement is possible in principle it's not recommended, as it will introduce a number of additional uncertainties (e.g. measurement distance). Especially in the case of a BEM based on transmitter output power or output power density for a radiated measurement the knowledge of certain parameters is necessary, which can be acquired only on-site; i.e. feeder loss and antenna gain."

4.3.4 FCC regulation in the U.S.

There are two recent publications by the FCC of an Administrative Requirements [11, 12] concerning measurements made on a device that employs multiple outputs in the same band. The documents treat both in-band and out-of-band/spurious emissions measurements.

For out-of-band/spurious emissions measurements from multiple outputs, two alternatives are given in [11]:

- (1) Measure and sum the spectra across the outputs and compare to the emission limit.
- (2) Measure each output and add $10 \log_{10}(N) dB$ to the value before comparing to the emission limit, where N is the number of outputs.

There is also guidance in [11] on calculating directional gain from antennas, which are applied e.g. when a conducted measurement is combined with a directional gain calculation to show compliance with a radiated limit:

- For cases where signals on different antennas are correlated (beam forming is given as an example), the antenna gain is $G_{ANT} + 10log_{10}(N) dBi$.
- For cases where all antennas signals are completely uncorrelated (Space Time Block Codes and Spatial Multiplexing MIMO are given as examples), the antenna gain is G_{ANT}.

Additional guidance is given in [12] for MIMO operation with cross-polarized antennas.

4.3.5 MIC regulation in Japan

Ordinance Regulating Radio Equipment [16] is stipulated by MIC in order to determine the conditions for radio equipment and high frequency based equipment. In [16], some details (e.g. the unwanted emissions of specific systems, the measurement and calculation method of output power etc.) are explained for each individual technical condition of a specific system. Regarding the 3GPP systems, the technical conditions of WCDMA/HSPA/DC-HSDPA/LTE were notified by MIC in [17].

In the technical conditions in [17], the measurement and calculation method of output power or unwanted emissions (both in-band and out-of-band/spurious emissions) from multiple outputs are given as follows:

• For an adaptive array antenna

- Measure and sum the output powers or emissions (which are specified by absolute values in the technical conditions) of all the antenna connectors.
- In this case, the output power of one array element shall be configured with the maximum output power. Then, the output powers of remaining array elements shall be configured as the sum of output powers of all array elements are maximized.
- For MIMO
 - Measure the output power or emission on each antenna connector.

5 Study of AAS deployment scenarios

5.1 AAS applications

Examples of AAS applications are provided in this section.

5.1.1 Tilt and radiation pattern control

Antennas are usually manufactured with a fixed beamwidth, and antenna manufacturers typically offer a limited number of beamwidth variations within their conventional product lines. Conventional BS installations often introduce physical tilt to the antenna in order to orient the main lobe of the antenna response towards the ground. Antenna tilt is selected to optimize desired cell coverage and to minimize interference to and from adjacent cells. Some installations employ Remote Electrical Tilt (RET) devices which allow adjustment of the phase shift to facilitate remote control of the antenna tilt angle.

An AAS may dynamically control the elevation and azimuth angles, as well as the beamwidth of its radiation pattern via electronic means. Electronic control may be used along with mechanical control, The AAS radiation pattern may be adapted to the specific deployment scenario and possibly to changing traffic patterns. The AAS radiation pattern may also be independently optimized for different links such as independently for uplink and downlink, for coverage and beam forming gain purposes.

5.1.1.1 Cell partitioning in the horizontal and vertical plane

The concepts of tilt and beamwidth control can be extended by a technique known as cell partitioning in which the cell is subdivided in vertical or horizontal directions by adjustment of the antenna pattern. For example one cell partition is located close to the BS and the other cell partition is located farther away from the BS.

5.1.2 Multiple input multiple output (MIMO)

MIMO is a general terminology that includes the following spatial processing techniques: Beamforming, Diversity, and Spatial Multiplexing. A brief description of each is provided below.

- Beamforming: The use of a dedicated beam formed towards the UE when data demodulation using a dedicated reference signal is supported by the UE.
- Diversity: The use of diversity techniques to jointly optimize in the spatial and frequency domain through the use of, for example, Spatial-Frequency Block Code (SFBC) or Frequency Switching Transmit Diversity (FSTD), or combinations of both;
- Spatial Multiple xing: The transmission of multiple signal streams to one (SU-MIMO) or more (MU-MIMO) UEs using multiple spatial layers created by combinations of the available antennas.

5.1.3 Differentiated antenna behaviours at different carrier frequencies

AAS supports the use of different antennas at different carrier frequencies and for different RATs. For example, an AAS may create 4 virtual antennas for an LTE carrier and 2 antennas for a GSM or HSPA carrier.

5.1.4 Per RB (or UE) Transmission and Reception

In this case, each UE may get its own beam that tracks the movement of the UE.

The current specification support for Spatial Multiplexing, Beamforming and Transmit Diversity includes the ability to schedule transmission and reception to one UE within one Resource Block. This allows beamforming to individual UEs with adaptation to mobility, as an example.

5.2 Deployment and coexistence scenarios

5.2.1 Deployment scenarios

The AAS BS can be deployed for Wide Area, Medium Range, and Local Area coverage.

- The Wide Area coverage deployment scenario is typically found in outdoor macro environments, where the BS antennas are located on masts, roof tops or high above street level. An AAS BS designed for wide area coverage is called a Macro AAS.
- The Medium Range coverage deployment scenario is typically found in outdoor micro environments, where the AAS BSs are located below roof tops. An AAS BS designed for medium range coverage is called a Micro AAS.
- The Local Area BS deployment scenario is typically found indoors (offices, subway stations etc.) where antennas are located on ceilings or walls. Deployment scenarios for local area coverage can also be found outdoors in hot spot areas like marketplaces, high streets or railway stations. An AAS BS designed for local area coverage is called a Pico AAS.

5.2.2 Coexistence scenarios

The radiation pattern for an AAS BS can be dynamically adjustable, while a fixed beam pattern is assumed for the conventional BS. A dynamic radiation pattern has been considered for UTRA 1.28Mcps TDD system and the beam pattern can be found in Annex B in TR36.942 [19].

Coexistence of an AAS BS with a conventional BS based on an un-coordinated deployment shall be considered. Analytical approaches can be used to study the coexistence requirements based on existing results, supplemented with additional simulations when necessary.

The following initial scenarios are identified for the purpose of studying the spatial characteristics for AAS BS:

- E-UTRA Macro AAS BS co-located with another E-UTRA Macro AAS BS
- E-UTRA Macro AAS BS co-located with E-UTRA Macro legacy BS

NOTE: The scenarios that would impact the RF requirements are TBD

5.3 Classifications of AAS BS

TR25.951 and TR25.952 define deployment scenarios for UTRA Wide-Area, Medium-Range, Local-Area, and Home base stations. The Base Station RF requirements in 3GPP specifications are specified for those BS classes based on studying characteristics of the deployment scenarios in TR25.951/952 using the methodologies specified in TR25.942. RF requirements for E-UTRA base stations are based on studies using the methodologies specified in TR36.942.

The methodologies in TR25.942 and TR36.942 can be extended to study AAS characteristics for Wide-Area, Medium-Range, and Local-Area BS deployment scenarios, or where necessary further methodologies can be derived based on the defined deployment scenarios. The scope of the work item will be limited to study of these classes. Employing those methodologies may result in a restatement of existing RF requirements transferred to AAS specific reference points, or may result in new RF requirements for AAS BS.

Further details are within the scope of the WI phase.

5.4 Simulation study

5.4.1 Objectives

The coexistence simulation objectives include the following:

- 1. Establishment of coexistence system simulations based on 3-dimensional antenna patterns for AAS and non-AAS BS systems.
 - The coexistence characteristics for non-AAS BS systems are presented to establish baseline performance.
 - Coexistence performance of AAS BS systems with both AAS BS systems and non-AAS systems in uncoordinated deployment scenarios is evaluated.
- 2. Evaluate the transmitter and receiver spatial characteristics of AAS BS.
- 3. Define and derive a proposal for how to set measurable RF requirements.

5.4.2 Simulation scenarios

5.4.2.1 Initial simulation cases

The initial simulation cases are based on the AAS fundamental applications where the AAS BS is used for a 3-sector/site coverage. This is similar to the legacy passive antenna system.

Note: Simulation scenarios for other applications will be added later.

For initial consideration, the E-UTRA Macro to E-UTRA Macro coexistence scenario is identified for the purpose of studying the spatial characteristics of an AAS BS. Simulation cases as shown in Table 5.4.2.1-1 and Table 5.4.2.1-2 are applied for evaluating in-band blocking and ACLR for AAS BS.

Table 5.4.2.1-1: Simulation cases for in-band blocking

Case	Aggressor	Victim	Simulated link	Statistics
1-a	Legacy E-UTRA Macro system	AAS E-UTR A Macro system	Uplink	Interferer levels at victim BS
1-b	AAS E-UTR A Macro system	AAS E-UTR A Macro system	Uplink	Interferer levels at victim BS
1-c(Baseline)	Legacy E-UTRA Macro system	Legacy E-UTRA Macro system	Uplink	Interferer levels at victim BS

Table 5.4.2.1-2: Simulation cases for ACLR

Case	Aggressor	Victim	Simulated link	Statistics
1-a	AAS E-UTR A Macro system	Legacy E-UTRA Macro system	Downlink	Throughput loss
1-b	AAS E-UTR A Macro system	AAS E-UTR A Macro system	Downlink	Throughput loss
1-c(Baseline)	Legacy E-UTRA Macro system	Legacy E-UTRA Macro system	Downlink	Throughput loss

5.4.2.2 Simulation cases based on the other AAS applications

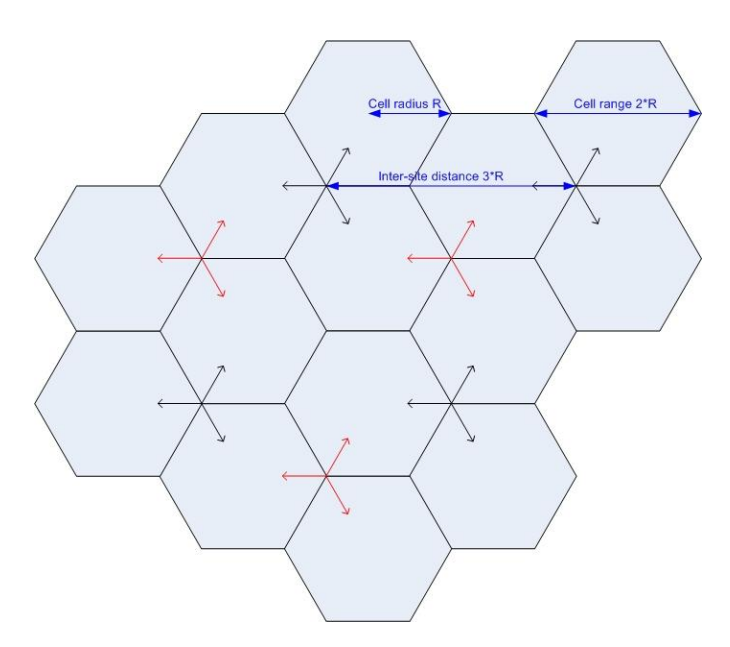
<Reserved for future use>

5.4.3 Simulation assumptions

5.4.3.1 Assumptions for the initial simulation cases

5.4.3.1.1 Network layout

The macro cell network is a tri-sector layout placed on a hexagonal grid with distance of $3 \times R$, where R is the cell radius with wrap around. For uncoordinated network simulations, identical cell layouts for each network are applied, with worst case shift between sites. The second network's sites are located at the first network's cell edge, as shown in Figure 5.4.3.1.1-1[19]. The ISD is 750 m.



18

Figure 5.4.3.1.1-1 Multi operator cell layout - uncoordinated deployment

5.4.3.1.2 Propagation model

The path loss model is defined as below

$$Path_Loss = max \{L(R), Free_Space_Loss\} + shadowfading$$

where the free space loss is defined as

Free_Space_Loss =
$$98.46 + 20 \log_{10}(R)$$
 (R in kilometre)

and L(R) is defined as below [19]

$$L(R) = 128.1 + 37.6 \cdot Log_{10}(R) (dB)$$

The shadow fading is modelled as a log-normal distribution.

Then the final coupling loss model is defined as [20]:

where G_Tx is the transmitter antenna gain and the G_Rx is the receiver antenna gain.

5.4.3.1.3 Down-tilt angle setting

For the coexistence study, the setting of the antenna down-tilt angle is selected by choosing the angle which produces the highest system throughput in a set of simulations. For a Macro cell with ISD of 750m, the downlink and uplink throughput of the AAS single system is evaluated by scanning BS down-tilt angle (both electrically and mechanically) from 5 degrees to 20 degrees, as shown in Figure 5.4.3.1.3-1 to Figure 5.4.3.1.3-4.

From the simulation results, it can be observed that:

- 1. For down link system throughput, the system throughput reaches its maximum with BS down-tilt angle of about 9 degree, for both electrical and mechanical down-tilt.
- 2. The average uplink throughput is relatively insensitive to the down-tilt angle. This is mainly due to the uplink power control which could fully or partially compensate the difference of the coupling loss (antenna gain) caused by different down-tilt angles and ensures the signal power received at BS from different users is similar. The uplink edge throughput at cell edge is sensitive to the down-tilt angle. The maximum throughput is reached at about 9 degrees down-tilt. This down-tilt angle also maximises the down link throughput.

3. A down-tilt angle of 9 degrees can be used for the specific scenario under the assumptions defined in Section 5.4 (e.g. ISD, height of BS and UE, antenna pattern, etc.) for the fundamental AAS coexistence simulation as a baseline because it maximises throughput. In other scenarios and in particular in a real network deployment, different down-tilt angles may maximise throughput and may be applied.

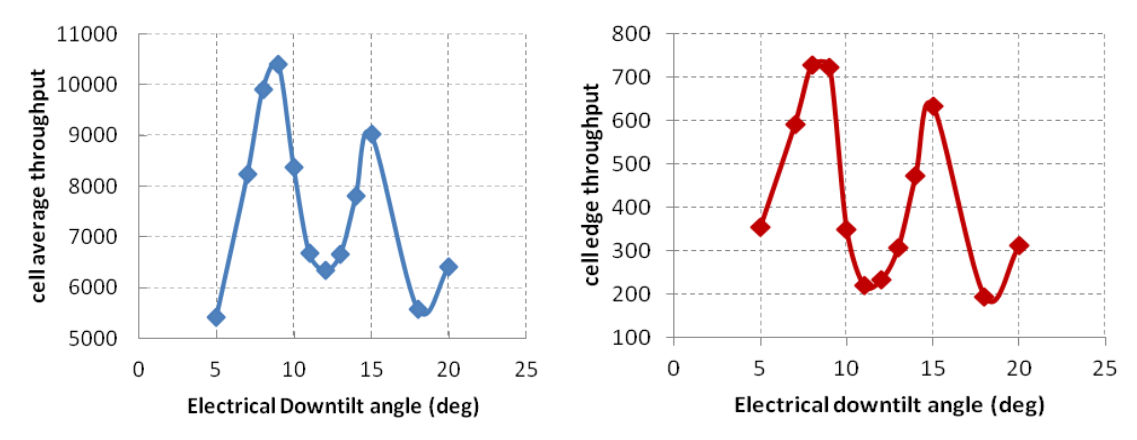


Figure 5.4.3.1.3-1 Downlink cell average and cell edge throughput with different electrical down-tilt angles

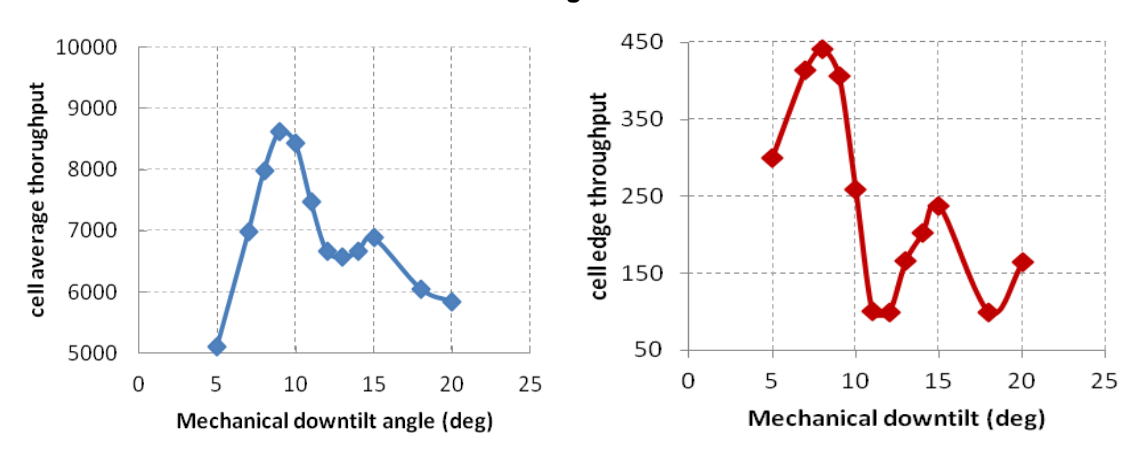


Figure 5.4.3.1.3-2 Downlink cell average and cell edge throughput with different mechanical down-tilt angles

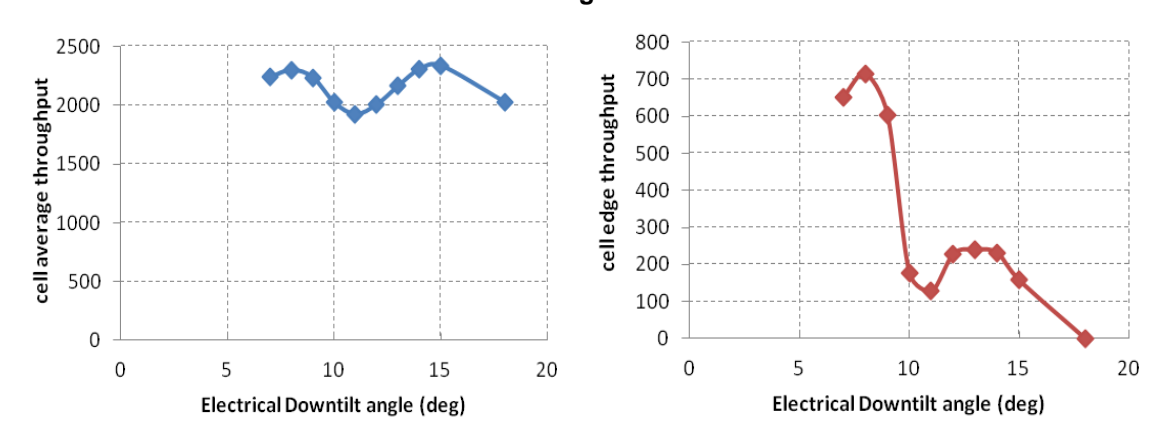


Figure 5.4.3.1.3-3 Uplink cell average and cell edge throughput with different electrical down-tilt angles

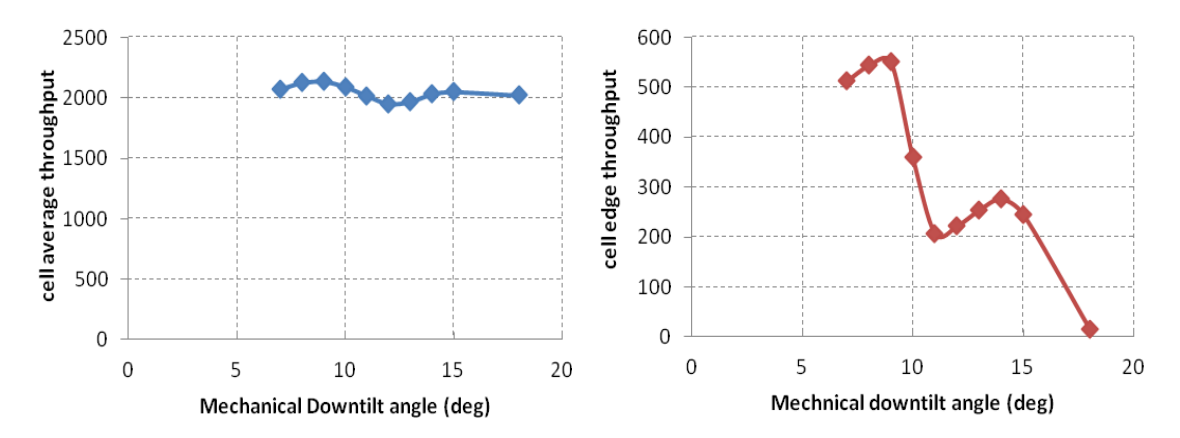


Figure 5.4.3.1.3-4 Uplink cell average and cell edge throughput with different mechanical down-tilt angles

5.4.3.1.4 General simulation parameters for the initial simulation cases

Table 5.4.3.1.4-1 General simulation parameters

Parameters	Values	
Cellular layout	Hexagonal, 3 sectors/cell (19 cell wrap-around), uncoordinated	
UE distribution	Average 10 UEs per sector. UEs on flat ground	
Carrier frequency	2GHz	
System bandwidth	10MHz	
Inter Site Distance (ISD)	750m	
Minimum distance UE<->BS	35m	
Log normal shadowing	Standard Deviation of 10 dB	
Shadow correlation coefficient	0.5 (inter site) / 1.0 (intra site)	
Scheduling algorithm	Round Robin, Full buffer	
RB number per active UEs	UL: 16RBs (total: 48 RBs)	
KB Humber per active OES	DL: 50RBs	
Number of active UEs	UL: 3 UEs	
Number of active OES	DL: 1 UE	
UE max Tx power	23 dBm	
UE min Tx power	-40 dBm	
BS maxTx power	46dBm	
	(TR36.942 Section 12.1.4)	
Power control parameters	PC Set 1 (alpha=1; P0=-101dBm)	
	PC Set 2 (alpha=0.8; P0=-92.2dBm)	
Antenna configuration at UE	Omni-directional	
The height of BS	30 m	
The height of UE	1.5 m	
	9 degrees as the baseline (can be combination of mechanical and electrical), which	
Down-tilt angle	corresponds to $\theta_{\it etilt}$ = 9 degrees as defined in Section 5.4.3.	
Antenna array configuration	40×4	
$(Row \times Column)$	10×1	
ACS of LTE UE	33 dB	
Radiation pattern of the antenna	The same as AAS 3D antenna pattern as introduced in section 5.4.3.	

inatallad far lagagy DC	
Installed for legacy BS	
1	

5.4.3.2 Assumptions for the other applications

<Reserved for future use >

5.4.4 Array antenna model

Currently a passive antenna is modeled as a single radiating source according to definition in TR 36.814, Table A.2.1.1 - 2. For AAS BS it was decided extend the antenna model and define an array antenna model based on multiple radiating sources.

5.4.4.1 Methodology

For a uniformly distributed array (ULA) antenna, as shown in Figure 5.4.4.1-1, the radiation elements are placed uniformly along the vertical **z**-axis in the Cartesian coordinate system. The **x-y** plane constructs the horizontal plane. A signal acting at the array elements is in the direction of **u**. The elevation angle of the signal direction is denoted as θ (defined between 0° and 180° , 90° represents perpendicular angle to the array antenna aperture) and the azimuth angle is denoted as ϕ (defined between -180° and 180°).

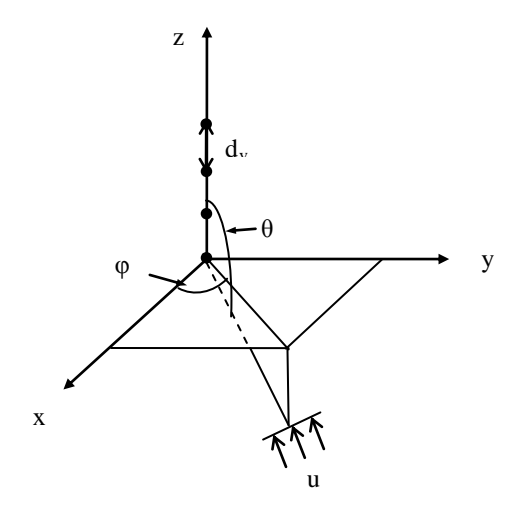


Figure 1.4.4.1-1. Antenna Array Geometry

The array antenna radiation is created by super-position including three main components:

- · The element radiation pattern
- The array factor
- The signals applied to the system

Each component is defined in details in Section 5.4.4.1.1 to 5.4.4.1.5:

5.4.4.1.1 Element Pattern

A method similar to current 3GPP modelling used for passive antennas is applied for the element radiation pattern model, which is

$$20 \times \log_{10}(P_E(\theta, \varphi)) = G_{E,Max} - \min\left\{-\left[A_{E,H}(\varphi) + A_{E,V}(\theta)\right]A_m\right\}$$

Where

- $P_E(\theta, \varphi)$ is the magnitude of the element pattern
- $-\theta$ is the elevation angle, defined between 0° and 180° (90° represents perpendicular to the array antenna aperture)
- $-\varphi$ is the azimuth angle, defined between -180° and 180°

- $=G_{EMax}$ is the maximum directional gain of the radiation element (in dB), which is assumed to be 8dBi;
- $A_{EH}(\varphi)$ is the horizontal pattern of the radiation element,

$$A_{E,H}(\varphi) = -\min \left[12 \left(\frac{\varphi}{\varphi_{3dB}} \right)^2, A_m \right]$$

where ϕ_{3dB} is the horizontal 3dB beam-width, and A_m is the front-back ratio.

- $A_{FV}(\theta)$ is the vertical radiation pattern of the radiation element offset by 90° to point perpendicular to array,

$$A_{E,v}(\theta) = -\min \left[12 \left(\frac{\theta - 90}{\theta_{3dB}} \right)^2, SLA_v \right]$$

where θ_{3dB} is the vertical 3dB beam-width and SLA_{v} is the side-lobe level limit.

 $A_{E,V}(\theta)$ and $A_{E,H}(\varphi)$ is plotted in Figure 5.4.4.1.1-1 when $\theta_{3dB}=65^{\circ}$, $SLA_{v}=30\,dB$, $\phi_{3dB}=65^{\circ}$ and $A_{m}=30\,dB$.

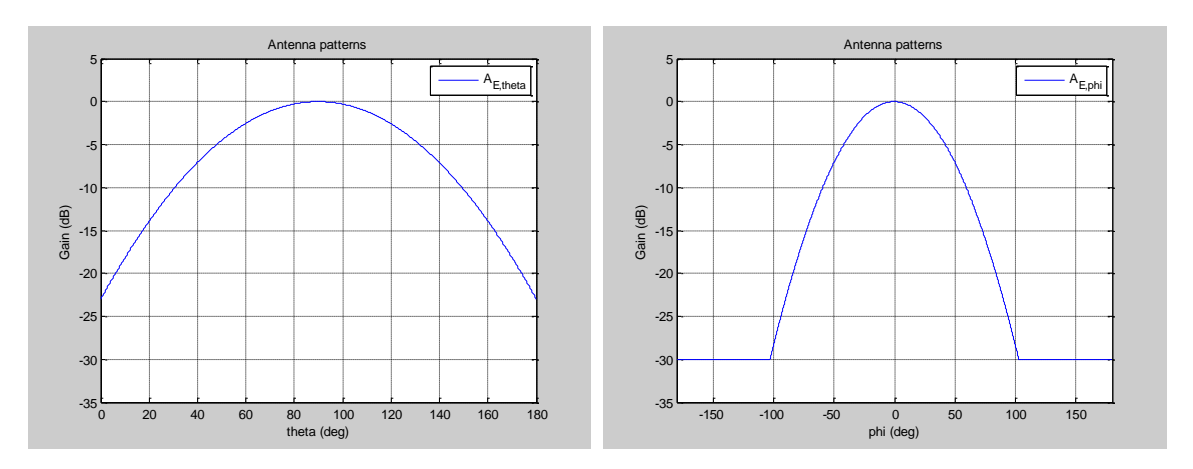


Figure 5.4.4.1.1-1. Vertical and Horizontal element radiation patterns

5.4.4.1.2 Array factor for single column

The performance of the array depends on the spacing and weighting of the radiation elements, which can be represented by \widetilde{W} as the Hadamard product, i.e.,

$$\widetilde{W} = W \cdot V$$

in which V is the phase shift due to array placement, denoted as

$$V = [v_1, v_2, \dots, v_N]^T$$
, where

$$v_n = \exp\left(-2\pi \cdot i \cdot (n-1) \cdot \frac{d_v}{\lambda} \cdot \cos(\theta)\right) \quad n = 1, 2, \dots N;$$

and W is the weighting factor, which can provide control of side lobe levels and can also provide electrical down-tilt. For simplicity, the amplitude of the weighting vector is assumed to be identical for each radiation element. The phase of the weighting vector is used to implement electrical down tilt and is dependent on the required tilt and the element spacing.

$$W = \left[w_1, w_2, \dots, w_N \right]^T$$

$$\omega_n = \frac{1}{\sqrt{N}} \exp\left(2\pi \cdot i \cdot (n-1) \cdot \frac{d_v}{\lambda} \cdot \cos(\theta_{etilt})\right), \quad n = 1, 2, \dots N$$

where, θ_{etilt} is defined as the down-tilt angle as defined in TR 36.814 (Meaning that for θ_{etilt} =0 degrees the main beam is pointing perpendicular to the array antenna aperture).

For mechanical down-tilt, this can be handled by a coordinate system transformation described in TR 36.814 section A2.1.6.2 in details.

5.4.4.1.3 Array factor for multiple column

A planar uniform rectangular array (URA) antenna with $N_V \times N_H$ radiation elements is employed for modelling AAS with multiple columns, as shown in figure 5.4.4.1.3-1. The numbers of the elements placed along y-axis and z-axis are N_H and N_V , respectively.

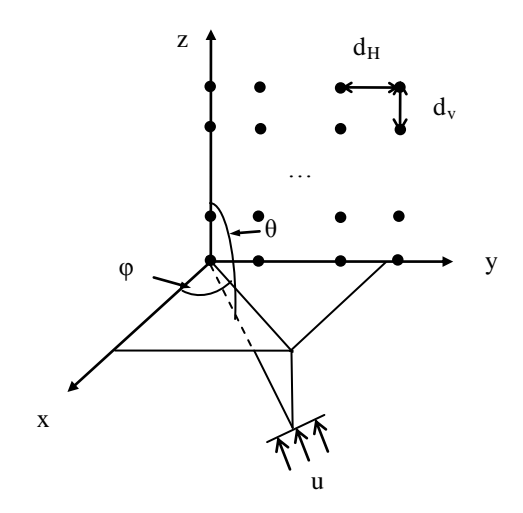


Figure 2.4.4.1.3-1 Geometry distribution of AAS with multiple columns array

The array factor of the planar array can be represented by \widetilde{W} , i.e.,

$$\widetilde{W} = W \cdot V$$

in which V is the phase shift due to array placement, denoted as

$$V = \begin{bmatrix} v_{1,1}, v_{1,2}, \dots, v_{1,N_V}, \dots, v_{N_H,1}, v_{N_H,2}, \dots, v_{N_H,N_V} \end{bmatrix}^T,$$

$$v_{m,n} = \exp\left(-i \cdot 2\pi \left((n-1) \cdot \frac{d_V}{\lambda} \cdot \cos(\theta) + (m-1) \cdot \frac{d_H}{\lambda} \cdot \sin(\theta) \cdot \sin(\varphi)\right)\right),$$

$$m = 1, 2, \dots, N_H; n = 1, 2, \dots, N_V;$$

W is the weighting factor, which can provide control of side lobe levels and can also provide electrical steering, both horizontal and vertical. For simplicity, the amplitude of the weighting vector is assumed to be identical for each radiation element. The phase of the weighting vector is used to implement electrical steering and is dependent on the required horizontal and vertical steering angle and the element spacing.

$$W = \left[w_{1,1}, w_{1,2}, \dots, w_{1,N_V}, \dots, w_{N_H,1}, w_{N_H,2}, \dots, w_{N_H,N_V} \right]^T$$

$$w_{m,n} = \frac{1}{\sqrt{N_H N_V}} \exp \left(i \cdot 2\pi \left((n-1) \cdot \frac{d_V}{\lambda} \cdot \sin(\theta_{etilt}) + (m-1) \cdot \frac{d_H}{\lambda} \cdot \cos(\theta_{etilt}) \cdot \sin(\varphi_{escan}) \right) \right),$$

$$m = 1, 2, \dots, N_H; n = 1, 2, \dots, N_V;$$

where $\, heta_{etilt}$ is the electrical down-tilt steering, and $\, heta_{escan}$ is the electrical horizontal steering.

5.4.4.1.4 Signals and correlation matrix for single column

Correlation of 2 transceiver paths is represented by a correlation coefficient, $0 \le \rho \le 1$, defined below as the similarity of the unwanted signals at the output of 2 paths when an identical signal is applied at the input. Unwanted signals generated in the transceivers can under different circumstances be regarded as correlated, $\rho = 1$, (e.g. unwanted signals generated by CFR (Crest Factor Reduction) will be generated digitally and hence identical in each path), or uncorrelated, $\rho = 0$, (e.g. amplified thermal noise is random in nature and hence will have no similarity in different paths). As the type of unwanted signal is implementation specific and hence unknown, the correlation matrix allows varying levels of correlation to be investigated so the worst case can be identified for specification purposes.

The signals at all elements are defined as

$$S(t) = [s_1(t), s_2(t), ..., s_N(t)]^T$$

The complex output of the array system at far field becomes

$$y(\theta, \varphi, t) = \sum_{n=1}^{N} s_n(t) \cdot w_n \cdot E_n(\theta, \varphi) = P_E(\theta, \varphi) \cdot \widetilde{W}^H \cdot S(t)$$

where $E_n(\theta, \varphi)$ denotes the complex gain of the *n*th radiation element, together with the phase shift due to array place ment, expressed as

$$E_n(\theta,\varphi) = P_E(\theta,\varphi) \cdot \exp\left(-2\pi \cdot i \cdot (n-1) \cdot \frac{d_v}{\lambda} \cdot \cos(\theta)\right), \quad \theta = 0, \dots 180, \varphi = -180, \dots 0, \dots 180.$$

Then the radiation pattern of the antenna array is the mean output power which can be obtained by taking conditional expectation over $|y(\theta, \varphi, t)|^2$,

$$P(\theta, \varphi) = E \left[y(\theta, \varphi, t)^{2} \right] = P_{E}^{2}(\theta, \varphi) \cdot \widetilde{W}^{H} \cdot E[S(t) \cdot S^{H}(t)] \cdot \widetilde{W} = P_{E}^{2}(\theta, \varphi) \cdot \widetilde{W}^{H} \cdot R \cdot \widetilde{W}$$

and R is the array correlation matrix defined by

$$R = E(S(t) \cdot S^{H}(t)) = \begin{bmatrix} R_{11} & R_{12} & \cdots & R_{1N} \\ R_{21} & R_{22} & \cdots & R_{2N} \\ \cdots & \cdots & R_{nm} & \cdots \\ R_{N1} & R_{N2} & \cdots & R_{NN} \end{bmatrix}$$

Elements of this matrix denote the correlation between signals in the various transceiver paths. For example, R_{nm} denotes the correlation between the signals in the nth and the mth transceiver paths, assuming that the fast fading between antenna elements is spatially correlated.

$$R_{nm} = \frac{\sum_{k=1}^{K} s_{n,k} \cdot s_{m,k}^{*}}{\sqrt{\sum_{k=1}^{K} \left| s_{n,k} \right|^{2}} \cdot \sqrt{\sum_{k=1}^{K} \left| s_{m,k} \right|^{2}}}$$

For simplicity but still having the correlation sufficiently modelled in the coexistence study, it is proposed to assume the same correlation level ρ , where ρ is a value between 0 and 1, between signals in transceiver paths, or

$$R = E(S(t) \cdot S^{H}(t)) = \begin{bmatrix} 1 & \rho & \cdots & \rho \\ \rho & 1 & \cdots & \rho \\ \cdots & \cdots & 1 & \cdots \\ \rho & \rho & \cdots & 1 \end{bmatrix}$$

25

Note that uniform correlation may be an over-simplification of an active array implementation. When multiple sub-arrays are within the antenna elements, it is possible they have different correlation levels. The modelling of this effect is FFS.

It is clear that

$$R = \rho \cdot (U - I) + I = \rho \cdot U + (1 - \rho) \cdot I$$

where U is the all-1 matrix and I is the unit matrix with 1 on the diagonal elements only. The radiation pattern is simplified as

$$A_{A}(\theta, \varphi) = A_{E}(\theta, \varphi) + 10 \log_{10} \left[1 + \rho \cdot \left(\left| \sum_{n=1}^{N} w_{n} \cdot v_{n} \right|^{2} - 1 \right) \right]$$

When $\rho = 1$, the correlation matrix R is an all-1 matrix U, and the radiation pattern is the same as a passive antenna if their weighting vector W is configured the same. Therefore the following equation can be used for a legacy system with a passive array antenna as well.

$$A_{A}(\theta,\varphi) = A_{E}(\theta,\varphi) + 10\log_{10}\left(\left|\sum_{n=1}^{N} w_{n} \cdot v_{n}\right|^{2}\right)$$

When $\rho = 0$, the correlation matrix R is the unit matrix I with 1 on the diagonal elements and the radiation pattern is the same as the radiation element, or the antenna shows no array gain for uncorrelated inputs.

$$A_{A}(\theta,\varphi) = A_{E}(\theta,\varphi)$$

5.4.4.1.5 Signals and correlation matrix for multiple column

The methodology of antenna modelling for multiple columns follows the same procedure with that for single column in Section 5.4.4.1.4.

The signals at all elements are defined as

$$S(t) = \left[s_{1,1}(t), s_{1,2}(t), \dots, s_{1,N_V}(t), \dots, s_{N_H,1}(t), s_{N_H,2}(t), \dots, s_{N_H,N_V}(t) \right]^T$$

The complex output of the array system at far field becomes

$$y(\varphi,\theta,t) = \sum_{m=1}^{N_H} \sum_{n=1}^{N_V} S_{m,n}(t) \cdot w_{m,n} \cdot E_{m,n}(\varphi,\theta) = P_E(\varphi,\theta) \cdot \widetilde{W}^H \cdot S(t)$$

where $E_{m,n}(\varphi,\theta)$ denotes the complex gain of the radiation element of *m*-th column and the *n*-th row, together with the phase shift due to array placement, expressed as

$$E_{m,n}(\varphi,\theta) = P_{E}(\varphi,\theta) \cdot \exp\left(-2\pi \cdot i \cdot \left((n-1) \cdot \frac{d_{v}}{\lambda} \cdot \cos(\theta) + (m-1) \cdot \frac{d_{H}}{\lambda} \cdot \sin(\theta) \sin(\varphi)\right)\right)$$

Then the radiation pattern of the antenna array is the mean output power which can be obtained by taking the conditional expectation over $|y(\varphi,\theta,t)|^2$,

$$P(\varphi,\theta) = E\left[y(\varphi,\theta,t)\right]^{2} = P_{E}^{2}(\varphi,\theta) \cdot \widetilde{W}^{H} \cdot E\left[S(t) \cdot S^{H}(t)\right] \cdot \widetilde{W} = P_{E}^{2}(\varphi,\theta) \cdot \widetilde{W}^{H} \cdot R \cdot \widetilde{W}$$

and R is the array correlation matrix defined by

$$R = E(S(t) \cdot S^{H}(t)) = \begin{bmatrix} R_{1,1} & R_{1,2} & \cdots & R_{1,N_{V}} \dots & R_{1,N_{V}N_{H}} \\ R_{2,1} & R_{2,2} & \cdots & R_{2,N_{V}} \dots & R_{2,N_{V}N_{H}} \\ \cdots & \cdots & R_{(i-1)N_{V} + (j-1),(k-1)N_{V} + (t-1)} \\ R_{N_{V}N_{H},1} & R_{N_{V}N_{H},2} & \cdots & \cdots & R_{N_{V}N_{H},N_{V}N_{H}} \end{bmatrix}$$

Elements of this matrix denote the correlation between signals in the various transceiver paths. For example,

 $R_{(i-1)N_V+(j-1),(k-1)N_V+(t-1)}$ denotes the correlation between the signals in the {ith column, jth row} and the {kth column, th row} transceiver paths, assuming that the fast fading between antenna elements is spatially correlated.

For simplicity but still having the correlation sufficiently modelled in the coexistence study, it is proposed to assume the same correlation level ρ , where ρ is a value between 0 and 1, between signals in transceiver paths, or

$$R = E(S(t) \cdot S^{H}(t)) = \begin{bmatrix} 1 & \rho & \cdots & \rho \\ \rho & 1 & \cdots & \rho \\ \cdots & \cdots & 1 & \cdots \\ \rho & \rho & \cdots & 1 \end{bmatrix}$$

Note that uniform correlation may be an over-simplification of an active array implementation. When multiple subarrays are within the antenna elements it is possible they have different correlation levels. The modelling of this effect is FFS.

It is clear that

$$R = \rho \cdot (U - I) + I = \rho \cdot U + (1 - \rho) \cdot I$$

where U is the all-1 matrix and I is the unit matrix with 1 on the diagonal elements only. The radiation pattern is simplified as

$$A_{A}(\varphi,\theta) = A_{E}(\varphi,\theta) + 10\log_{10} \left[1 + \rho \cdot \left(\left| \sum_{m=1}^{N_{H}} \sum_{n=1}^{N_{V}} w_{m,n} \cdot v_{m,n} \right|^{2} - 1 \right) \right]$$

When $\rho = 1$, the correlation matrix R is an all-1 matrix U, and the radiation pattern is the same as a passive antenna.

$$A_{A}(\varphi,\theta) = A_{E}(\varphi,\theta) + 10\log_{10}\left[\left|\sum_{m=1}^{N_{H}} \sum_{n=1}^{N_{V}} w_{m,n} \cdot v_{m,n}\right|^{2}\right]$$

When $\rho = 0$, the correlation matrix R is the unit matrix I with 1 on the diagonal elements and the radiation pattern is the same as the radiation element, or the antenna shows no array gain for uncorrelated inputs.

$$A_{\scriptscriptstyle A}(\theta,\varphi) = A_{\scriptscriptstyle F}(\theta,\varphi)$$

5.4.4.2 Summarized functions and parameters

The parameters for the array antenna model are defined in Table 5.4.4.2-1 and Table 5.4.4.2-2 below:

Table 5.4.4.2-1 Element pattern

Horizontal Radiation Pattern	$A_{E,H}(\varphi) = -\min\left[12\left(\frac{\varphi}{\varphi_{3dB}}\right)^2, A_m\right] dB$
Front-to-back ratio	$A_m = 30dB$
Vertical Pattern method	$A_{E,V}(\theta) = -\min\left[12\left(\frac{\theta - 90}{\theta_{3dB}}\right)^2, SLA_v\right]$

Side Lobe lower level	SLA _v =30 dB
Element Pattern	$A_{E}\left(\varphi,\theta\right) = G_{E,\max} - \min\left\{-\left[A_{E,H}\left(\varphi\right) + A_{E,V}\left(\theta\right)\right], A_{m}\right\}$
Element Gain	G _{E, max} =8 dBi *
NOTE: For a type A10 antenna according to Table 5.4.4.2.1-1 8 dBi corresponds to 18 dBi array gain.	

Table 5.4.4.2-2 Composite array pattern for single column

Configuration	Single column (N-elements)	
Composite Array radiation pattern in dB $A_{\scriptscriptstyle A}(\theta,\varphi)$	$A_{A}(\theta,\varphi) = A_{E}(\theta,\varphi) + 10\log_{10}\left[1 + \rho \cdot \left(\left \sum_{n=1}^{N} w_{n} \cdot v_{n}\right ^{2} - 1\right)\right]$ the super position vector is given by $v_{n} = \exp\left(-2\pi \cdot i \cdot (n-1) \cdot \frac{d_{v}}{\lambda} \cdot \cos(\theta)\right), n = 1,2,N$ the weighting is given by $\omega_{n} = \frac{1}{\sqrt{N}} \exp\left(2\pi \cdot i \cdot (n-1) \cdot \frac{d_{v}}{\lambda} \cdot \sin(\theta_{etilt})\right), n = 1,2,N$	
Active array loss	l 0 dB	
Additional parameters are provided for antenna type A10 in Table 5.4.4.2.1-1		

Table 5.4.4.2-3 Composite array pattern for multiple column

Configuration	Multiple columns (N∨xN _H elements)						
	$A_{A}(\theta,\varphi) = A_{E}(\theta,\varphi) + 10\log_{10}\left[1 + \rho \cdot \left(\left \sum_{m=1}^{N_{H}} \sum_{n=1}^{N_{V}} w_{m,n} \cdot v_{m,n}\right ^{2} - 1\right)\right]$						
	the super position vector is given by						
Composite Array radiation pattern in dB $A_{\!\scriptscriptstyle A}\!\left(heta,arphi ight)$	$v_{m,n} = \exp\left(-i \cdot 2\pi \left((n-1) \cdot \frac{d_V}{\lambda} \cdot \cos(\theta) + (m-1) \cdot \frac{d_H}{\lambda} \cdot \sin(\theta) \cdot \sin(\varphi)\right)\right)$ $m = 1, 2,, N_H; n = 1, 2,, N_V;$						
	the weighting is given by						
	$w_{m,n} = \frac{1}{\sqrt{N_H N_V}} \exp \left(i \cdot 2\pi \left((n-1) \cdot \frac{d_V}{\lambda} \cdot \sin(\theta_{etilt}) + (m-1) \cdot \frac{d_H}{\lambda} \cdot \cos(\theta_{etilt}) \cdot \sin(\varphi_{escan}) \right) \right)$						
	$m = 1, 2,, N_H; n = 1, 2,, N_V;$						
Active array loss	0 dB						
Additional parameters are provi	ded in Table 5.4.4.2.1-1.						

5.4.4.2.1 Typical array antenna parameters

Table 5.4.4.2.1-1 Parameter for typical passive antenna types

Antenna type	A 1	A5	A10	A15	B5	B10	B15	D5	D10	D15
No of radiation elements	1	5	10	15	5	10	15	5	10	15
No of columns	1	1	1	1	2	2	2	4	4	4
Maxarray gain for a single column / dBi	8.7	15	18	19.5	14.5	17	18.5	14.5	17	18.5

Max antenna gain / dBi	8.7	15	18	19.5	17	19.5	21	20	22.5	24
Vertical radiating element spacing d/λ	-	0.9	0.9	0.9	0.9	0.9	0.9	0.9	0.9	0.9
Horizontal radiating element spacing d/λ	-	-	-	-	0.6	0.6	0.6	0.5	0.5	0.5
Vertical 3dB bandwidth of single element / deg	65	65	65	65	65	65	65	65	65	65
Horizontal 3dB bandwidth of single element / deg	65	65	65	65	80	80	80	80	80	80
Losses of cable network / dB	0.5	0.8	1.0	1.2	0.8	1.0	1.2	0.8	1.0	1.2

Note: For single column AAS antenna, to calculate the gain of an active antenna the losses of the cable network must be added to the maximum gain.

AAS Max antenna gain = passive Max antenna gain + Losses of cable network

6 Study of AAS transmitter characteristics

6.1 General review of transmitter characteristics

General transmitter characteristics are discussed in the following sections to facilitate the feasibility study. Particularly, ACLR is studied in the present document as typical examples. Detailed considerations for each of the transmitter characteristics will be considered in the future.

6.2 Transmitter spatial characteristics

AAS experiences different spatial selectivity compared to the conventional BS. Due to the discrepancies among multiple Tx chains, the unwanted in-band/out-band emissions in general do not follow the beam forming as the wanted signal does. This leads to the RF performance of AAS BS, such as ACLR, EVM, varies with different directions in spatial domain.

6.3 Simulation results

6.3.1 ACLR

Adjacent Channel Leakage power Ratio (ACLR) is the ratio of the filtered mean power centred on the assigned channel frequency to the filtered mean power centred on an adjacent channel frequency.

System simulations were performed to evaluate the downlink average and 5% CDF throughput loss of the victim system while coexisting with the adjacent system by varying ACLR value at the antenna connector. Requirement definition point is FFS. For AAS, different correlation levels between transmitters were performed to evaluate the impact on the system performance degradation.

The detailed simulation results are present in Annex. B.

6.3.1.1 Observations

- 1. Cell average and 5% CDF throughput loss caused by aggressor AAS in Case 1a (AAS to Legacy) are consistent with that caused by legacy BS in Case 1c (Legacy to Legacy) with the same ACLR (per connector) assumption.
- 2. The impact of correlation level to the system coexistence is evaluated. Simulation results in Case 1a(AAS to Legacy) and Case 1b(AAS to AAS) show that different correlation levels have little impact on the throughput loss due to the fact that the dominant source of adjacent channel interference is due to UE ACS.
- 3. The impact of other down-tilt values (5/20 degrees) applied in aggressor system is also investigated to check how sensitive the co-existence is dependent on the down-tilt value. Simulation results in Case 1b indicate that generally the throughput impact is not sensitive to the amount of tilt in the aggressor system.
- 4. The impact of different down-tilt methods (electrical / mechanical) on the system coexistence is also evaluated. Simulation results in Case 1a~1c show that in most cases, the difference is small.

6.4 Requirements for AAS transmitters

The term "requirements in the far field" is used as example in this section to demonstrate feasibility of specifying radiated requirements. Requirements are said to be radiated if the requirements are set on the AAS BS system shown in figure 4.2-1, including the radiating elements.

6.4.1 Output power

In current 3GPP specifications, several different terms for the output power of the BTS are defined. All definitions are based on measuring the mean power at the antenna connector in the transmitter ON period. The test purpose is to verify the actual capability of the transmitter to feed an antenna and the accuracy of the maximum output power under normal and extreme conditions for all transmitters.

Two approaches have been considered for defining AAS Output power requirements.

6.4.1.1 Approach 1

Approach 1 is to define requirements at the boundary of the transceiver array that can be translated as test requirements at either the transceiver array boundary or in the far field.

Requirements for testing in the far field would be obtained by adding appropriate antenna array gain characteristics relating to the AAS under test to the transceiver array boundary requirement.

The accuracy of the maximum total output power shall be consistent with current 3GPP specification.

6.4.1.2 Approach 2

Approach 2 is to define requirements in the far field that can be translated as test requirements at either the transceiver array boundary or in the far field.

Requirements for testing at the transceiver array boundary would be obtained by subtracting appropriate antenna array gain characteristics relating to the AAS under test.

The definition of points in space at which the power requirements should be defined (e.g. in the main lobe, or around the whole base station) should be studied further and decided in the work item (WI).

The description of the requirements by Approach 1 would be similar to existing specifications; Approach 2 would require the requirements to be described in a different manner from existing specification. How to describe the requirements is actually the work of the WI stage.

6.4.1.3 Study Item conclusions on output power

The AAS Study Item came to the following conclusions on the way forward for defining the output power requirement in the work item:

- 1. Capture the two approaches in the Technical Report.
- 2. The output power requirements can be specified as EIRP at the far field. However, the requirements shall be specified in the way that the equivalent requirements can be translated at the boundary of the transceiver array.
 - The impacts imposed on the transceiver array and the antenna array by the requirements at either transceiver array or far field shall be the same.
- 3. The output power requirement can be specified at the transceiver array boundary. The requirements shall be specified in the way that the equivalent requirements can be translated at the far field.
- 4. Further details are within the scope of WI phase.

6.4.2 ACLR requirements

In the current UMTS and LTE specifications, ACLR is defined as the ratio of the filtered mean power centred on the assigned channel frequency to the filtered mean power centred on an adjacent channel frequency. This definition can be considered for AAS BS. However, the ACLR performance of the AAS BS observed in space varies with different directions. The definition of the reference point locations in space at which the assigned channel and adjacent channel power are specified needs further study in the work item phase.

For an AAS BS, simulation results indicated that for the specific scenarios studied, ACLR of 45dB per transceiver is sufficient to fulfil the co-existence studies as detailed in TR36.942 and TR25.942. These simulations estimate the mean and 5th percentile throughput impact, while future simulations may consider and study the impact of the spatial distribution of ACLR on the spatial distribution of throughput.

The ACLR requirements can potentially be defined either at the far field or at the transceiver array boundary. Preferably, the requirement definition point for ACLR should aim to be consistent with other AAS requirements. If the ACLR requirements for AAS BS are specified at one point or more points at the far field, how to equivalently translate between per transceiver ACLR requirements and the ACLR requirements at the far field should be within the scope of the work item phase.

7 Study of AAS receiver characteristics

7.1 General review of receiver characteristics

General receiver characteristics are discussed in the following sections to facilitate the feasibility study. Particularly, inband blocking is studied in the present document as typical examples. Detailed considerations for each of the receiver characteristics will be considered in the future.

7.2 Receiver spatial characteristics

AAS experiences different spatial selectivity compared to fixed beam antennas. In figure 7.2-1, a visualization of spatial selectivity loss in AAS is shown. The AAS system does not achieve full spatial selectivity until after digital baseband processing of the multiple elements in the array. Hence, an interfering UE close to antenna would pose higher interferer level towards a sub-array compared to full array antenna pattern.

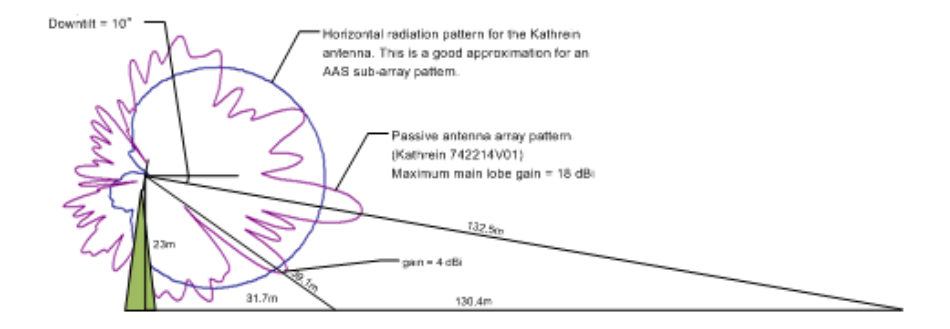


Figure 7.2-1 AAS Receiver Array Patterns

7.2.1 Element or Sub array characteristics

The effective power level of the interferer UE (or the composite power summation of multiple interferer UEs) is higher due to the lack of multi-element pattern. The close-in interferers do not experience antenna gain suppression as there is no array pattern yet. Instead, the interference signals experience the less selective pattern (more omni-directional) of the element or sub-array.

In addition the effective gain in the direction of the desired UE is lower until the spatial gain has been realized, again due to the lack of multi-element summation to/from the array pattern in the antenna. Instead the signal from the faraway desired UE experiences the same less selective pattern (low gain) pattern. Thus the desired signal appears lower in level to the front end stages.

7.2.2 AAS system characteristics

<reserved for future use>

7.3 Simulation results

7.3.1 In-band blocking

The in-band blocking characteristic is a measure of the receiver's ability to detect a wanted signal at its assigned channel in the presence of an unwanted interferer inside the operating band.

The methodology of defining BS in -band blocking requirements for UTRA and E-UTRA is described in TR25.942 and TR36.942, i.e. system simulations were performed to evaluate the CDF distribution of the received power. In these simulations the RX power has been measured at the antenna connector (via the connected antenna) from UEs within the systems at the adjacent channel, pending discussion on requirement definition points. The in-band blocking requirement shall be the power level that the BS may receive with very low probability, for example, 0.01% for Macro BS.

In this section the simulation results for in band blocking from different companies have been captured based on the simulation scenarios and assumptions described in Section 5.4.

7.3.1.1 Case 1a: Uplink E-UTRA AAS interferer- legacy system victim

Simulations are based on the following assumptions:

Aggressor system: 10 MHz E-UTRA with passive antenna system

Victim system: 10 MHz E-UTRA with AAS

Simulation frequency: 2000 MHz

Environment: Macro Cell, Urban Area, uncoordinated deployment

Cell Range 750 m

The blocking level measured at the antenna connector of AAS single radiation element from UEs within the adjacent legacy system is presented in table 7.3.1.1-1.

Table 7.3.1.1-1 Blocking level for a 99.99% probability for Case 1a

Down-tilt	Power Control	Huawei	ZTE	Ericsson
		R4-124174/R4-125469	R4-125244	R4-125431
Electrical down-tilt : 9 degrees	PC1	-44.92	-44.8	-43.3
	PC2	-54.69	-52.72	-53.7
Mechanical down-tilt: 9 degrees	PC1	-45.39	-46.13	-43.5
	PC2	-53.94	-57.85	-53.4

7.3.1.2 Case 1b: Uplink E-UTRA AAS interferer- AAS victim

Simulations are based on the following assumptions:

Aggressor system: 10 MHz E-UTRA with AAS

Victim system: 10 MHz E-UTRA with AAS

Simulation frequency: 2000 MHz

Environment: Macro Cell, Urban Area, uncoordinated deployment

Cell Range 750 m

The blocking level measured at the antenna connector of AAS single radiation element from UEs within adjacent AAS system is presented in table 7.3.1.2 -1.

Table 7.3.1.2-1 Blocking level for a 99.99% probability for Case 1b

Down-tilt	Power Control	Huawei	ZTE	Ericsson
		R4-124174/R4-125469	R4-125244	R4-125431
Electrical down-tilt: 9 degrees	PC1	-45.03	-45.12	-43.4
	PC2	-55.49	-52.82	-56.3
Mechanical down-tilt: 9 degrees	PC1	-46.18	-46.21	-42.4
	PC2	-54.74	-57.69	-54.2

7.3.1.3 Case 1c: Uplink E-UTRA legacy system interferer- legacy system victim

Simulations are based on the following assumptions:

Aggressor system: 10 MHz E-UTRA with passive antenna system

Victim system: 10 MHz E-UTRA with passive antenna system

Simulation frequency: 2000 MHz

Environment: Macro Cell, Urban Area, uncoordinated deployment

Cell Range 750 m

The blocking level measured at the antenna connector of legacy BS from UEs within adjacent legacy system is presented in table 7.3.1.3-1.

Table 7.3.1.3-1 Blocking level for a 99.99% probability for Case 1c

Down-tilt	Power Control	Huawei	ZTE	Ericsson
		R4-124174/R4-125469	R4-125244	R4-125431
Electrical down-tilt: 9 degrees	PC1	-46.6	-44.35	-41.6
	PC2	-55.89	-55.63	-55.4
Mechanical down-tilt: 9 degrees	PC1	-49.08	-41.79	-42.8
	PC2	-59.15	-53.69	-54.8

7.3.1.4 Discussion

Simulation results show that,

- 1. Comparing Case 1a and Case 1c, the blocking interference signals presented at the individual receivers relating to radiating elements of the AAS are within around 1-5dB of those at the receiver of a BS equipped with passive antenna for both mechanical and electrical tilt.
- 2. The blocking interference signal obtained from Case 1a is a little higher than that from Case 1b. The reason is the legacy BS with a passive antenna has a higher cable loss than the AAS, resulting in the transmit power of the UE's being higher and hence leading to a higher blocking level in the victim network.

Other scenarios, in particular involving different element beam-width properties or AAS dimensionality have not been studied.

7.4 Requirements for AAS receivers

The term "requirements in the far field" is used as example in this section to demonstrate feasibility of specifying radiated requirements. Requirements are said to be radiated if the requirements are set on the AAS BS system shown in figure 4.2-1, including the radiating elements.

7.4.1 Requirement Reference Point

The requirement reference point is the point at which a core RF requirement is specified. Tests are defined at test requirement point(s), and the criteria for passing the test which verify the core RF requirements are test requirements. Test requirements are derived from the core RF requirements set at the requirement reference points.

7.4.2 Reference sensitivity

There are two approaches to define the reference sensitivity level requirements.

7.4.2.1 Approach 1

Approach 1 is to define the requirements at the boundary of the transceiver array such that they can be translated as test requirements at either the transceiver array boundary or at the far field.

The transceiver array boundary requirement may be derived taking into account the noise figure achievable in AAS transceivers and considering the difference in gain between AAS antenna systems and legacy antenna systems in order to achieve as a minimum requirement similar coverage to legacy base stations.

The Work Item would need to further consider whether to trade off noise figure and coverage when higher AAS array gains are available. Trading the noise figure for option 1 would require setting multiple requirements.

Requirements for OTA tests would be derived by adding the known gain of the AAS under test to the core requirement.

7.4.2.2 Approach 2

Approach 2 is to define the requirements AAS in the far field such that they can be translated to test requirements either in the far field or at the transceiver array boundary.

When setting the minimum far field requirement the achievable noise figure in AAS transceivers and the coverage achievable in legacy systems may be taken into account.

AAS systems with different levels of AAS array gain would not change a core requirement defined in far field. A large AAS gain could be used to either exceed the minimum requirement or to accept a higher noise figure in the individual transceivers.

Transceiver array boundary tests for far field requirements would be derived by subtracting the array gain of the specific AAS under test.

The question of whether to trade off noise figure and coverage when higher AAS antenna array gains are available is also applicable to approach 2 and pending further investigation in the WI phase.

7.4.2.3 Study Item conclusions on reference sensitivity

The AAS Study Item came to the following conclusions on the way forward for defining the reference sensitivity requirement in the work item:

- 1. The reference sensitivity level requirements can be specified to meet the throughput requirements by receiving a wanted signal at the far field or at the transceiver array boundary. However, this reference sensitivity level requirements shall be specified in the way that the equivalent requirements can be translated for conformance test
 - The impacts imposed on the transceiver array and the antenna array by the requirements at either transceiver array or far field shall be the same.
- 2. Whether or not to trade off between the noise figure and antenna gain are within the scope of the work item.
- 3. Further details are within the scope of WI phase.

Editor Note: Reference sensitivity refers to the minimum RX signal level that can be detected and relates to receiver internal noise. Receiver noise will not add coherently when combined in the baseband, whereas an applied signal will. Thus the applied signal to receiver noise level will differ between the individual transceivers and the combined signal, and the SNR for the combined signal will be modified by the spatial processing. The term "sub array reference sensitivity" refers to the reference sensitivity defined at sub array level prior to RDN combining, and "system reference sensitivity" to the reference sensitivity defined after baseband combining.

7.4.3 In-band blocking

The receiver in-band blocking requirement for BS with AAS is defined to protect against high mean power level of the interferers or blocker signals. A different interferer level could potentially arise in AAS systems compared to legacy systems as a result of the difference in antenna gain between an antenna array and a single element or sub-array of an antenna array.

The in-band blocking power level is obtained by system level simulation based on un-coordinated deployment, and the in-band blocking level is the 99.99% level of the CDF of the total received power at the transceiver input. Contributors to this power level include multiple UEs which are distributed at multiple locations.

Preliminary simulation results for a single column AAS system observed that the blocking power level for each individual receiver channel of the AAS system was similar to the in-band blocking level for a legacy BS installed with an assumed typical reference passive antenna array. Final determination will be completed in the WI phase.

The in-band blocking requirements can be specified at either the transceiver array boundary or in the far field.

The details as to how to implement the RF requirements in the core and testing specifications will be completed in the WI phase.

8 AAS test aspects

The purpose of testing is to verify the requirements for AAS transmitter(s) and receiver(s). This section captures the study results on the testing of AAS BS.

There could be multiple measurement setups capable of testing AAS BS, such as Conducted Test, Over-the-Air Test, Coupling Test, Combined Test, and etc. Some of the measurement setups were studied and the key aspects are introduced in this section.

In case a BS design does not support access to the antenna connectors for conductive tests, radiated tests can be the alternative. Use of more than one measurement setup is not precluded if the same level of measurement accuracy and compliance can be ensured. In this case, using the radiated measurement setup to test BS with access to antenna connectors could also be possible.

In existing BS test specifications for core requirement verification, such as TS36.141, the measurement setup is specified in the Annex part in informative clauses. For a BS with AAS, the measurement setups will also be specified as informative clause, such as one for AAS with access to antenna connector(s), and the others for AAS without accessibility of antenna connector(s).

8.1 Comparison of different test methods

Methodologies under consideration for AAS testing are presented in 8.1.2. Each methodology has strengths and weaknesses which are considered in developing compliance tests.

Test methodologies are compared on multiple criteria:

- Completeness. A methodology is considered complete if it can provide sufficient data to demonstrate compliance.
- Accuracy. The methodologies must provide results that correctly characterize the performance of the equipment
 under test. Methodologies that require extensive calibration or numerous calibration factors are sensitive to
 systematic error.
- Measurement Equipment Capabilities. The methodologies must be possible to implement with commonly available test equipment. Sufficient margin must exist between the test equipment noise floor or other test equipment limitations and the characteristic in question. Results recorded near the limits of the equipment capabilities tend to have poor accuracy.
- Repeatability. Repeatability is a measure of the ability of a methodology to produce the same measurement results for multiple test iterations conducted by multiple test operators at multiple test sites. Methodologies that are very sensitive to calibration or subtle changes in the test environment are associated with questionable repeatability.
- Cost-effectiveness. Given sufficient resources, any of the test methodologies could conceivably be demonstrated to
 produce acceptable results. However, some methodologies require significant effort and test discipline (and thus
 expense) to produce results with the required accuracy and place extensive demands upon test facilities. Reasonable
 compromises must be considered where the cost of producing acceptable results with a more complicated
 methodology is prohibitive.
- Implementation neutrality. The methodology should not place constraints on implementations. Requirements for test ports and test fixtures should be minimized.

8.2 AAS test methodologies

Several test methodologies have been proposed during the discussion. In this sub-clause the potential test methodologies for AAS testing are documented to facilitate the further study.

8.2.1 Conducted Test

Conducted testing is performed via ohmic contact at the antenna connector(s). Each transceiver can be tested independently or multiple transceivers can be combined through passive combiners and tested simultaneously.

Independent characterization of individual transceivers follows the existing 3GPP practice of specifying requirements at the antenna connector. Such testing requires no new procedures. Comparison of AAS conducted requirements to existing 3GPP requirements is a straightforward process of adjusting existing requirements by the gains and losses associated with the antenna array configuration.

Spatial performance of the combined transceiver and antenna array may be extrapolated from independent conducted test results, but the procedure is not straightforward and requires assumptions regarding coherent vs. non-coherent combining of differing signal types and assumptions about the uniformity of gain between the array elements. As such, conducted tests have limited value in characterizing spatial performance.

Spatial characteristics can be simulated by connecting multiple transceivers to test equipment though passive combiners and adjusting phase and attenuation for each path. TS 36.104 and TS 36.141 illustrate such testing. However, the necessary phase and attenuation adjustments require detailed knowledge of the AAS architecture under test to accurately simulate spatial characteristics. The combining apparatus induces additional loss and phase uncertainties, which may challenge the dynamic range and noise floor of test equipment. Hence, the ability of passive combiner tests to characterize spatial performance with sufficient accuracy is FFS.

The FCC has stated [11][12] that test results for multiple-antenna transmitter emissions that are based on measurements of combined signals are not acceptable for FCC type certification. The FCC allows test results to be derived by measuring individual transceivers and combined in a worst-case fashion.

A practical limitation of both independent and combined testing methodologies is that antenna connectors in an AAS may be optimized for connection to the antenna radiator elements. This may render the connectors incompatible with commercially available test equipment.

8.2.1.1 Combiner and Splitter Approach

As an example of a conducted test, the combiner approach for the transmitter test combines the antenna array elements output into a single BS transmit output connector where tests can be performed. Similarly, a splitter approach is used for the receiver conducted tests. An illustration of conducted tests for an $M \times N$ Antenna Array using the Combiner and Splitter approach for the transmitter and receiver tests is shown in Figure 8.2.1.1-1 and Figure 8.2.1.1-2, respectively.

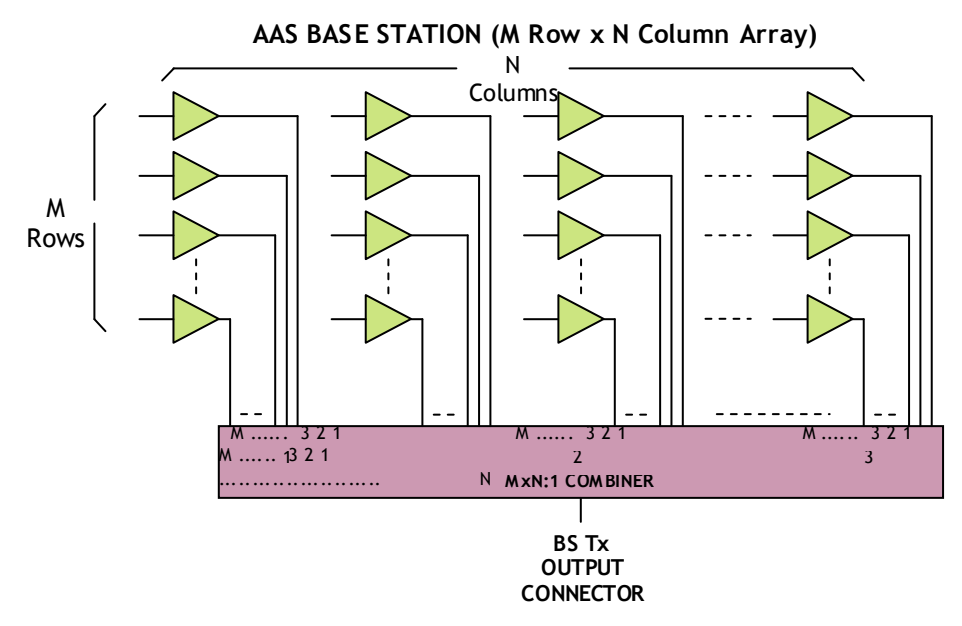


Figure 8.2.1.1-1: Combiner Approach -Transmitter test set-up for BS with AAS

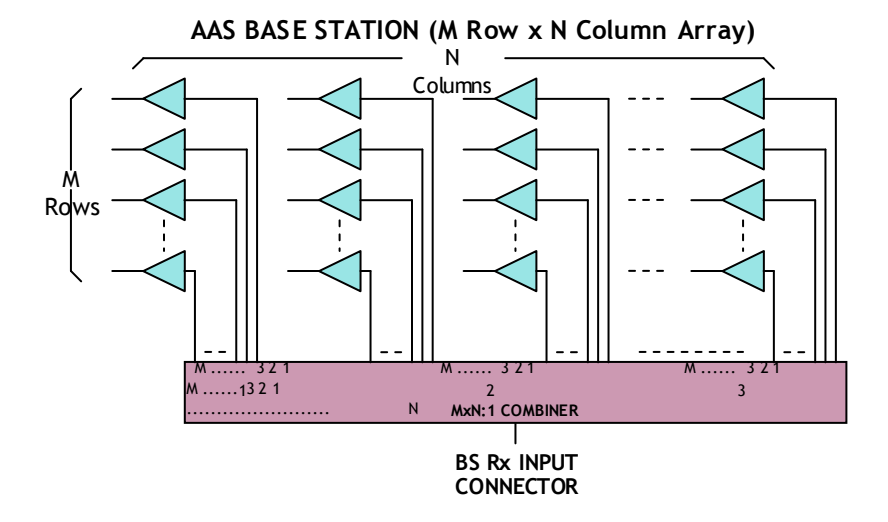


Figure 8.2.1.1-2: Splitter Approach - Receiver test set-up for BS with AAS

8.2.2 Far Field Over-the-Air Test

Far Field Over-the-Air (OTA) testing is performed in an anechoic chamber or some other far-field test facility (e.g. outdoor open field). In OTA test data would be collected at required angle(s) which details are FFS.

OTA testing offers the potential to provide a complete spatial characterization of an antenna system and the far field behaviours (e.g. EIRP and EIRS). In principle, it is similar to open-field testing which is frequently required by regulatory agencies for equipment type certification. Although specific OTA procedures are FFS, the test steps should at least include calibration and requirements tests. Great care must be taken with the calibration of such sites (in addition to test equipment calibration) to obtain repeatable and stable results and to avoid perturbations to the AAS system characteristics. To reduce the potential test costs the exact characteristics tested with far field OTA should be carefully studied and chosen.

All existing 3GPP requirements are stated in terms that correspond to conducted tests. Developing corresponding tests for radiated tests in three dimensions would require the development of new test procedures. It also requires a corresponding translation between the current requirements and equivalent three dimensional OTA requirements. As the requirement reference point in sub-clause 6.4.1 is not decided yet, the process for translating between current measurements to OTA requirements is FFS.

8.2.3 Coupling Test

Coupling tests are close-field tests conducted by arranging an array of field strength probes in a fixture which aligns the probes with the radiators of the AAS. Figure 8.2.3-1 is an illustration of the Coupling Test concept.

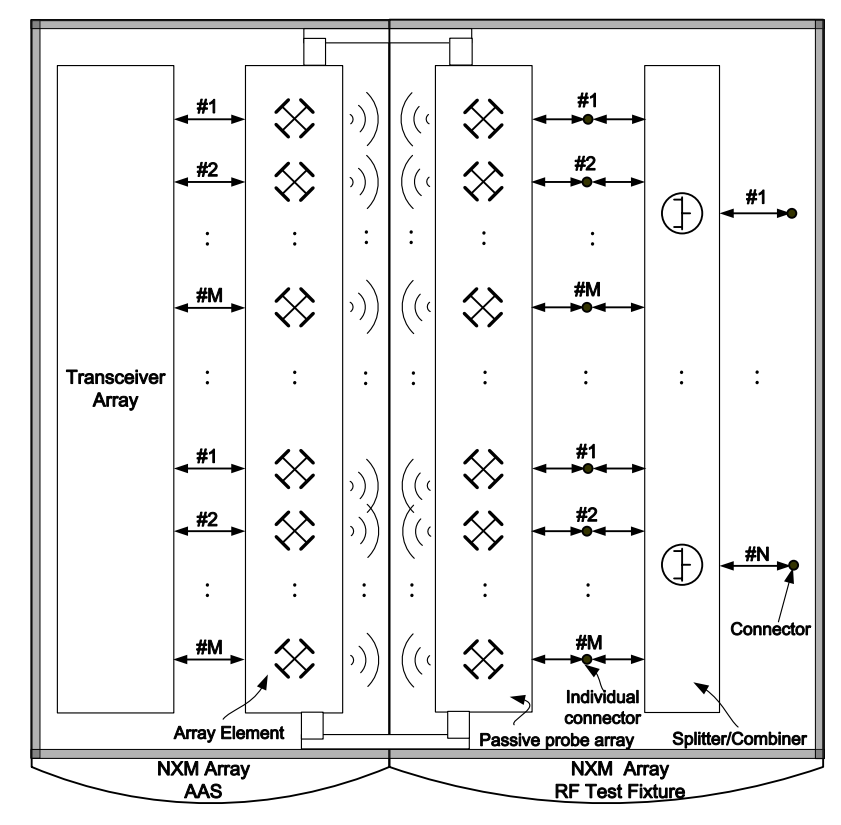


Figure 8.2.3-1 Coupling Test Diagram

From Figure 8.2.3-1, the RF test fixture consists of a passive RF distribution splitter/combiner and a passive probe array. The splitter/combiner conducts the RF signal to individual probe ports (i.e. RF connectors) and combines the RF signal from each individual probe port. The number of probes in the test fixture is not necessarily equal to the number of radiators in the AAS

Far-field performance can be estimated from close-field measurements using calculations derived from electro magnetic theory. The calculations are very sensitive to the precision and accuracy of the close-field measurements, and simplifying assumptions are required to manage the complexity of the calculations. The required degree of accuracy and adequate estimation formulas are FFS. Though the details are FFS, the test should at least include two steps: calibration and measurement.

This form of testing provides a single connection point for testing the receiver and transmitter sections of the AAS. It avoids the need for direct connection to the AAS transceiver but requires the design of a custom close passive coupler device. The fixture must be accurately aligned to the AAS enclosure to ensure repeatable measurements with required accuracy.

The Coupling test method also presents challenges to the test equipment. The close-field coupler should allow testing over the entire frequency range covered by the Technical Standards (i.e., 9 kHz to 12.75/19 GHz for spectral emissions, even if only CATA/CATB requirements apply). The setup should support all applicable UTRA and E-UTRA bands for collocation and coexistence measurements. The electrical characteristics of the close-field probe should be characterized very accurately over this entire frequency band so that the probe response can be de-embedded from the measurements.

8.2.4 Combined Test

8.2.4.1 Combined Conducted and Over-the-Air Test

In this section, the combined use of Conducted and Over-the-Air test approaches is described. It consists of first using the Over-the-Air test (OTA) methodology, as described in Section 8.2.2 to measure and quantify some aspect of the antenna performance followed by a Conducted test of the transceiver.

In the first step, antenna performance obtained during the validation phase where measurements using OTA can be employed e.g. the difference in antenna gains between the single element antenna and the complete passive array antenna over a range of azimuth and elevation angles, which are measured using OTA test. The results of these measurements are then processed to be applied towards the second step where Conducted tests, as described in Section 8.2.1 can be employed.

A Combined Test approach can be illustrated below in Figure 8.2.4.1-1.

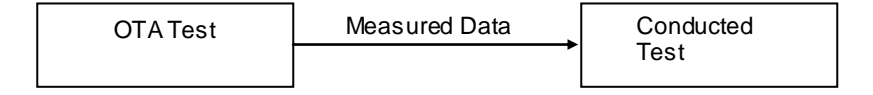


Figure 8.2.4.1-1: Combined Conducted-OTA Test

The details of processing in the two steps are to be defined later for the specific RF requirement.

8.2.4.2 Combined Close Field Coupling and Over-the-Air Test

In this section, the combined use of closed field coupling and Over-the-Air test approaches is described. It consists of first using the Over-the-Air Test methodology to measure and quantify some aspect of the antenna performance followed by a Conducted test of the transceiver array.

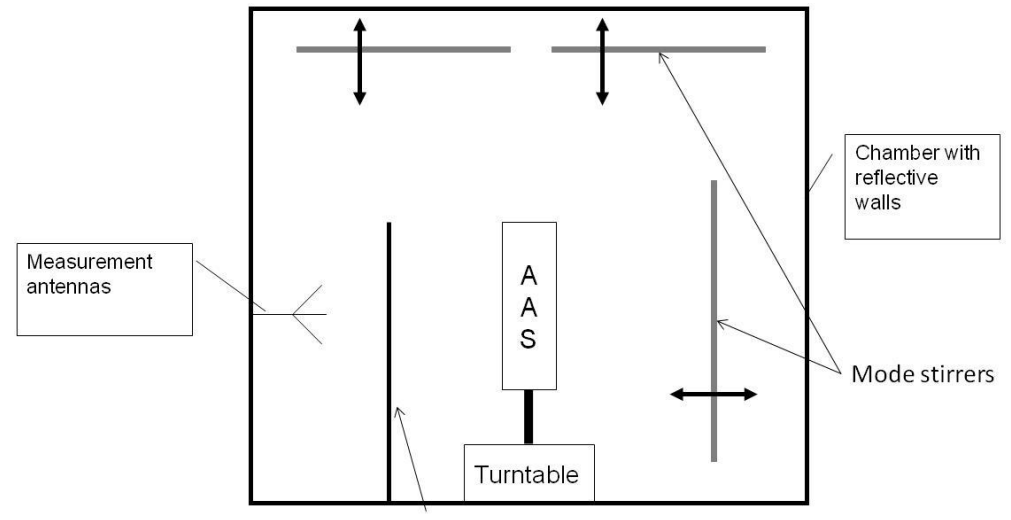
In the first step, antenna performance is obtained by OTA testing and the measurements are then processed to be applied towards the second step. In the second step, coupling test is employed to achieve RF requirements.

The test details are to be defined later.

8.2.5 Rayleigh Faded Multi-path Over-the-Air test

Rayleigh faded multi-path Over-the-Air test requires a reverberation chamber. Inside the chamber the mode stirrers and the reflecting metal walls generate a Rayleigh fading environment. The measurement antennas, or the AAS antennas if for receiver measurements collect the power representing the average from all directions if the measurement time is long enough. The Rayleigh faded multi-path Over-the-Air test is not capable of capturing the spatial effects of an AAS. The method gives Total Radiated Power (TRP) and Total Received Sensitivity (TRS) measured of the whole sphere.

Introducing absorption material in the reverberation chamber to change the propagation modes is also possible for particular measurements. The detailed test methods are FFS.



Reflector or absorber to remove/attenuate LOS signal

Figure 8.2.5-1 Rayleigh Faded Multi-path Over-the-Air test Diagram

8.2.6 Near-Field Probe Scanner Test

The physical dimensions of a test range can be reduced by adopting near-field probe scanner measurement method, where the near-field is measured in certain position by a measurement probe mounted in a mechanical scanner. Applying analytical methods the measured near-field can be converted to far-field radiation characteristics, such as gain patterns. The near-field measured data (amplitude and phase) is acquired by using a probe to scan field close to the radiating element. The position of the probe is characterized by coordinates (x, y, z_0) in the xyz-coordinate system of the antenna under test (AUT). During the scanning, z_0 is kept constant, while x and y are varied. The dimensions of the near-filed scanning aperture must be large enough to accept all significant energy radiated from the AUT. The measured

near-field data $E(x,y,z_0)$ is transformed into a plane wave spectrum, by a two-dimensional Fourier transform resulting in a far-field pattern. The probe response is de-convoluted from the AUT angular response.

For certain BS antenna configurations it may be better to utilize cylindrical or spherical scanning techniques where the near-field is probed on a cylindrical or spherical surface instead of a plane surface. In the cylindrical scanning technique, the AUT is rotated around the z-axis of a xyz-coordinate system in $\Delta \varphi$ steps, while the probe is moved on the cylindrical surface at various heights relative to the xy-plane in Δz steps. The probe is located at a distance, which is the smallest cylinder radius enclosing the AUT. The cylindrical scanning enables obtaining the exact azimuth pattern but limited elevation pattern due to the truncation of the scanning aperture in z direction. The cylindrical scanning technique is suitable for BS antenna measurements since it will capture the wide beam characteristics in the azimuth plane well and also capture the narrow beam characteristics in the vertical plane.

The accuracy of the near-field measurement is determined by: RF reflections, mechanical errors, truncations errors and system errors. A near field range is suitable for placement in a shielded chamber with absorption material on the inside minimizing reflections and RF interference.

This method is commercially accepted for BS antenna testing in transmission mode. The feasibility for testing BS antennas in reception mode is FFS.

9 Conclusions

The main purpose of the study item is to study the necessity and feasibility of specifying the necessary requirements for AAS BS.

The study resulted in the following findings:

- An examination of relevant international regulations revealed little guidance regarding the specifications that are explicitly applicable to AAS.
- An analysis of AAS RF transmission observes that undesired emissions from different transmitters will not be perfectly correlated. The uncorrelated parts of the undesired emissions will not be radiated in the same pattern as emissions which are correlated between different transmitters. This effect was studied in simulations of the spatial distribution of the Adjacent Channel Leakage Ratio (ACLR). Simulation results indicated that for the specific scenarios (an application with fixed beam pattern by a single column AAS) studied, ACLR of 45dB per transceiver is sufficient to fulfil the co-existence studies as detailed in TR36.942 and TR25.942. These simulations estimate the mean and 5th percentile throughput impact, while future simulations may consider and study the impact of the spatial distribution of ACLR on the spatial distribution of throughput.
- As an example of receiver impacts, the in-band blocking was simulated and analyzed for AAS BS. The results of a single column AAS model observed that the power level presented for each individual receiver of an AAS system was similar to the in-band blocking power level presented to a conventional BS receiver as a result of the difference in antenna gain and directivity between an antenna array and a single element or sub-array of the AAS antenna array.
- Existing RF requirements (in which some of the requirements are derived based the reference antennas) may be inadequate to ensure coexistence for unique AAS applications which may be difficult or impossible to support by conventional base stations. Examples of such applications include beam steering in elevation, azimuth or combinations of both.
- Two potential approaches for reference point definition were identified for requirements. Requirements should be specified at only one reference point. The SI did not reach consensus on the default reference point.
- The point of testing may differ from the requirement reference point; one example is a requirement may be specified in the far field but tested at the transceiver array boundary with an appropriate transformation, and vice versa.

Based on the above findings, the study item concluded that it is necessary and feasible to specify the requirements for AAS BS. The following topics shall be studied and evaluated for the purpose of developing the future AAS requirements

- Elaboration of the transformation from the requirement point to the test point.
- Spatial effects of multiple-column AAS BS on coexistence performance.
- Spatial variation of other RF characteristics which may be impacted by antenna characteristics. It may be necessary to evaluate these characteristics on a requirement by requirement basis.

- Development of application independent core requirements which ensure co-existence in generic applications. It may be necessary to evaluate detailed approaches on a requirement by requirement basis.
- Development of multiple testing approaches (e.g., far field, near field, and conductive testing at transceiver array boundary) to support AAS implementations with access to the transceiver array boundary, as well as AAS implementations without access to the transceiver array boundary.

Annex A: (Informative) Study Item plan and progress

A.1 The Study Item plan

The work plan for the present Study Item is below:

By end of RAN4 # 62bis (Mar 2012), to complete the study of the following aspects:

Study of AAS classifications

Study of AAS definitions and terminologies

By end of RAN4 # 65 (Nov 2012), to complete the following aspects:

Study of AAS transmitter characteristics (RF and/or EMC)

Study of AAS Receiver characteristics (RF and/or EMC)

Study of AAS test aspects

Capture the study results in clause 6, clause 7, and clause 8 in the present document.

Technical Report to be presented in RANP # 58 (Dec 2012) for information.

By end of RAN4 #66 (Jan 2013), to complete the following aspects:

Concluding the SI by completing the conclusion part (clause 9) in the present document.

Technical Report to be presented in RANP # 59 (Mar 2013) for approval.

A.2 The Study Item progress

RAN Plenary #54 Completion level 8%

RAN Plenary #55 Completion level 20%

RAN Plenary #56 Completion level 55%

RAN Plenary #57 Completion level 65%

RAN Plenary #58 Completion level 90%

A.3 The list of contributions

RAN4 #59, Barcelona, Spain, 9-13 May, 2011

R4-112779, Deployment Scenarios and RF Requirements for Base Station Systems, Huawei

RAN Plenary #52, Bratislava, Slovakia, May 31-June 3, 2011

RP-110858, RF Requirements for Active Antenna Array System (AAS) Base Station, Huawei

RAN4 #59 adhoc, Bucharest, Romania, June 27th – July 1st, 2011

R4-113380, Considerations for BS AAS Requirements, Alcatel-Lucent

R4-113423, Discussion of RF requirements for AAS BS, Huawei

R4-113594, BS antenna array aspects, Ericsson

RAN Plenary #53, Fukuoka, Japan, Sept 13-Sept 16, 2011, SI approved

RP-111349, Study of RF and EMC Requirements for Active Antenna Array System (AAS) Base Station, Huawei

RAN4 #60, Zhuhai, China, 10 Oct - 14 Oct, 2011

- R4-115008, Discussion on AAS spurious emission, Huawei
- R4-115009, Consideration of the framework for AAS study, Huawei
- R4-115010, Further considerations of AAS transmitter characteristics, Huawei
- R4-115011, Work plan for AAS study item, Huawei
- R4-115012, Possible application scenarios of AAS, Huawei
- R4-115176, On requirements for Active Antenna Array base-station, Ericsson
- R4-115177, On Reference point for requirements and test for AAS, Ericsson
- R4-115270, BS AAS Requirements & Specification Options, Alcatel-Lucent
- R4-115272, BS AAS: Preliminary List of Specifications Coverage, Alcatel-Lucent
- R4-115330, AAS Taxonomy, Nokia Siemens Networks
- R4-115457, Work plan for AAS study item, Huawei
- R4-115458, Consideration of the framework for AAS study, Huawei

RAN4 #61, San Francisco, CA, Nov. 14-18, 2011

- R4-115575, Considerations of system coexistence simulation for AAS, ZTE
- R4-115663, BS AAS Radio Architecture, Alcatel-Lucent
- R4-115667, BS AAS Acronym and Definition, Alcatel-Lucent
- R4-115987, Scope of AAS study item, NTT DOCOMO
- R4-116004, On need and feasibility of OTA test in AAS, Ericsson
- R4-116006, On spatial domain impact on receiver in AAS, Ericsson
- R4-116008, On the spatial domain in AAS and current specification, Ericsson
- R4-116010, On the scope for the AAS work, Ericsson
- R4-116011, Terminology and definitions for AAS, Erics son
- R4-116012, Overview of international regulation related to AAS, Ericsson
- R4-116015, TR ver 0.0.1 for AAS SI, Huawei (Rapporteur)
- R4-116073, Proposed text for the scope of the AAS technical report, Nokia Siemens Networks
- R4-116075, AAS nomenclature, Nokia Siemens Networks
- R4-116078, Baseline AAS deployment scenarios, Nokia Siemens Networks
- R4-116282, Harmonized AAS Nomenclature, Nokia Siemens Networks
- R4-116290, TP for Overview of international regulation related to AAS, Ericsson
- R4-116332, TP on BS AAS Radio Architecture, Alcatel Lucent

RAN Plenary #54, Berlin, Germany, Dec. 6-9, 2011

RP-111546, Status report for SI Study of RF and EMC Requirements for Active Antenna Array System (AAS) Base Station, Huawei

RAN4 #62, Dres don, Germany, Feb. 06-10, 2012

- R4-120051, Survey of AAS test options, Nokia Siemens Networks
- R4-120061, Initial simulation results for AAS blocking, ZTE
- R4-120062, Some antenna terminologies about AAS, ZTE
- R4-120063, Text proposal for simulation assumptions for AAS, ZTE
- R4-120064, Discussion on feasibility and necessity of OTA far field testing for AAS, ZTE
- R4-120185, TP subclause 3.1 and 3.2 Definitions and Abbr, Huawei
- R4-120189, TP subclause 4.2 reference structure, Huawei
- R4-120194, TP subclause 5.1 Applications, Huawei
- R4-120195, TP subclause 5.2 Deployment scenarios, Huawei
- R4-120196, TP subclause 5.3 Classifications, Huawei
- R4-120199, TP subclause 6.1 General review of the transmitter characteristic, Huawei
- R4-120200, TP subclause 6.2 The transmitter spatial characteristics, Huawei
- R4-120203, TP subclause 7.1: General review of receiver characteristics, Huawei
- R4-120210, TP subclause Annex A: The SI progress and work plan, Huawei
- R4-120215, Further consideration of AAS study, Huawei
- R4-120329, BS AAS Requirements and Tests, Alcatel-Lucent
- R4-120330, BS AAS Definition and Reference Points, Alcatel-Lucent
- R4-120487, On spatial distribution aspects of receiver performance requirements, Ericsson

- R4-120608, Application scenarios for AAS, Ericsson
- R4-120610, On spatial domain properties of the transmitter in AAS, Ericsson
- R4-120614, On AAS specification base-line, Ericsson
- R4-120674, AAS spatial aspects, Nokia Siemens Networks
- R4-120905, Spatial do main impact on AAS specification work, Ericsson
- R4-120908, Antenna Model for Active Antenna Array Systems, Kathrein
- R4-120987, Way forward for AAS study, Huawei
- R4-120988, TP for Overview of international regulation related to AAS, Ericsson, Huawei, NTT DOCOMO
- R4-120990, Radio Reference Architecture for BS with AAS, Alcatel-Lucent, Huawei
- R4-120992, TP subclause 4.1 SI Objective and methodologies, Huawei
- R4-120993, TP subclause 6.1 General review of the transmitter characteristic, Huawei
- R4-121094, Harmonized AAS Nomenclature, Nokia Siemens Networks, Huawei, ALU, ZTE

RAN Plenary #55, Xiamen, China, Feb. 28- Mar. 02, 2012

RP-120158, Status report for SI Study of RF and EMC Requirements for Active Antenna Array System (AAS) Base Station, Huawei

RAN4 #62bis, Jeju, Korea, Mar. 26-30, 2012

- R4-121200, TP for updating AAS definitions and abbreviations in 37.840, Ericsson
- R4-121201, OTA measurement of AAS unwanted emission, Ericsson
- R4-121212, Text Proposal for AAS Definition, Alcatel-Lucent
- R4-121213, Text Proposal for Combiner Approach, Alcatel-Lucent
- R4-121214, Further Considerations to the Combiner Approach, Alcatel-Lucent
- R4-121215, Active Antenna Modeling, Alcatel-Lucent
- R4-121216, A combined Conducted and OTA Approach, Alcatel-Lucent
- R4-121335, Text proposal for simulation objective for AAS, ZTE, Nokia Siemens Networks
- R4-121336, Text proposal for comparison of different test methods for AAS, ZTE
- R4-121337, OTA test methodologies for AAS, ZTE
- R4-121498, Baseline test methodologies with consideration of future OTA possibility, NTT DOCOMO
- R4-121623, Consideration of simulation for AAS study, Huawei
- R4-121624, TP for simulation assumptions for AAS, Huawei
- R4-121625, TR37.840 for AAS SI ver 010, Huawei
- R4-121626, Further considerations of the methologies for AAS study, Huawei
- R4-121627, TP for TR37840 AAS applications and coexistence scenarios, Huawei
- R4-121628, TP for AAS tests aspects, Huawei
- R4-121644, Multi carrier transmitter spatial do main impact, Ericsson
- R4-121647, AAS Reference Structure Update, Ericsson
- R4-121650, AAS Structure examples, Ericsson
- R4-121653, On AAS impacts to demodulation performance testing, Ericsson
- R4-121667, Demodulation performance testing, Ericsson
- R4-121835, Modeling Active Antennas, Kathrein
- R4-121917, On applications to be covered in AAS SI, Ericsson
- R4-121918, AAS applications, Erics son
- R4-121919, On parameterization of reference structure, Ericsson
- R4-121920, On AAS BS classification and output power definition, Ericsson
- R4-121921, On AAS co-existence scenarios, Ericsson
- R4-122100, AAS applications, Ericsson
- R4-122101, TP for TR37840 AAS applications and coexistence scenarios, Huawei
- R4-122102, Way forward of AAS study, Huawei, NTT DoCoMo, ALU, NSN, Ericsson, ZTE
- R4-122103, Text proposal for simulation objective for AAS, ZTE, Nokia Siemens Networks
- R4-122104, TP for simulation assumptions for AAS, Huawei
- R4-122195, Text proposal for comparison of different test methods for AAS, ZTE
- R4-122196, AAS Adhoc meeting minutes, Huawei
- R4-122197, Text Proposal for AAS Definition, Alcatel-Lucent
- R4-122198, AAS Reference Structure Update, Ericsson
- R4-122224, AAS Adhoc meeting minutes, Huawei

RAN4 #63, Prague, Czech Republic, May. 21-25, 2012

R4-122355 Extension of the new antenna model to a 2D antenna array, Kathrein R4-122378 Antenna tilt angle considerations, Nokia Siemens Networks R4-122379 Spatial aspects of passive antenna arrays, Nokia Siemens Networks R4-122380 AAS study item goals and outputs, Nokia Siemens Networks R4-122395 Discussion on modeling AAS antenna pattern, ZTE R4-122397 Text proposal for simulation assumptions for AAS, ZTE R4-122398 Discussion for ACLR requirements, ZTE R4-122399 Discussion for blocking requirements, ZTE R4-122400 Discussion for antenna requirements in AAS BS, ZTE R4-122402 Text proposal for comparison of different test methods for AAS, ZTE, Nokia Siemens Networks R4-122525 TR 37.840 ver 0.2.0, Huawei R4-122526 Corrections on TR 37.840 ver 0.2.0, Huawei R4-122529 Minimum coupling loss of AAS, Huawei R4-122530 TP on simulation assumptions for AAS studying, Huawei R4-122531 On AAS antenna modelling, Huawei R4-122533 Simulation results of in-band blocking for AAS receiver, Huawei R4-122534 Modeling of AAS transmitters spatail characteristics, Huawei R4-122536 On the RF requirements for AAS receiver, Huawei R4-122538 Lab results of the AAS transmitter spatial characteristics, R4-122543 On spatial ACLR of AAS, Huawei R4-122960 Text Proposal on AAS demodulation performance, Ericsson R4-122963 Text proposal on AAS areas to Study, Ericsson R4-122966 TP on AAS Scenarios, Ericsson R4-122968 TP on transmitter spatial domain aspects, Ericsson R4-122970 TP on receiver spatial do main aspects, Erics son R4-123004 Text proposal: Collection of AAS RF performance test methods, Ericsson R4-123010 AAS spatial performance simulation results, Ericsson R4-123011 AAS spatial performance simulation results, Ericsson R4-123072 Deployment Scenarios and Assumptions, Alcatel-Lucent R4-123077 Antenna Model for AAS, Alcatel-Lucent R4-123079 AAS RF Requirements, Alcatel-Lucent R4-123081 Further Considerations of Combined Conducted-OTA Approach, Alcatel-Lucent R4-123084 Text Proposal for Testing Methodologies, Alcatel-Lucent R4-123085 AAS example applications, Ericsson R4-123086 Example of reference structure parameterization, Ericsson R4-123092 Text Proposal for Combined Conducted-OTA Approach, Alcatel-Lucent R4-123368 On co-existence study of AAS, NTT DOCOMO R4-123518 AAS Adhoc meeting minutes, Huawei R4-123519 Way Forward on AAS Tx ACLR Requirement, Alcatel Lucent, NTT DOCOMO, Huawei R4-123521 AAS antenna modelling Way Forward, Huawei, Ericsson, Kathrein, Alcatel-Lucent, Alcatel-Lucent

RAN Plenary #56, Ljubljana, Slovenia, June 13 - 15, 2012

RP-120581 Status report for SI Study of RF and EMC Requirements for Active Antenna Array System (AAS) Base Station, Huawei

RAN4 #64, Qing dao, China, August. 13-17, 2012

Shanghai Bell, Nokia Siemens Networks

R4-123805	On ACLR requirement for BS with AAS, NTT DOCOMO
R4-123925	Discussion for composite radiation pattern of AAS, ZTE
R4-123926	Discussion for ACLR requirements, ZTE
R4-123957	Methodologies of Far field OTA test and Close field coupling test for AAS, ZTE
R4-123960	Text proposal for comparison of different test methods for AAS, ZTE
R4-124007	Antenna Tilt Considerations, Nokia Siemens Networks
R4-124033	TP on antenna model, Ericsson
R4-124034	TP on receiver spatial do main aspects, Ericsson
R4-124035	TP on AAS far-field characteristics for large tilt angles, Ericsson
R4-124036	TP on simulation parameter assumptions, Ericsson
R4-124041	TP on placing together AAS RF performance test methods, Ericsson
R4-124042	Impact of Coupling between Sub-Arrays, Ericsson

R4-124045	Spatial Modelling for BS with AAS, Alcatel-Lucent
R4-124046	ACLR Considerations, Alcatel-Lucent
R4-124047	Further Considerations of Combined Conducted-OTA Approach, Alcatel-Lucent
R4-124048	Receive Blocking Requirements: Simulation Results, Alcatel-Lucent
R4-124049	RF Requirements: Receive Blocking, Alcatel-Lucent
R4-124050	Spurious Emissions Requirements for AAS, Alcatel-Lucent
R4-124051	Text Proposal for Combined Conducted-OTA, Approach Alcatel-Lucent
R4-124053	Text Proposal for Testing Methodologies, Alcatel-Lucent
R4-124054	Text Proposal: Receive Blocking, Alcatel-Lucent
R4-124169	Text Proposal: 3D coexistence scenarios and simulation assumptions, Huawei
R4-124170	Text Proposal: 3D antenna modelling, Huawei
R4-124171	Discussion on BS down-tilt angle, Huawei
R4-124172	Simulation results for AAS spatial ACLR, Huawei
R4-124174	Simulation results: AAS in-band blocking, Huawei
R4-124175	Text Proposal: AAS receiver characteristics, Huawei
R4-124176	On AAS spatial EVM, Huawei
R4-124179	On AAS applications, Huawei
R4-124180	On the remaining work of AAS SI, Huawei
R4-124221	Close field coupling test methodology for the RF parameters of AAS, ZTE
R4-124222	Far field OTA test methodology for the spacial performance of AAS, ZTE
R4-124406	TP on AAS Scenarios, Ericsson
R4-124409	TP on transmitter spatial domain impacts of AAS, Ericsson
R4-124414	Legacy base-line E-UTRA co-existence simulation results for AAS, Ericsson, ST-Ericsson
R4-124416	Text proposal on impact of AAS on demodulation performance requirements, Ericsson
R4-124419	Downlink co-existence with electronic tilt, Ericsson
R4-124420	Further results on downlink AAS coexistence with non AAS, Ericsson
R4-124422	Further results on downlink AAS coexistence with AAS, Ericsson
R4-124425	On defining spatial ACLR, Ericsson
R4-124427	TP on general AAS TX characteristics, Ericsson
R4-124429	TP on general AAS RX characteristics, Ericsson
R4-124485	Consideration on AAS antenna modelling, CATT
R4-124571	AAS example applications, Ericsson
R4-124573	Further elaboration of AAS parametirization, Ericsson
R4-124576	Example for reference structure parameterization, Ericsson
R4-124578	Discussion on test and requirement points for AAS, Ericsson
R4-124749	Simulation results for AAS spatial ACLR, Huawei
R4-124885	AAS Ad Hoc minutes, Huawei
R4-124886	Text Proposal: 3D antenna modelling, Huawei
R4-124887	Text Proposal: 3D coexistence scenarios and simulation assumptions, Huawei
R4-124889	Way forward on AAS transmitter characteristics, Huawei, Ericsson, Alcatel Lucent, NSN, Kathrein
R4-124890	AAS RX characteristics, Alcatel Lucent
R4-124891	AAS example applications, Ericsson, Nokia Siemens Networks, Huawei, Kathrein, Alcatel-Lucent
R4-124978	Way forward on AAS test methodology, ZTE, Huawei, Alcatel Lucent, Kathrein, NSN

RAN Plenary #57, Chicago, USA, Sept 4 - 7, 2012

R4-124997 AAS Ad Hoc minutes, Huawei

 $RP-121081\ Status\ report\ for\ SI\ Study\ of\ RF\ and\ EMC\ Requirements\ for\ Active\ Antenna\ Array\ System\ (AAS)\ Base\ Station,\ Huawei$

RAN4#64Bis, Santa Rosa, USA, October 8-12, 2012

R4-125127	Transmitter Spurious Emission for AAS, Alcatel-Lucent
R4-125128	Text Proposal for Receiver Blocking Requirements, Alcatel-Lucent
R4-125131	Combined Test Methodology, Alcatel-Lucent
R4-125132	Testing Methodologies, Alcatel-Lucent
R4-125133	Requirement Points for AAS, Alcatel-Lucent
R4-125215	TP on modeling AAS with multiple-column array antenna, CMCC, Huawei
R4-125243	Updated simulation results on downlink AAS, ACLR ZTE
R4-125244	Simulation results for BS uplink in-band blocking requirements of AAS, ZTE
R4-125245	Correction on Composite Array Radiation Pattern for AAS, ZTE

R4-125247 Discussions on the reference point of the composite ACLR in AAS, R4-125248 Text Proposal on AAS spatial characteristics, ZTE Discussion on Far field OTA Test, ZTE R4-125249 R4-125251 Text Proposal on Far field OTA Test, ZTE R4-125253 Methodologies of Close field coupling test for AAS, ZTE R4-125254 Text proposal on close field coupling test for AAS, ZTE TP for 8.2.1 Conducted Test, Nokia Siemens Networks R4-125260 R4-125262 for 8.2.2 Far Field Over-the-Air Test, Nokia Siemens Networks R4-125263 TP for 8.2.3 Coupling Test, Nokia Siemens Networks R4-125265 TP for 8.2.4 Combined Test, Nokia Siemens Networks R4-125370 TP adding a 2D array model to TR 37.840, Erics son R4-125372 TP adding a sub-section with a second set of simulation parameters to the TR, Ericsson R4-125374 TP adding sub-section for directivity characteristics in Annex C, R4-125426 AAS impact on demodulation performance require ments, Ericsson R4-125427 Initial ACLR results considering horizontal domain beamforming, Ericsson R4-125428 Text Proposal on reference points for ACLR, Ericsson R4-125429 Considerations on further scenarios to investigate for RX blocking and ACLR, Ericsson R4-125430 TX ACLR simulations, Ericsson R4-125431 RX blocking simulations, Ericsson R4-125432 On the requirement definition points for RX blocking, Ericsson R4-125433 On requirement definition points for reference sensitivity, Ericsson R4-125434 TP on spatial domain impacts of AAS, Ericsson TR 37.840 v 030, Huawei R4-125456 Further considerations of AAS SI next step, Huawei R4-125458 Summary of the issues and solutions for AAS, R4-125462 Huawei R4-125466 TP on ACLR simulation results summary, Huawei R4-125467 TP analyzing directivity and gain of parameterized antenna element model, Ericsson R4-125469 Additional simulation results for AAS in-band blocking, Huawei R4-125471 TP adding introduction body text to section of TR 37.840, Ericsson R4-125474 Updated simulation results for AAS ACLR, Huawei R4-125475 TP with editorial corrections to TR 37.840, Ericsson, Huawei R4-125477 TP on BS down-tilt angle, Huawei R4-125481 TP on EVM simulation resuts summary, Huawei R4-125484 TP on in-band blocking simulation results summary, Huawei R4-125487 Text Proposal to clause 8: AAS Testing, Huawei R4-125491 Discussion of AAS transmitter characteristics and requirements, Huawei R4-125494 Discussion on AAS receiver characteristics and requirements, Huawei R4-125503 Test methodologies of Far field OTA test with reverberation chamber for AAS. Huawei Output power requirements for AAS, Ericsson R4-125708 Reference point principles, Ericsson R4-125711 R4-125712 On spatial EVM for AAS, Ericsson R4-125965 AAS Ad Hoc minutes, Huawei R4-125967 Text Proposal on Far field OTA Test, ZTE R4-125978 TP on modeling AAS with multiple-column array antenna, CMCC, Huawei, Ericsson R4-125980 TP on BS down-tilt angle, Huawei R4-125981 TP on ACLR simulation results summary, Huawei, Ericsson, ZTE R4-125982 TP on in-band blocking simulation results summary, Huawei, Ericsson, ZTE R4-125983 Text Proposal to clause 8: AAS Testing, Huawei, Alcatel Lucent R4-125984 TP for 8.2.3 Coupling Test, Nokia Siemens Networks, ZTE, Huawei R4-125985 TP for 8.2.1 Conducted Test, Nokia Siemens Networks, Alcatel-Lucent, Huawei, ZTE R4-125986 Combined Test Methodology, Alcatel-Lucent, Nokia Siemens Networks, ZTE R4-125987 Test methodologies of Far field OTA test with reverberation chamber for AAS, Huawei Summary of the issues and solutions for AAS, R4-125988 Huawei R4-125989 Requirement Points for AAS, Alcatel-Lucent R4-126073 Requirements for AAS, Huawei R4-126074 WF and Text Proposal for Requirements Points for AAS, Alcatel-Lucent, Ericsson

RAN4#65, New Orleans, USA, November 12-16, 2012

R4-126323 TR37.840 ver 040, Huawei R4-126872 AAS Ad Hoc minutes, Huawei R4-126882 AAS Ad Hoc minutes, Huawei

R4-127000

Nokia Siemens Networks R4-126537 AAS study item completion, R4-126547 Way forward for AAS, Ericsson On the inclusion of radiating elements for AAS, Ericsson R4-126548 R4-126551 TP: Requirement and test point approach for AAS, Ericsson R4-126685 TP: TP on spatial domain impacts of AAS, Ericsson R4-126688 TP: Aligning section 3 with TR 37.840 version 0.4.0, TP: TP on spatial domain impacts of AAS, Ericsson R4-126888 R4-126890 TP: Aligning section 3 with TR 37.840 version 0.4.0, R4-126898 TP: Way forward for output power requirement, Ericsson R4-126899 TP: Way forward for reference sensitivity requirement, Ericsson, Huawei R4-126532 AAS classification, Nokia Siemens Networks R4-126885 AAS classification, Nokia Siemens Networks, Huawei R4-126571 TP on Section 5.4.4.2. for general parameters on the AAS antenna model, Kathrein R4-126689 TP: Adding directivity and gain to definitions in section 3 of 37.840. Ericsson TP: Adding directivity analysis to Annex C or TR 37.840, Ericsson R4-126692 R4-126886 TP on Section 5.4.4.2. for general parameters on the AAS antenna model, Kathrein R4-126887 TP: Adding directivity and gain to definitions in section 3 of 37.840. Ericsson R4-126889 TP: Adding directivity analysis to Annex C or TR 37.840, Ericsson TP on Section 5.4.4.2. for general parameters on the AAS antenna model, Kathrein R4-126977 R4-126324 Update of the SI plan, Huawei R4-126325 Review of the requirements and antenna for legacy BS, Huawei R4-126326 Summary of the methodologies for AAS study, Huawei Output power requirements for AAS, Huawei R4-126328 ACLR requirements for AAS, Huawei R4-126329 Spurious emission requirements for AAS, Huawei R4-126330 R4-126331 EVM requirements for AAS, Huawei R4-126332 Reference sensitivity requirements for AAS, Huawei R4-126333 In-band blocking requirements for AAS, Huawei Text proposal for TR37.840 Subclause 9, Huawei R4-126396 R4-126458 Guideline for specifying AAS requirements, Huawei R4-126515 AAS Requirements, Alcatel-Lucent Reference sensitivity requirement definition, Ericsson R4-126534 Reference point for AAS receiver requirements, Nokia Siemens Networks R4-126535 Output power requirements definition, Ericsson R4-126541 R4-126543 Receiver blocking requirements definition, Ericsson R4-126544 ACLR requirement definition, Ericsson R4-126545 Unwanted emissions requirements definition, Ericsson R4-126549 Further elaboration on spatial EVM for AAS, Ericsson R4-126550 EVM requirements definition, Ericsson Update of the SI plan, Huawei R4-126883 R4-126884 Text proposal for TR37.840 Subclause 9, Huawei R4-126896 TP for AAS ACLR, ZTE, Huawei, Ericsson, Alcatel Lucent, Nokia Siemens Networks In-band blocking requirements for AAS, Huawei, Ericsson, Alcatel Lucent, Nokia Siemens R4-126897 Networks, ZTE R4-126917 Summary of the methodologies for AAS study, Huawei Further explanation on the near-field coupling test fixture, ZTE Corporation R4-126114 R4-126115 TP on improved diagram of the coupling test, ZTE Corporation R4-126334 TP on reverberation chamber OTA test for AAS, Huawei R4-126520 Combined OTA-Conducted Test, Alcatel-Lucent R4-126536 AAS test methods comparison, Nokia Siemens Networks R4-126686 TP: Adding Near-Field Probe Scanner Test method to section 8, Ericsson R4-126891 AAS test methods comparison, Nokia Siemens Networks R4-126892 Combined OTA-Conducted Test, Alcatel-Lucent TP: Adding Near-Field Probe Scanner Test method to section 8, R4-126893 Ericsson

Updated on AAS TR TR37.840 v0.5.0, Huawei

RAN4 #66, St. Julian's, Malta, 28th January – 1st February 2013

R4-130130	AAS Feasibility Study Summary, Alcatel-Lucent
R4-130140	Far field and transceiver boundary testing examples, Ericsson
R4-130144	Further extensions to array antenna model, Ericsson
R4-130145	TP: Aligning section 3 with version 1.0.0 of TR 37.840, Ericsson
R4-130259	The need for defining minimum steering range of AAS transmission beam, ZTE
R4-130268	Way forward on how to introduce AAS to the requirement, NTT DOCOMO
R4-130428	Consideration of AAS WI, Huawei
R4-130431	Draft AAS work item proposal, Huawei
R4-130520	Text proposal for the technical report conclusion, Nokia Siemens Networks
R4-130524	Corrections for Deployment Scenarios section, Nokia Siemens Networks
R4-130685	Discussion on the response to ITU and WI prioritization, Ericsson
R4-130686	On the WI scope, Ericsson
R4-130775	Some considerations on the AAS WI phase, ZTE
R4-130904	TP for receiver reference point, Nokia Siemens Networks, Huawei, Alcatel-Lucent, ZTE, Ericsson
R4-130905	Text proposal for TR37.840 Clause 9: Conclusion, Huawei, Alcatel-Lucent, Kathrein, NSN
R4-130906	TP for capturing non-core requirements, Ericsson, Huawei, Alcatel-Lucent
R4-130908	AAS reference structure, Ericsson
R4-130909	TP: Editorial corrections for TR 37.840 version 1.0.0, Ericsson
R4-130910	TP: Editorial corrections of TR 37.840 section 5.4.4, Ericsson
R4-130911	Text Proposal on remaining sections in TR37.840, Huawei
R4-130977	Relation between transceiver boundary and far-field, Ericsson, CATR
R4-130978	TP defining Far field and transceiver boundary requirement definitions, Ericsson, Huawei, ZTE, NSN
R4-130984	TR update 37.840 v 1.1.0, Huawei

Annex B: Simulations results

The simulation results for ACLR (per element) from different companies have been captured based on the simulation scenarios and assumptions described in Section 5.4.

B.1 Case 1a: Downlink E-UTRA AAS interferer- legacy system victim

Simulations are based on the following assumptions:

Aggressor system: 10 MHz E-UTRA with AAS

Victim system: 10 MHz E-UTRA with passive antenna system

Down-tilt angle: 9 degrees down-tilt in aggressor and victim system

Correlation level: 0, 0.2, 0.4, 0.6, 0.8. 1.0

Environment: Macro Cell, Urban Area, uncoordinated deployment

Cell Range 750 m

Simulation results are presented in Table B.1-1 for electrical down-tilt and Table B.1-2 for mechanical down-tilt.

Table B.1-1 Case 1a simulation results summary (Electrical down-tilt)

Huawei (R4- 125474)	Correlation: 0		Correlation: 0.2		Correlation: 0.4		Correlation: 0.6		Correlation: 0.8		Correlation: 1	
ACLR per element (dBc)	cell average through put loss (%)	5% CDF through put loss (%)	cell average through put loss (%)	5% CDF through put loss (%)	cell average throughp ut loss (%)	5% CDF throughp ut loss (%)	cell average throughp ut loss (%)	5% CDF throughp ut loss (%)	cell average through put loss (%)	5% CDF through put loss (%)	cell average through put loss (%)	5% CDF throughp ut loss (%)
30	6.0929	23.9549	6.4980	22.8180	6.8261	22.2874	7.0837	21.5957	7.2587	21.1872	7.2207	19.0198
35	4.8476	15.9239	4.9697	15.5777	5.0757	15.2120	5.1605	14.7111	5.2134	13.5116	5.1733	12.1408
40	4.2737	11.1952	4.3016	10.9334	4.3254	10.6982	4.3435	10.4384	4.3519	10.1315	4.3193	9.5474
45	4.0276	9.4984	4.0326	9.3892	4.0358	9.3027	4.0377	9.2495	4.0364	9.2104	4.0149	8.8281
50	3.9307	8.9929	3.9309	8.9722	3.9308	8.9707	3.9303	8.9687	3.9287	8.9602	3.9147	8.6013

ZTE (R4- 125243)	Correlation: 0		Correlation: 0.2		Correlation: 0.4		Correlation: 0.6		Correlation: 0.8		Correlation: 1	
ACLR per element (dBc)	cell average through put loss (%)	5% CDF through put loss (%)	cell average through put loss (%)	5% CDF through put loss (%)	cell average throughpu t loss (%)	5% CDF through put loss (%)	cell average throughp ut loss (%)	5% CDF throughp ut loss (%)	cell average through put loss (%)	5% CDF through put loss (%)	cell average through put loss (%)	5% CDF throughp ut loss (%)
30	5.9106	20.2684	6.3600	21.1764	6.7141	21.6916	7.0187	21.6602	7.2652	20.4283	7.3705	19.6064
35	4.7621	15.6824	4.8974	15.6195	5.0092	15.1871	5.1078	14.6385	5.1895	14.2075	5.2250	13.9391
40	4.2324	12.5605	4.2647	12.0792	4.2914	11.6938	4.3147	11.5711	4.3341	11.5945	4.3429	11.4494
45	4.0085	11.0662	4.0143	10.8066	4.0194	10.7919	4.0240	10.7722	4.0279	10.7015	4.0290	10.6069
50	3.9222	10.5553	3.9231	10.4964	3.9242	10.3897	3.9251	10.3154	3.9254	10.2912	3.9259	10.3006

Ericcso n (R4- 125430)			Correlation: 0.2		Correlation: 0.4		Correlation: 0.6		Correlation: 0.8		Correlation: 1	
ACLR per element (dBc)	cell average through put loss (%)	5% CDF through put loss (%)	cell average through put loss (%)	5% CDF through put loss (%)	cell average throughpu t loss (%)	5% CDF through put loss (%)	cell average throughp ut loss (%)	5% CDF throughp ut loss (%)	cell average through put loss (%)	5% CDF through put loss (%)	cell average through put loss (%)	5% CDF throughp ut loss (%)

30	5.8010	22.6056	6.1369	24.5186	6.4065	25.8766	6.6207	27.2267	6.7697	27.9175	6.6685	28.2114
35	4.4337	16.7285	4.5551	17.9056	4.6530	18.3543	4.7301	18.5422	4.7794	18.9312	4.7216	18.9885
40	3.7465	15.5633	3.7923	15.7568	3.8253	15.8147	3.8494	16.0168	3.8622	16.1395	3.8357	16.2241
45	3.4539	15.2556	3.4756	15.5620	3.4880	15.7127	3.4960	15.7257	3.4995	15.7262	3.4899	15.7264
50	3.3466	15.0479	3.3607	15.1163	3.3669	15.1163	3.3705	15.2062	3.3722	15.2062	3.3693	15.2513

Table B.1-2 Case 1a simulation results summary (Mechanical down-tilt)

Huawei (R4- 125474)	Correlation: 0		Correlation: 0.2		Correlation: 0.4		Correlation: 0.6		Correla	tion: 0.8	Correlation: 1		
ACLR per element (dBc)	cell average through put loss (%)	5% CDF through put loss (%)	cell average through put loss (%)	5% CDF through put loss (%)	cell average throughp ut loss (%)	5% CDF throughp ut loss (%)	cell average throughp utloss (%)	5% CDF throughp ut loss (%)	cell average through put loss (%)	5% CDF through put loss (%)	cell average through put loss (%)	5% CDF throughp ut loss (%)	
30	3.5786	14.0827	3.7739	14.6345	3.9308	13.5067	4.0493	12.9034	4.1144	12.3559	4.0003	10.6685	
35	2.7853	6.0808	2.8304	6.0181	2.8649	6.1911	2.8853	6.3956	2.8844	6.4574	2.7976	5.8873	
40	2.4138	4.7018	2.4171	4.6158	2.4165	4.6766	2.4111	4.5316	2.3975	4.3468	2.3427	3.4315	
45	2.2442	3.8258	2.2407	3.8030	2.2360	3.6515	2.2293	3.4225	2.2193	3.3515	2.1877	2.8893	
50	2.1687	3.2419	2.1661	3.2200	2.1630	3.1969	2.1588	3.1850	2.1531	3.0401	2.1373	2.7372	

ZTE (R4- 125243)	Correlation: 0		Correlation: 0.2		Correlation: 0.4		Correlation: 0.6		Correlation: 0.8		Correlation: 1	
ACLR per element (dBc)	cell average through put loss (%)	5% CDF through put loss (%)	cell average through put loss (%)	5% CDF through put loss (%)	cell average throughp ut loss (%)	5% CDF throughp ut loss (%)	cell average throughp utloss (%)	5% CDF throughp ut loss (%)	cell average through put loss (%)	5% CDF through put loss (%)	cell average through put loss (%)	5% CDF throughp ut loss (%)
30	2.9219	10.6241	3.1098	10.4443	3.2741	10.2447	3.3983	9.9706	3.4709	9.3203	3.4760	8.9923
35	2.1550	6.5387	2.1979	6.5004	2.2324	6.0789	2.2565	5.9615	2.2651	5.7411	2.2545	5.6770
40	1.7968	5.2378	1.8021	5.0606	1.8045	4.9980	1.8046	4.7461	1.8012	4.6654	1.7933	4.5784
45	1.6466	4.4512	1.6461	4.4493	1.6444	4.3635	1.6425	4.3368	1.6397	4.3388	1.6362	4.3424
50	1.5905	4.2997	1.5897	4.3022	1.5887	4.3048	1.5877	4.2946	1.5865	4.2972	1.5852	4.2998

Ericsso n (R4- 125430)	Correlation: 0		Correlation: 0.2		Correlation: 0.4		Correlation: 0.6		Correlation: 0.8		Correlation: 1	
ACLR per element (dBc)	cell average through put loss (%)	5% CDF through put loss (%)	cell average through put loss (%)	5% CDF through put loss (%)	cell average throughp ut loss (%)	5% CDF throughp ut loss (%)	cell average throughp ut loss (%)	5% CDF throughp ut loss (%)	cell average through put loss (%)	5% CDF through put loss (%)	cell average through put loss (%)	5% CDF throughp ut loss (%)
30	6.0587	24.1687	6.4010	26.8229	6.6808	28.7331	6.9009	30.6639	7.0547	31.4792	6.9464	32.0624
35	4.6905	19.2959	4.8131	19.7520	4.9126	20.2582	4.9912	21.0362	5.0415	21.7296	4.9762	21.9114
40	3.9775	17.1361	4.0239	17.2949	4.0568	17.5085	4.0805	17.6989	4.0919	17.7632	4.0583	17.7985
45	3.6598	16.5307	3.6815	16.5307	3.6937	16.5307	3.7012	16.5840	3.7037	16.6371	3.6904	16.6371
50	3.5371	15.3523	3.5510	15.3523	3.5571	15.2786	3.5604	15.2786	3.5616	15.3117	3.5574	15.3523

B.2 Case 1b: Downlink E-UTRA AAS interferer- AAS victim with equal down-tilt angles

Simulations are based on the following assumptions:

Aggressor system: 10 MHz E-UTRA with AAS

Victim system: 10 MHz E-UTRA with AAS

Down-tilt angle: 9 degrees down-tilt in aggressor and victim system

Correlation level: 0, 0.2, 0.4, 0.6, 0.8. 1.0

Environment: Macro Cell, Urban Area, uncoordinated deployment

Cell Range 750 m

Simulation results are presented in Table B.2-1 for electrical down-tilt and Table B.2-2 for mechanical down-tilt.

Table B.2-2 Case 1b simulation results summary (Electrical down-tilt)

Huawei (R4- 125474)	Correlation: 0		Correlation: 0.2		Correlation: 0.4		Correlation: 0.6		Correlation: 0.8		Correlation: 1	
ACLR per element (dBc)	cell average through put loss (%)	5% CDF through put loss (%)	cell average through put loss (%)	5% CDF through put loss (%)	cell average throughp ut loss (%)	5% CDF throughp ut loss (%)	cell average throughp ut loss (%)	5% CDF throughp ut loss (%)	cell average through put loss (%)	5% CDF through put loss (%)	cell average through put loss (%)	5% CDF throughp ut loss (%)
30	5.3426	20.7257	5.7125	20.6483	6.0130	19.6488	6.2501	18.9976	6.4128	18.4933	6.3846	16.4072
35	4.2216	13.9657	4.3328	13.4933	4.4275	12.9340	4.5035	11.7741	4.5532	11.1628	4.5205	10.0884
40	3.7069	9.5738	3.7325	9.4169	3.7543	9.2403	3.7712	8.9711	3.7799	8.7062	3.7521	8.2707
45	3.4894	8.2557	3.4939	8.2009	3.4973	8.1578	3.4992	7.8511	3.4983	7.8027	3.4798	7.4957
50	3.4042	7.6123	3.4045	7.6022	3.4046	7.5994	3.4044	7.5965	3.4033	7.5935	3.3902	7.3285

ZTE (R4- 125243)	Correla	ation: 0	Correla	tion: 0.2	Correla	tion: 0.4	Correla	tion: 0.6	Correla	tion: 0.8	Correl	ation: 1
ACLR per element (dBc)	cell average through put loss (%)	5% CDF through put loss (%)	cell average through put loss (%)	5% CDF through put loss (%)	cell average throughp ut loss (%)	5% CDF throughp ut loss (%)	cell average throughp ut loss (%)	5% CDF throughp ut loss (%)	cell average through put loss (%)	5% CDF through put loss (%)	cell average through put loss (%)	5% CDF throughp ut loss (%)
30	5.1803	18.3029	5.5833	18.2090	5.9016	19.0236	6.1745	18.5968	6.3992	17.8076	6.4967	17.0596
35	4.1436	13.7661	4.2639	13.5598	4.3624	13.3167	4.4492	12.9323	4.5225	12.1806	4.5546	12.0952
40	3.6667	10.2602	3.6949	10.0423	3.7185	10.3673	3.7388	10.0804	3.7563	9.9191	3.7633	9.6364
45	3.4650	8.7739	3.4704	8.7962	3.4749	8.6918	3.4786	8.5830	3.4821	8.5761	3.4837	8.5224
50	3.3879	8.1770	3.3890	8.1593	3.3900	8.1476	3.3905	8.0914	3.3913	8.1011	3.3919	8.1166

Ericsso n (R4- 125430)	Correla	ation: 0	Correla	tion: 0.2	Correla	tion: 0.4	Correla	tion: 0.6	Correla	tion: 0.8	Correl	ation: 1
ACLR per element (dBc)	cell average through put loss (%)	5% CDF through put loss (%)	cell average through put loss (%)	5% CDF through put loss (%)	cell average throughp ut loss (%)	5% CDF throughp ut loss (%)	cell average throughp ut loss (%)	5% CDF throughp ut loss (%)	cell average through put loss (%)	5% CDF through put loss (%)	cell average through put loss (%)	5% CDF throughp ut loss (%)
30	5.0490	17.8383	5.3526	19.5973	5.6014	20.9169	5.7976	21.9064	5.9365	23.1688	5.8565	23.3411
35	3.8246	14.7246	3.9346	15.2660	4.0231	15.6994	4.0934	15.9439	4.1396	16.2466	4.0959	16.3624
40	3.2277	12.9305	3.2703	13.2089	3.3006	13.2937	3.3228	13.5048	3.3355	13.8731	3.3159	13.9720
45	2.9813	12.6096	3.0021	12.7990	3.0139	12.7990	3.0217	12.7990	3.0258	12.8705	3.0188	12.8884
50	2.8928	11.9565	2.9067	12.0287	2.9128	12.0287	2.9164	12.1007	2.9183	12.1007	2.9164	12.1007

Table B.2-2 Case 1b simulation results summary (Mechanical down-tilt)

Huawei (R4-	Correlation: 0	Correlation: 0.2	Correlation: 0.4	Correlation: 0.6	Correlation: 0.8	Correlation: 1
125474)						

ACLR per element (dBc)	cell average through put loss (%)	5% CDF through put loss (%)	cell average through put loss (%)	5% CDF through put loss (%)	cell average throughp ut loss (%)	5% CDF throughp ut loss (%)	cell average throughp ut loss (%)	5% CDF throughp ut loss (%)	cell average through put loss (%)	5% CDF through put loss (%)	cell average through put loss (%)	5% CDF throughp ut loss (%)
30	3.1517	12.6415	3.3151	11.2450	3.4472	10.9667	3.5461	10.0202	3.5983	10.3055	3.4909	9.1215
35	2.4489	4.9736	2.4862	4.8950	2.5143	4.9382	2.5298	5.0418	2.5261	4.9831	2.4476	3.7916
40	2.1205	3.9868	2.1222	4.0009	2.1216	3.9035	2.1171	3.7370	2.1046	3.4180	2.0560	2.5176
45	1.9721	3.2334	1.9692	3.0999	1.9648	2.9193	1.9589	2.7357	1.9501	2.6623	1.9218	2.1941
50	1.9060	2.6029	1.9037	2.5789	1.9010	2.5674	1.8972	2.5558	1.8923	2.3469	1.8785	2.1037

ZTE (R4- 125243)	Correla	ation: 0	Correla	tion: 0.2	Correla	tion: 0.4	Correla	tion: 0.6	Correla	tion: 0.8	Correl	ation: 1
ACLR per element (dBc)	cell average through put loss (%)	5% CDF through put loss (%)	cell average through put loss (%)	5% CDF through put loss (%)	cell average throughp ut loss (%)	5% CDF throughp ut loss (%)	cell average throughp ut loss (%)	5% CDF throughp ut loss (%)	cell average through put loss (%)	5% CDF through put loss (%)	cell average through put loss (%)	5% CDF throughp ut loss (%)
30	2.5076	9.1243	2.6635	9.3049	2.7988	8.8567	2.9014	8.1983	2.9604	7.5941	2.9599	7.5392
35	1.8262	5.6494	1.8604	5.4981	1.8876	5.4054	1.9065	5.3499	1.9113	5.0218	1.9007	4.8700
40	1.5113	4.2005	1.5145	4.3511	1.5159	4.1487	1.5160	4.1416	1.5123	4.1069	1.5048	4.1283
45	1.3804	3.6771	1.3797	3.7099	1.3780	3.6046	1.3760	3.5769	1.3734	3.5799	1.3701	3.6423
50	1.3315	3.3844	1.3308	3.4067	1.3298	3.4301	1.3288	3.4487	1.3277	3.4654	1.3265	3.4778

Ericsso n (R4- 125474)	Correla	ation: 0	Correla	tion: 0.2	Correla	tion: 0.4	Correla	tion: 0.6	Correla	tion: 0.8	Correl	ation: 1
ACLR per element (dBc)	cell average through put loss (%)	5% CDF through put loss (%)	cell average through put loss (%)	5% CDF through put loss (%)	cell average throughp ut loss (%)	5% CDF throughp ut loss (%)	cell average throughp ut loss (%)	5% CDF throughp ut loss (%)	cell average through put loss (%)	5% CDF through put loss (%)	cell average through put loss (%)	5% CDF throughp ut loss (%)
30	5.2893	20.4516	5.6017	22.7150	5.8575	24.1853	6.0644	25.5291	6.2092	27.0379	6.1231	27.2605
35	4.0603	15.6654	4.1745	16.2303	4.2659	17.2965	4.3376	17.6232	4.3842	17.8159	4.3319	18.2315
40	3.4365	14.0680	3.4805	14.0881	3.5119	14.1446	3.5344	14.1516	3.5466	14.3692	3.5212	14.3769
45	3.1658	13.6960	3.1866	13.6960	3.1988	13.6960	3.2065	13.6965	3.2098	13.6971	3.2003	13.6977
50	3.0638	13.4009	3.0775	13.4021	3.0835	13.4021	3.0869	13.4033	3.0884	13.4044	3.0855	13.4054

B.3 Case 1b: Downlink E-UTRA AAS interferer- AAS victim with non-optimal down-tilt angles

Simulations are based on the following assumptions:

Aggressor system: 10 MHz E-UTRA with AAS

Victim system: 10 MHz E-UTRA with AAS

Down-tilt angle: 9 degrees down-tilt in victim system;

5, 20 degrees down-tilt in aggressor system

Correlation level: 0, 0.2, 0.4, 0.6, 0.8. 1.0

Environment: Macro Cell, Urban Area, uncoordinated deployment

Cell Range 750 m

Simulation results are presented in Table B.3-1and Table B.3-2 for 5 degrees of electrical/mechanical down-tilt being used in aggressor system, respectively, and Table B.3-3 and Table B.3-4 for 20 degrees of electrical/mechanical down-tilt being used in aggressor system, respectively.

Table B.3-3 Case 1b simulation results summary (Aggressor: eDT of 5 deg, Victim: eDT of 9deg)

Huawei (R4- 125474)	Correla	ation: 0	Correla	tion: 0.2	Correla	tion: 0.4	Correla	tion: 0.6	Correla	tion: 0.8	Correl	ation: 1
ACLR per element (dBc)	cell average through put loss (%)	5% CDF through put loss (%)	cell average through put loss (%)	5% CDF through put loss (%)	cell average throughp ut loss (%)	5% CDF throughp ut loss (%)	cell average throughp ut loss (%)	5% CDF throughp ut loss (%)	cell average through put loss (%)	5% CDF through put loss (%)	cell average through put loss (%)	5% CDF throughp ut loss (%)
30	5.1610	19.7218	5.5890	19.7181	5.9519	19.1890	6.2481	17.5939	6.4592	15.9986	6.4905	13.1144
35	3.9495	13.3687	4.0605	12.6874	4.1541	12.1554	4.2261	10.9186	4.2695	10.2342	4.2501	8.4364
40	3.3650	8.3973	3.3836	8.0171	3.3969	7.7662	3.4043	7.5594	3.4030	6.9639	3.3854	6.0968
45	3.1061	6.5258	3.1060	6.4226	3.1045	6.3248	3.1016	6.1217	3.0967	5.8349	3.0876	5.4293
50	3.0031	5.8116	3.0016	5.7074	2.9998	5.5951	2.9977	5.4788	2.9953	5.3967	2.9910	5.2054

Ericsso n (R4- 125430)	Correla	ation: 0	Correla	tion: 0.2	Correla	tion: 0.4	Correla	tion: 0.6	Correla	tion: 0.8	Correl	ation: 1
ACLR per element (dBc)	cell average through put loss (%)	5% CDF through put loss (%)	cell average through put loss (%)	5% CDF through put loss (%)	cell average throughp ut loss (%)	5% CDF throughp ut loss (%)	cell average throughp ut loss (%)	5% CDF throughp ut loss (%)	cell average through put loss (%)	5% CDF through put loss (%)	cell average through put loss (%)	5% CDF throughp ut loss (%)
30	5.1914	18.0054	5.5806	19.8025	5.9110	20.7884	6.1914	22.4449	6.4110	22.9942	6.4062	23.3760
35	3.9267	12.4522	4.0634	13.7554	4.1779	14.1611	4.2740	15.0396	4.3452	15.3576	4.3245	15.4526
40	3.3133	11.4236	3.3640	11.5677	3.4023	11.6132	3.4329	11.9213	3.4535	12.0033	3.4410	12.1838
45	3.0611	11.3447	3.0845	11.4197	3.0989	11.4197	3.1092	11.4224	3.1157	11.4224	3.1109	11.4249
50	2.9708	11.2740	2.9856	11.2749	2.9925	11.2745	2.9969	11.2745	2.9996	11.2740	2.9984	11.2740

Table B.3-2 Case 1b simulation results summary (Aggressor: mDT of 5 deg, Victim: mDT of 9deg)

Huawei (R4- 125474)	Correla	ation: 0	Correla	tion: 0.2	Correla	tion: 0.4	Correla	tion: 0.6	Correla	tion: 0.8	Correl	ation: 1
ACLR per element (dBc)	cell average through put loss (%)	5% CDF through put loss (%)	cell average through put loss (%)	5% CDF through put loss (%)	cell average throughp ut loss (%)	5% CDF throughp ut loss (%)	cell average throughp ut loss (%)	5% CDF throughp ut loss (%)	cell average through put loss (%)	5% CDF through put loss (%)	cell average through put loss (%)	5% CDF throughp ut loss (%)
30	3.0679	11.6197	3.2427	10.4943	3.3904	9.2671	3.5052	8.7004	3.5757	8.0609	3.5133	5.3592
35	2.3301	5.4686	2.3666	5.2448	2.3959	4.8107	2.4134	3.6796	2.4141	3.2744	2.3595	2.5943
40	1.9897	2.7419	1.9932	2.6126	1.9933	2.4249	1.9885	1.6957	1.9780	1.5678	1.9460	1.0906
45	1.8408	1.3827	1.8388	1.3377	1.8359	1.3052	1.8312	1.2287	1.8244	0.9765	1.8084	0.7852
50	1.7804	0.8569	1.7789	0.8343	1.7771	0.8147	1.7746	0.7917	1.7710	0.7350	1.7638	0.7128

Ericsso						
n (R4-	Correlation: 0	Correlation: 0.2	Correlation: 0.4	Correlation: 0.6	Correlation: 0.8	Correlation: 1
125430)						

ACLR per element (dBc)	cell average through put loss (%)	5% CDF through put loss (%)	cell average through put loss (%)	5% CDF through put loss (%)	cell average throughp ut loss (%)	5% CDF throughp ut loss (%)	cell average throughp ut loss (%)	5% CDF throughp ut loss (%)	cell average through put loss (%)	5% CDF through put loss (%)	cell average through put loss (%)	5% CDF throughp ut loss (%)
30	4.2973	14.9384	4.7065	16.3019	5.0652	18.3227	5.3815	19.3731	5.6540	21.1699	5.7957	22.2737
35	3.5404	12.0871	3.6840	12.4732	3.8102	12.7342	3.9246	13.4003	4.0237	14.2156	4.0724	14.5000
40	3.2023	10.3409	3.2554	10.4495	3.2984	10.4966	3.3365	10.6089	3.3687	10.9148	3.3831	11.0234
45	3.0682	10.3257	3.0923	10.3257	3.1082	10.3257	3.1213	10.4144	3.1319	10.4442	3.1364	10.4589
50	3.0203	9.9770	3.0352	9.9770	3.0426	9.9732	3.0479	9.9760	3.0520	9.9770	3.0538	10.0001

Table B.3-3 Case 1b simulation results summary (Aggressor: eDT of 20 deg, Victim: eDT of 9deg)

Huawei (R4- 125474)	Correla	ation: 0	Correla	tion: 0.2	Correla	tion: 0.4	Correla	tion: 0.6	Correla	tion: 0.8	Correl	ation: 1
ACLR per element (dBc)	cell average through put loss (%)	5% CDF through put loss (%)	cell average through put loss (%)	5% CDF through put loss (%)	cell average throughp ut loss (%)	5% CDF throughp ut loss (%)	cell average throughp utloss (%)	5% CDF throughp ut loss (%)	cell average through put loss (%)	5% CDF through put loss (%)	cell average through put loss (%)	5% CDF throughp ut loss (%)
30	3.5321	24.9152	3.3497	26.1466	3.1374	26.6997	2.8883	27.0329	2.5950	26.8593	2.1796	25.8399
35	2.2273	19.5129	2.1402	19.5166	2.0448	19.6223	1.9372	19.5456	1.8148	19.5207	1.6470	19.6573
40	1.6599	16.7480	1.6213	16.6986	1.5803	16.6737	1.5357	16.7019	1.4863	16.6608	1.4192	16.5114
45	1.4307	15.8894	1.4157	15.8990	1.4003	15.8597	1.3833	15.8119	1.3641	15.7863	1.3376	15.6971
50	1.3463	15.1493	1.3410	15.4107	1.3353	15.4138	1.3287	15.4134	1.3209	15.4157	1.3110	15.4178

Ericsso n (R4- 125430)	Correlation: 0		Correlation: 0.2		Correlation: 0.4		Correlation: 0.6		Correlation: 0.8		Correlation: 1	
ACLR per element (dBc)	cell average through put loss (%)	5% CDF through put loss (%)	cell average through put loss (%)	5% CDF through put loss (%)	cell average throughp ut loss (%)	5% CDF throughp ut loss (%)	cell average throughp ut loss (%)	5% CDF throughp ut loss (%)	cell average through put loss (%)	5% CDF through put loss (%)	cell average through put loss (%)	5% CDF throughp ut loss (%)
30	3.2834	12.2470	3.3768	13.1667	3.4342	13.6213	3.4583	13.7961	3.4415	13.9851	3.2505	13.6983
35	2.1561	7.5908	2.1985	7.6184	2.2218	7.9897	2.2307	8.3053	2.2208	8.3232	2.1393	8.3149
40	1.6419	6.4718	1.6629	6.6668	1.6734	6.6684	1.6767	6.7225	1.6719	6.6699	1.6409	6.7212
45	1.4381	6.1523	1.4522	6.4673	1.4576	6.4673	1.4594	6.5469	1.4582	6.5469	1.4483	6.6262
50	1.3660	6.0972	1.3779	6.1522	1.3820	6.1522	1.3838	6.1522	1.3840	6.1522	1.3811	6.1522

Table B.3-4 Case 1b simulation results summary (Aggressor: mDT of 20 deg, Victim: mDT of 9deg)

Huawei (R4- 125474)	Correla	Correlation: 0.2		Correlation: 0.4		Correlation: 0.6		Correlation: 0.8		Correlation: 1		
ACLR per element (dBc)	cell average through put loss (%)	5% CDF through put loss (%)	cell average through put loss (%)	5% CDF through put loss (%)	cell average throughp ut loss (%)	5% CDF throughp ut loss (%)	cell average throughp utloss (%)	5% CDF throughp ut loss (%)	cell average through put loss (%)	5% CDF through put loss (%)	cell average through put loss (%)	5% CDF throughp ut loss (%)
30	2.5711	10.7954	2.5160	11.3001	2.4383	11.0524	2.3368	11.0892	2.1976	12.3859	1.9214	12.1904

35	1.8309	6.1074	1.7975	6.5883	1.7565	6.7182	1.7042	6.5232	1.6365	6.1193	1.5112	5.8223
40	1.4970	3.8662	1.4790	3.7678	1.4579	3.5091	1.4326	3.3754	1.4021	3.2465	1.3458	3.5312
45	1.3550	2.7577	1.3462	2.7474	1.3364	2.7369	1.3257	2.7260	1.3130	2.6868	1.2879	2.5604
50	1.2963	2.4456	1.2928	2.4401	1.2889	2.4346	1.2844	2.4246	1.2795	2.4100	1.2683	2.3951

Ericsso n (R4- 125430)	Correlation: 0		Correlation: 0.2		Correlation: 0.4		Correlation: 0.6		Correlation: 0.8		Correlation: 1	
ACLR per element (dBc)	cell average through put loss (%)	5% CDF through put loss (%)	cell average through put loss (%)	5% CDF through put loss (%)	cell average throughp ut loss (%)	5% CDF throughp ut loss (%)	cell average throughp ut loss (%)	5% CDF throughp ut loss (%)	cell average through put loss (%)	5% CDF through put loss (%)	cell average through put loss (%)	5% CDF throughp ut loss (%)
30	2.6459	15.9192	2.7573	16.9524	2.8373	17.5192	2.8928	17.5799	2.9179	17.9168	2.8296	17.6816
35	1.9455	13.4507	1.9908	13.3129	2.0224	13.3092	2.0438	13.3092	2.0520	13.3129	2.0124	13.2312
40	1.6208	11.3959	1.6429	11.3959	1.6551	10.8433	1.6622	10.8463	1.6638	10.8487	1.6477	10.8744
45	1.4872	10.8328	1.5015	10.8328	1.5076	10.7930	1.5108	10.7930	1.5116	10.7930	1.5060	10.7929
50	1.4381	10.6954	1.4500	10.6954	1.4544	9.7687	1.4565	9.7758	1.4574	9.7829	1.4560	9.7900

B.4 Case 1c: Downlink E-UTRA legacy system interferer- legacy system victim

Simulations are based on the following assumptions:

Aggressor system: 10 MHz E-UTRA with passive antenna system

Victim system: 10 MHz E-UTRA with passive antenna system

Down-tilt angle: 9 degrees down-tilt in aggressor and victim system

Environment: Macro Cell, Urban Area, uncoordinated deployment

Cell Range 750 m

Simulation results are presented in Table B.4-1 for electrical down-tilt and Table B.4-2 for mechanical down-tilt.

Table B.4-4 Case 1c simulation results summary (Electrical down-tilt)

	Huawei (R	(4-125474)	ZTE (R4	-125243)	Ericsson(R4-125430)		
ACLR per element (dBc)	cell average throughput loss (%)	cell edge throughput loss (%)	cell average throughput loss (%)	cell edge throughput loss (%)	cell average throughput loss (%)	cell edge throughput loss (%)	
30	6.3859	16.4113	6.4934	17.0554	5.4533	24.4796	
35	4.5223	10.0939	4.5520	12.0912	3.8742	17.2686	
40	3.7541	8.2778	3.7610	9.6536	3.2146	14.3383	
45	3.4818	7.5024	3.4815	8.5370	2.9805	13.0830	
50	3.3923	7.3351	3.3898	8.2019	2.9036	11.9269	

Table B.4-2 Case 1c simulation results summary (Mechanical down-tilt)

	Huawei (R	(4-125474)	ZTE (R4	-125243)	Ericsson (R4-125430)		
ACLR per element (dBc)	cell average throughput loss (%)	cell edge throughput loss (%)	cell average throughput loss (%)	cell edge throughput loss (%)	cell average throughput loss (%)	cell edge throughput loss (%)	
30	3.4918	9.1213	2.9593	7.5394	5.6895	29.4684	
35	2.4486	3.7918	1.9003	4.8682	4.0673	19.3364	

40	2.0570	2.5194	1.5044	4.1353	3.3908	14.7612
45	1.9229	2.1965	1.3697	3.6460	3.1497	13.7009
50	1.8796	2.1061	1.3262	3.4793	3.0674	13.6154

Annex C: (Informative) AAS spatial domain aspects

The purpose of this informative annex is to collect the studies and aspects considering the spatial effects observable with AAS systems. To illustrate the spatial effects under consideration, a theoretical model of a uniform linear array is examined. The parameters chosen for the model are strictly for this examination and are not claimed to be an accurate representation of physical systems. Common antenna array features such as power tapering are not considered. Note that the results given in this annex are link oriented. The spatial characteristics given in this annex may suggest further system analysis and studies where the results are captured in the main body of this TR.

C.1 Transmitter spatial characteristics

Interference emitted from AAS BS system may show different spatial characteristics to that from conventional BS, depending on the extent of beam-forming effects on the interference. Adjacent channel emissions, spurious emissions and intermodulation may be affected.

The transmitter intermodulation as a function of angle and frequency for an active Uniform Linear Array (ULA) has been elaborated by means of simulations. Power Amplifiers on each antenna element within the array were modelled with respect to non-linear behaviour to simulate the contribution from several power amplifiers / sub-arrays. Simulations were made over separate carrier frequencies, but also using the same carrier frequency. Results showed that intermodulation products may occur outside the main beams of the carriers, and are then also in general split into several sub-beams according to general side lobe behaviour of linear array antennas. The radiating elements were modelled based on agreed antenna models and the distance between radiating elements was chosen to be $0.9~\lambda$.

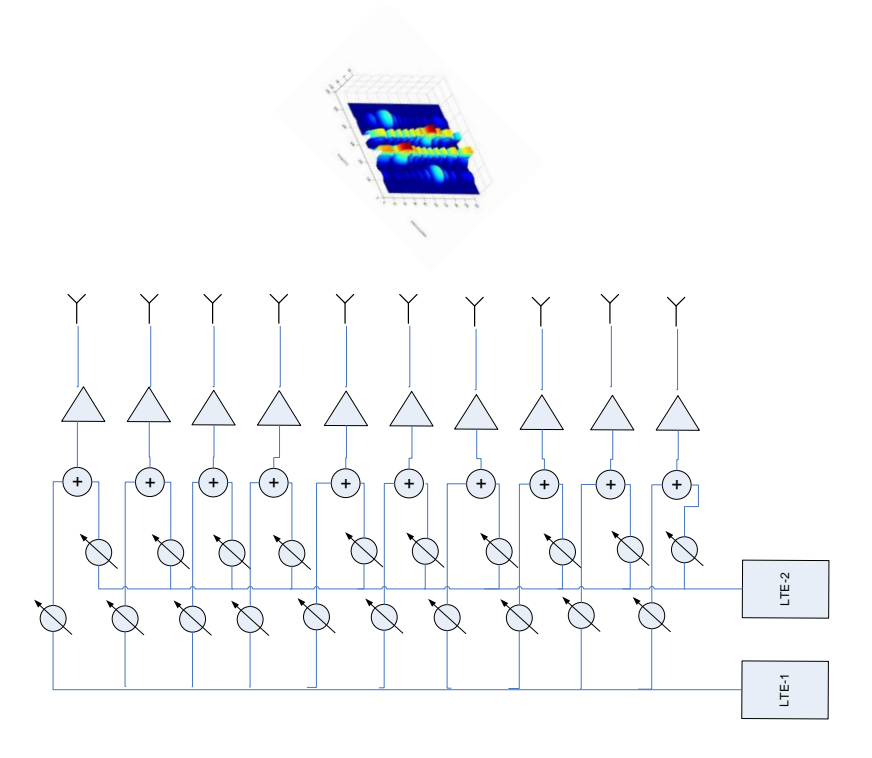


Figure C.1-1, ULA configuration for the simulation

C.1.2 Simulation assumptions

The simulations of AAS intermodulation spatial characteristics assume a number of antenna elements radiating into free space. Each of radiating elements is connected to an active amplifier which outputs non-linear distortion still remaining despite pre-distortion. That is, some non-linear components still do exist in order to study how these distribute over the antenna angular range.

As an example scenario a Uniform Linear Array (ULA) which has the characteristics of having all of its elements aligned along a straight line is selected. The inter-element distance is all equal among the elements and is set to 0.9λ (see figure C.1-1).

In some of the plots due to chosen inter-element distance, the grating lobes which occurs at inter-element distance of larger than 0.5λ become visible.

Another assumption is that the array antenna is fed by two E-UTRA-signals of 20 MHz, being un-correlated and having phase offsets on each antenna element corresponding to a particular scanning angle for the array. The number of antenna elements is 10

The non-linearity of each amplifier is modelled by a simple polynomial approach having the magnitude as a variable for the non-linearity. The PA characteristics may be most conveniently described by the following equation:

$$PA[x(t)] = x(t) \cdot \left[\alpha_1 + \alpha_2 | x(t)| + \alpha_3 | x(t)|^2 + \alpha_4 | x(t)|^3 \dots \right]$$

Each coefficient may be a complex number associated with the IM-level for the third order intermodulation, the fifth order intermodulation and so forth. Each antenna element is connected to one such amplifier which may either have the same coefficients or they may all have different coefficients, depending on the simulation scenario.

In the simulations only the third order intermodulation is retained, and the phase of this coefficient is varied with the index of the antenna. The magnitude is kept the same over all amplifiers. This is done in a random manner over 360° . Thus, the representation of the PAs boils down to the following:

$$PA[x(t)] = x(t) \cdot \left[\alpha_1 + |\alpha_3| \cdot e^{j\varphi} |x(t)|^2\right]$$

$$\varphi = random(2\pi)$$

The combination of having the summation of two different E-UTRA signals fed into the PA leads to some interesting results with regard to where in the angular space different IM components may occur. For the simulations in this section a few examples are shown just to highlight the behaviour.

The resulting signal as a function of the angle θ may be described by the following equation:

$$F(\theta,t) = \sum_{n=1}^{N} PA_n[x_n(t)] \cdot e^{-jk \cdot n \cdot d \cdot \cos(\theta)}$$

Where θ is to be taken as the observation angle from broadside direction. If the output signal is transferred into frequency domain, by use of for example the FFT, then the radiation pattern may be plotted in two dimensions being angle in one dimension and frequency in the other direction.

C.1.3 Simulation results

With the method described in above, the 2D radiation patterns may be plotted when different PA's are configured in various ways and at the same time the beam for the two E-UTRA signals is steered towards different directions. Note that the E-UTRA signals may be deployed at different carrier frequencies or even at the same carrier frequency (spatial multiplexing/MIMO).

Figure C.1.3-1 represents the scenario where the PAs have only 3:rd order intermodulation products and the PA non-linear characteristics to be identical. The two E-UTRA-signals are phase adjusted differently into all the 10 PAs such as to form a constructive antenna pattern in some direction for the first E-UTRA carrier while letting the second carrier radiate constructively in a yet another direction.

The result shows that if all the PAs can be assumed identical, then the intermodulation also shows an ordered radiation pattern with its associated side-lobe pattern very much like the radiation pattern for the two carriers themselves. However, it can be noted that the 3rd order intermodulation is radiated into slightly different angles being it one left or right side of the carrier spectrum. Note the pronounced antenna lobe for the intermodulation in two distinct directions.

The blue area represents the carriers while the red/yellow areas in the plots represent the intermodulation / unwanted emissions.

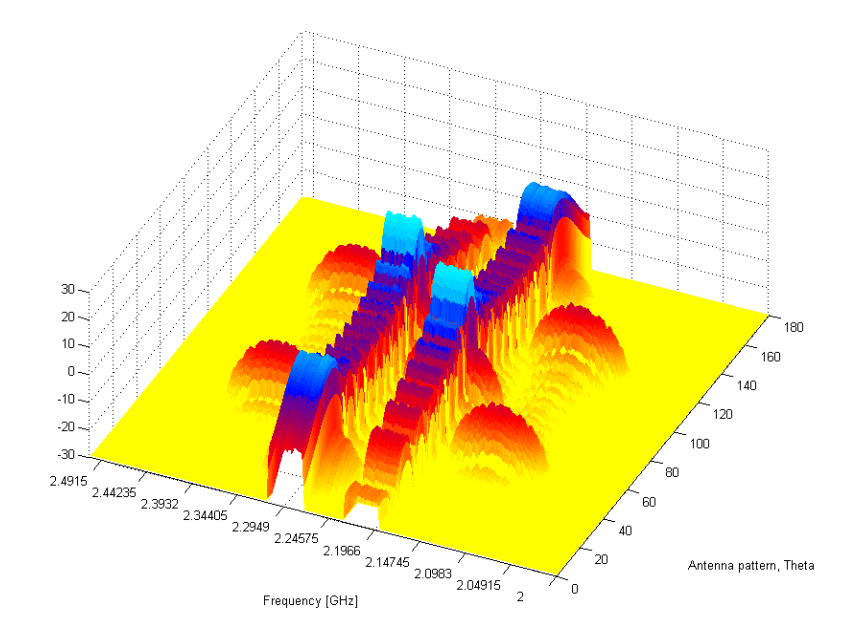


Figure C.1.3-1, Same PAs, two different E-UTRA carriers, different scan angles.

In figure C.1.3-2 similar to figure C.1.3-1, the two E-UTRA carriers were given phase distributions to produce beams in slightly different direction. It can be seen that the intermodulation follows the main beams and also similar to figure C.1.3-1, the angular distribution of the two 3:rd order IM bumps are aligned asymmetrically with respect to the angular beam directions.

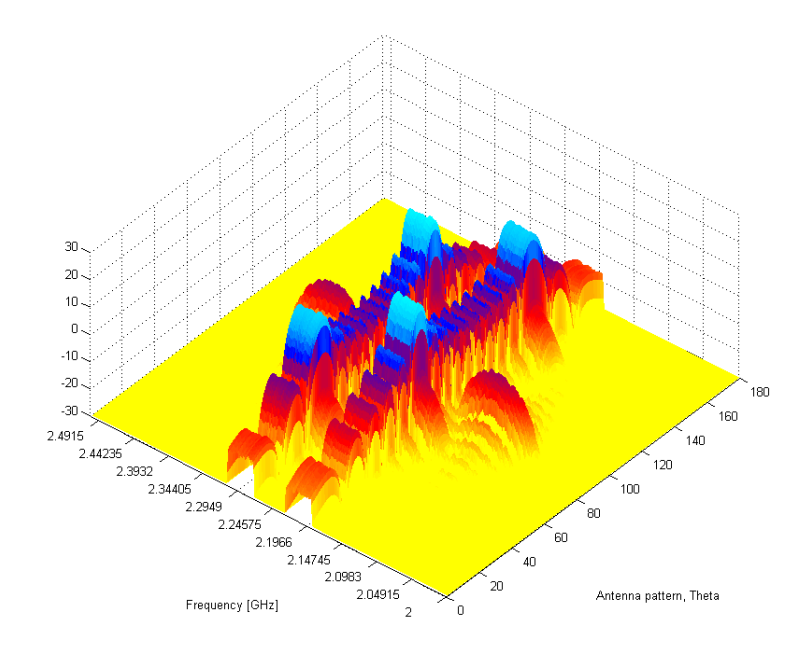


Figure C.1.3-2, Same PAs, two different E-UTRA carriers, yet another scan angles.

In figure C.1.3-3 to C.1.3-7, the different PAs were given individual non-linear characteristics. A set of randomly picked phases (0-360°) has been chosen for each PA. The results may be seen in the 2D-plot where the intermodulation now has become more smeared out over all angles, but with still the typical side-lobe behaviour of a linear uniform array is maintained.

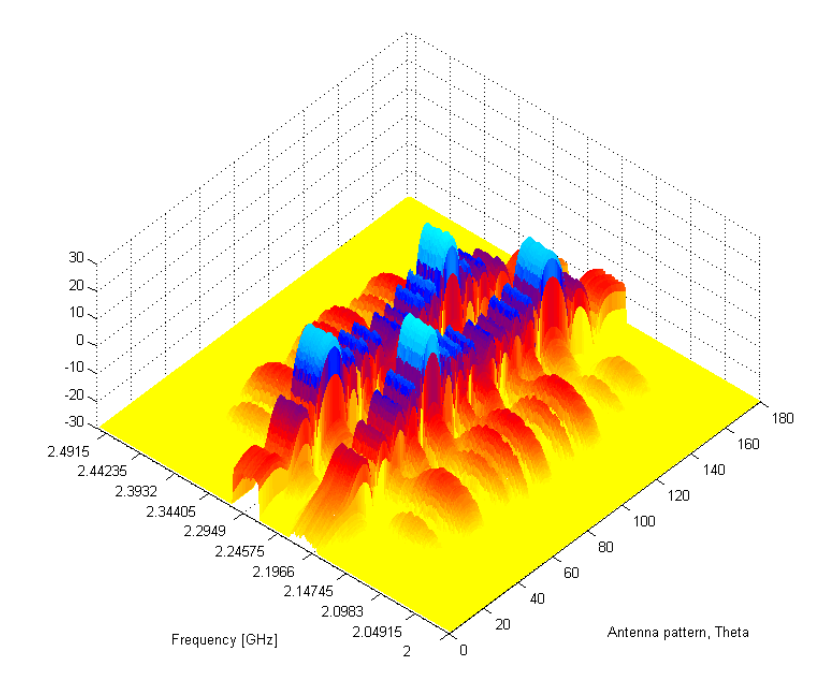


Figure C.1.3-3, Same PAs, two different E-UTRA carriers, different scan angles.

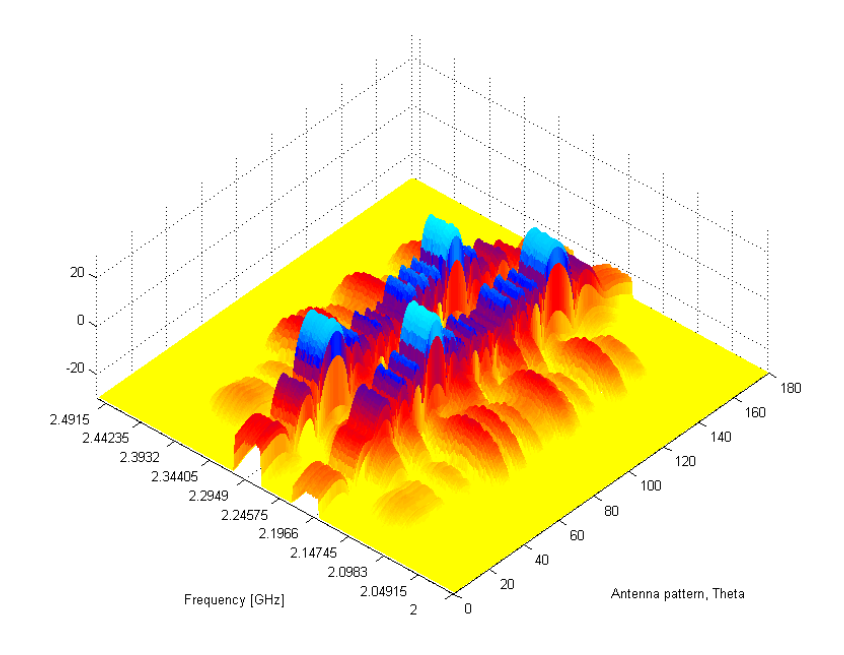


Figure C.1.3-4, Same PAs, two different E-UTRA carriers, different scan angles.

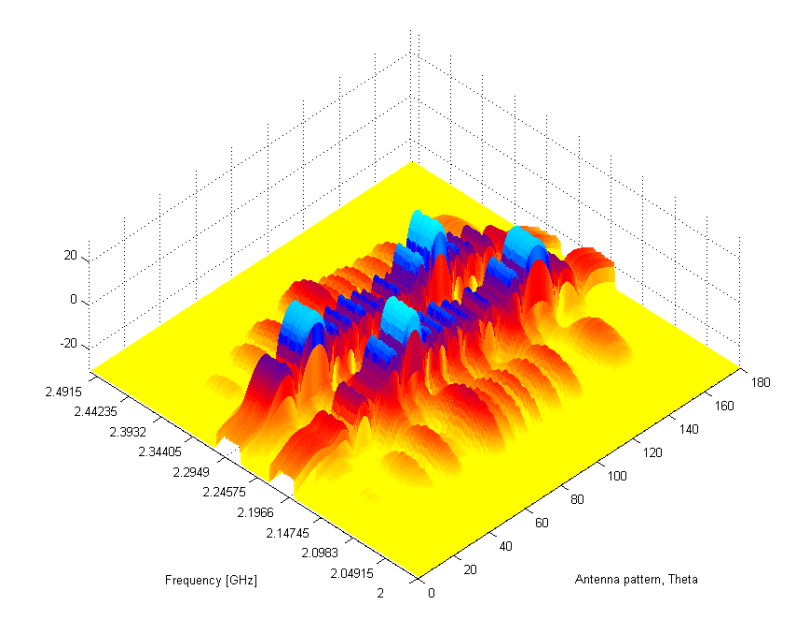


Figure C.1.3-5, Same PAs, two different E-UTRA carriers, different scan angles.

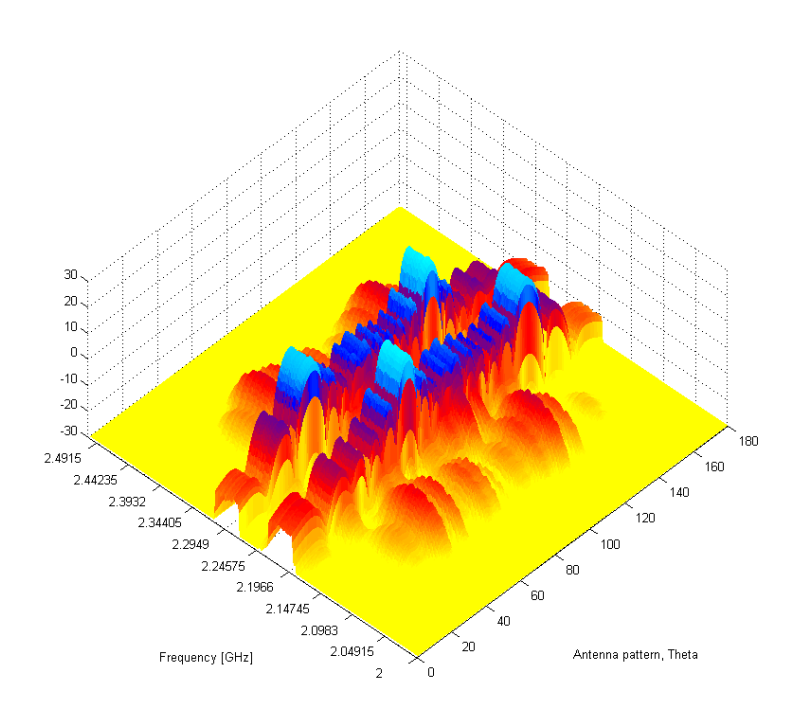


Figure C.1.3-6, Same PAs, two different E-UTRA carriers, different scan angles.

Figure C.1.3-7 and C.1.3-8 represent the behaviour when the two E-UTRA signals are actually placed at the same carrier frequency which would resemble a dual layer beam-forming. In first scenario, the phase of the third order intermodulation coefficient is the same over all 10 amplifiers which lead to the intermodulation being well concentrated around the carriers. In second scenario where the phases of the coefficient for the third order intermodulation is each given a different phase, it can be observed that the intermodulation products are smeared out over the angular space.

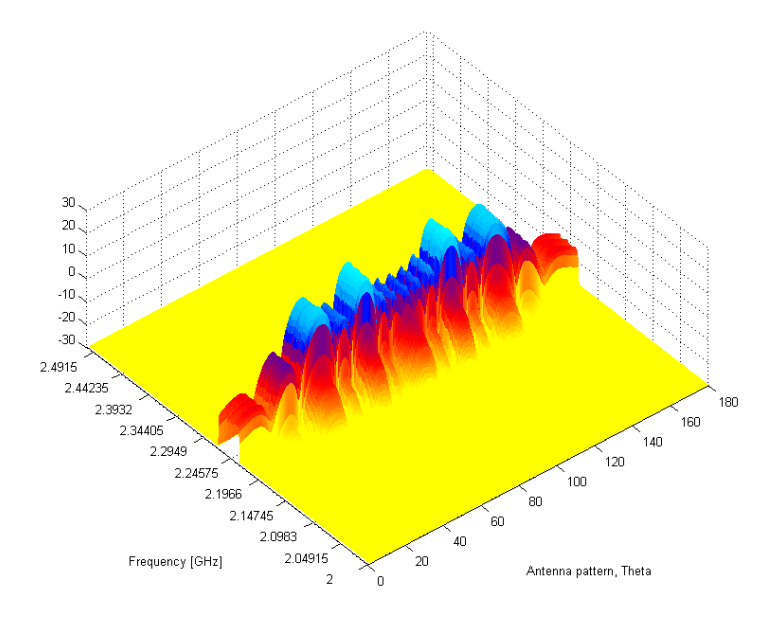


Figure C.1.3-7, Same PAs, two different E-UTRA carriers, same frequency and different scan angles.

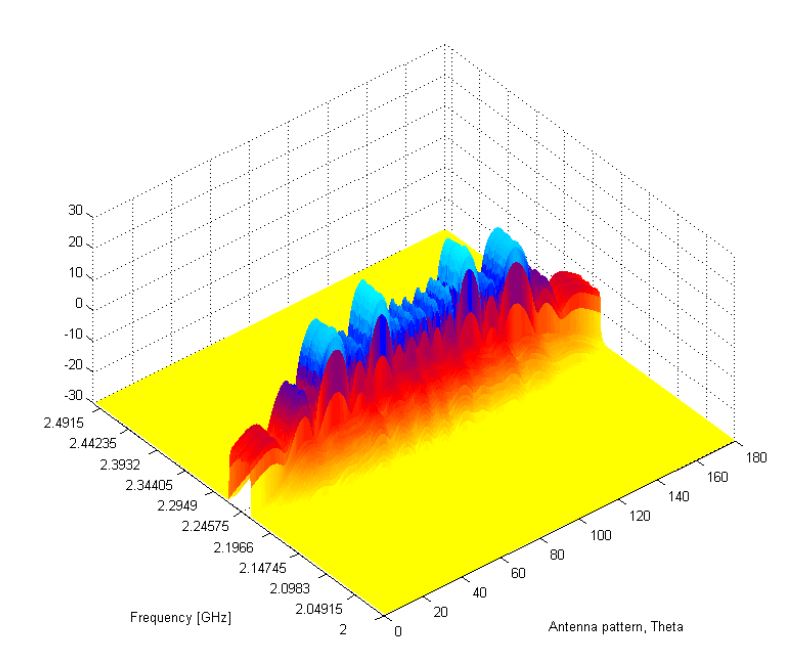


Figure C.1.3-8, Different PAs, two different E-UTRA carriers, same frequency and different scan angles.

The simulations above indicate that there is a difference on how unwanted emission expressed as transmitter intermodulation can vary in spatial domain, depending on the beam-forming applied to each carrier and the amount of correlation between third order intermodulation products. This emphasises the need for carefully investigating the spatial domain aspects for AAS transmitters.

C.2 Receiver spatial characteristics

AAS sub-arrays experience different spatial selectivity compared to fixed beam antennas. Furthermore, a sub-array may experience a differing spatial selectivity to the AAS array as a whole. In figure C.2-1, a visualization of spatial selectivity loss in AAS is given where an interfering UE close to antenna would pose higher interferer level towards a sub-array compared to full antenna beam.

Since the receiver spatial characteristics of the sub-arrays would influence the minimum coupling loss and thus receive requirements for AAS, the spatial aspects of the receiver and its possible impact in terms of minimum coupling loss of an example AAS implementation based on several sub-arrays compared to a fixed beam antenna was investigated. In sub-clause C.2.1 simulations of simple example antenna indicate that the height, direction and distance would influence coupling loss and consequently the blocking interferer level.

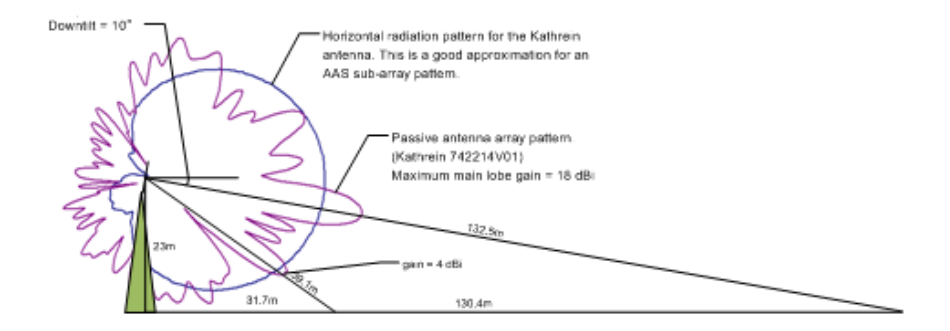


Figure C.2-1, Visualization of spatial selectivity loss in AAS.

C.2.1 Simulation results

Simulation results for the minimum coupling loss of an example antenna array at 2 GHz and compared to various number of array elements for various cases are presented in the following sub-clauses.

C.2.1.1 Antenna patterns for sub-arrays

For this simulation the element far-field pattern is defined by elements models defined in section 5.4.4.2.

The element separation was set to 0.9λ . The composite sub-array pattern is calculated using the superposition principle. The sub-array gain is obtained from the maximum normalized far-field pattern compensated with respect to the antenna directivity.

The sub-array gain patterns for a single, 2, 4 and 8 element array is shown in Figure C.2.1.1-1.

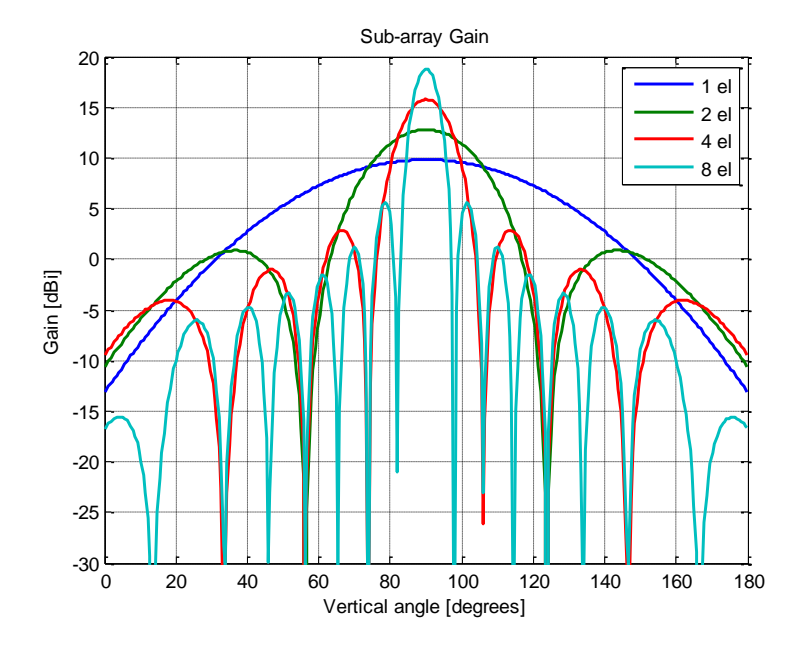


Figure C.2.1.1-1, Gain pattern for different sub-array configurations.

C.2.1.2 Coupling loss

Considering the example antenna (2 GHz) and taking into account 1,2, 4 and 8 element arrays, the coupling loss for 1, 2, 4, 8 element-arrays are compared for the down tilt angles of 0° and 10° respectively is given in figure C.2.1.2-1 to C.2.1.2-2. Base station antenna height was set to h=30 m.

The coupling loss is calculated with free space path loss as propagation model.

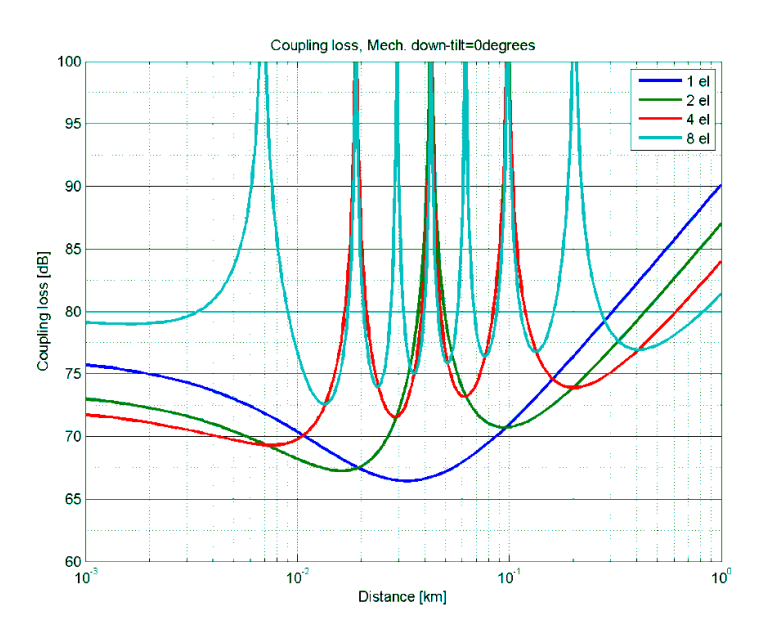


Figure C.2.1.2-1, Coupling loss, 0 degrees tilt for an antenna with 1, 2, 4 and 8 elements

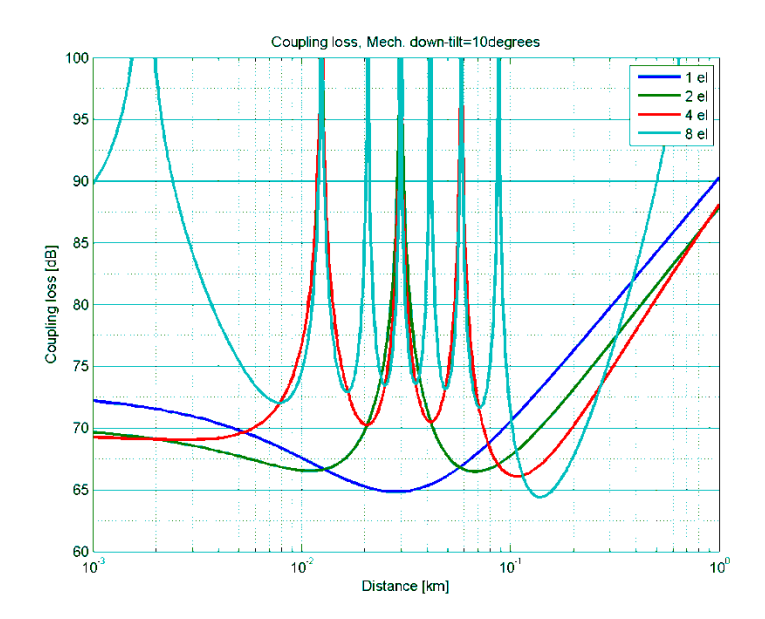


Figure C.2.1.2-2, Coupling loss, 10 degrees tilt for 1, 2, 4 and 8 elements.

The simulation results indicate that there is a distance and tilt dependent minimum coupling loss comparing a full antenna beam and also 2, 4 and 8-element arrays.

C.3 Impact of mutual coupling

Coupling between sub-arrays in a base station antenna array can in general have an impact on antenna performance since some of the energy coupled to other sub-arrays is re-radiated. In this sub-clause, the impact of coupling between sub-arrays on the sub-array patterns and on the composite patterns for a simple example antenna is shown.

The sub-array pattern as a function of the coupling magnitude has been simulated for an arrangement of four sub-arrays as shown in Figure C.3-1. The horizontal spacing between sub-arrays is 0.5λ .

The input signals to the sub-arrays are given by:

$$S = [s_1, s_2, s_3, s_4]$$

Each sub-array has a horizontal radiation pattern defined by:

$$A_{E,H}(\varphi) = -\min\left[12\left(\frac{\varphi}{\varphi_{3dB}}\right)^2, A_m\right],$$

where φ_{3dB} is 65 degrees and A_m is 25 dB.

The composite array pattern is given by:

$$A = \widetilde{W}(\varphi) \cdot 10^{\left(\frac{A_{E,H}(\varphi)}{20}\right)},$$

where $\widetilde{W}(\varphi)$ is the array factor.

The re-radiated energy due to mutual coupling between sub-arrays is represented by a coupling matrix C, where

$$C = \begin{bmatrix} 1 \angle 0^{\circ} & c \angle 160^{\circ} & \frac{c}{2} \angle 320^{\circ} & \frac{c}{4} \angle 480^{\circ} \\ c \angle 160^{\circ} & 1 \angle 0^{\circ} & c \angle 160^{\circ} & \frac{c}{2} \angle 320^{\circ} \\ \frac{c}{2} \angle 320^{\circ} & c \angle 160^{\circ} & 1 \angle 0^{\circ} & c \angle 160^{\circ} \\ \frac{c}{4} \angle 480^{\circ} & \frac{c}{2} \angle 320^{\circ} & c \angle 160^{\circ} & 1 \angle 0^{\circ} \end{bmatrix}$$

The coupling to an adjacent sub-array is $c \angle 160^\circ$ (e.g. from sub-array 1 to 2), to an alternate sub-array is $(c/2) \angle 320^\circ$ (e.g. from sub-array 2 to 4), and to a second alternate sub-array is $(c/4) \angle 480^\circ$ (e.g. from sub-array 4 to 1). The actual amount of coupling in practice will depend on many factors such as element design, sub-array spacing, impedance matching etc.

The horizontal radiation pattern is determined by the following matrix product:

$$P = SCA$$

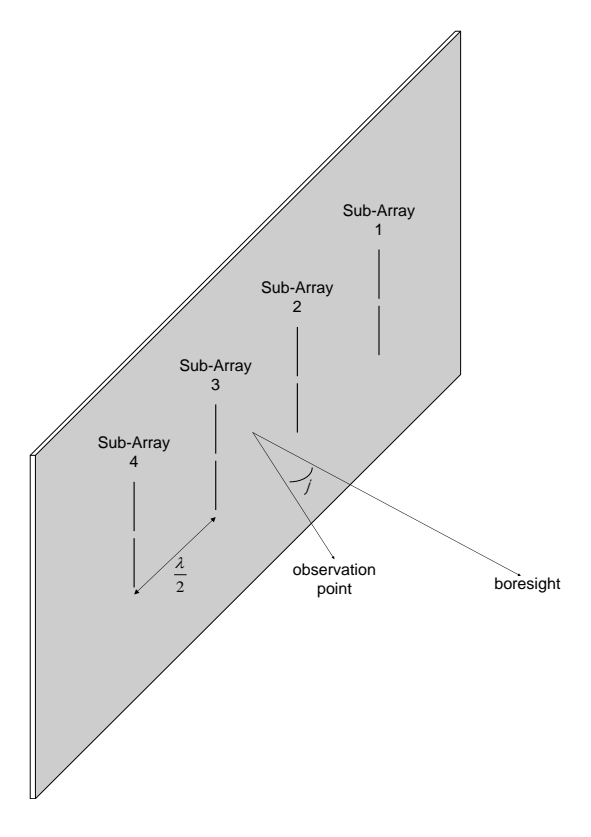


Figure C.3-1, Geometry of four sub-Arrays.

C.3.1 Simulation results

The coupling impact to the sub-array patterns is simulated by applying a signal to each sub-array in turn and applying the coupling matrix C (e.g. $S = \begin{bmatrix} 1,0,0,0 \end{bmatrix}$ for Sub-Array 1 of 4) The total power into the sub-arrays is normalized to the level corresponding to the case when c=0 (i.e. no coupling).

Composite patterns are determined by vector addition of the normalized sub-array patterns using a magnitude weighting of ¼ and applying a fixed phase progression.

Figure C.3.1-1 represents the coupling impact with a signal fed into the leftmost sub-array (Sub-Array 1 of 4) represented by the top row of C and where the coupling c ranges from 0 to 0.25.

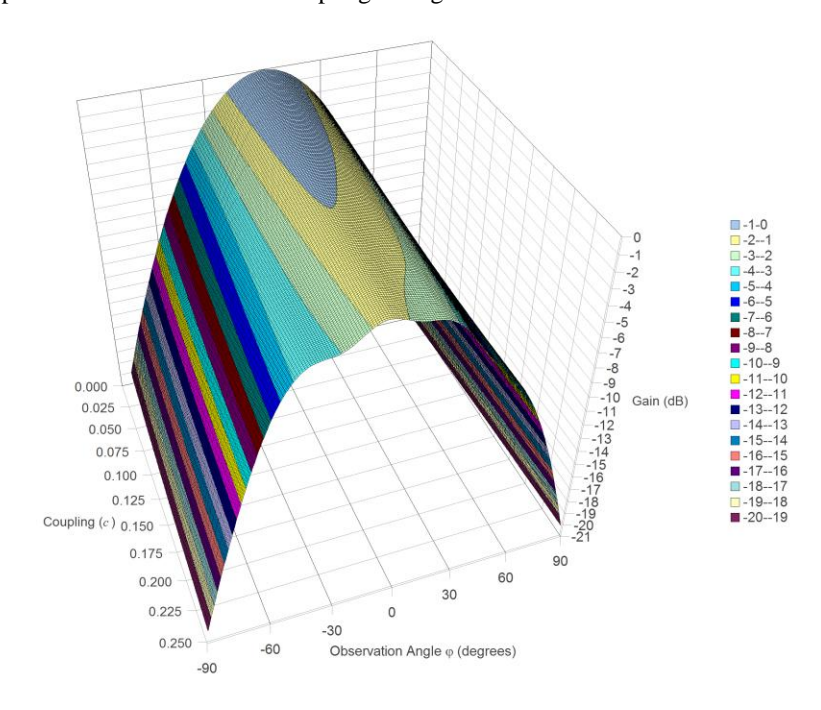


Figure C.3.1-1, Coupling impact on Sub-Array Patterns (Sub-Array 1 of 4).

The coupling impact with a signal fed into the rightmost sub-array (Sub-Array 4 of 4) represented by the fourth row of *C* will be the same as that in Figure C.3.1-1 but flipped left-right.

Figure C.3.1-2 represents the coupling impact with a signal fed into the second sub-array (Sub-Array 2 of 4) represented by the second row of C and where the coupling c ranges from 0 to 0.25.

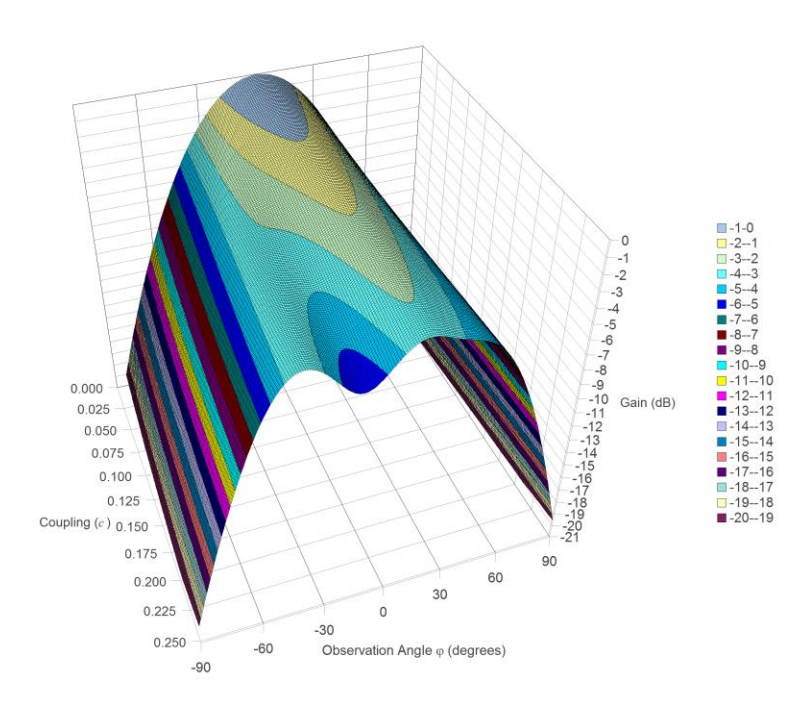


Figure C.3.1-2, Coupling impact on Sub-Array Patterns (Sub-Array 2 of 4).

The coupling impact with a signal fed into the third sub-array (Sub-Array 3 of 4) represented by the third row of C will be the same as that in Figure C.3.1-2 but flipped left-right.

With some level of coupling the sub-array bore site gain is not necessarily the highest, the sub-array pattern may not be symmetrical and the 3 dB beam width can be affected.

Figure C.3.1-3 represents the coupling impact on the composite horizontal pattern with equal magnitude weighting and a phase progression of 0 degrees.

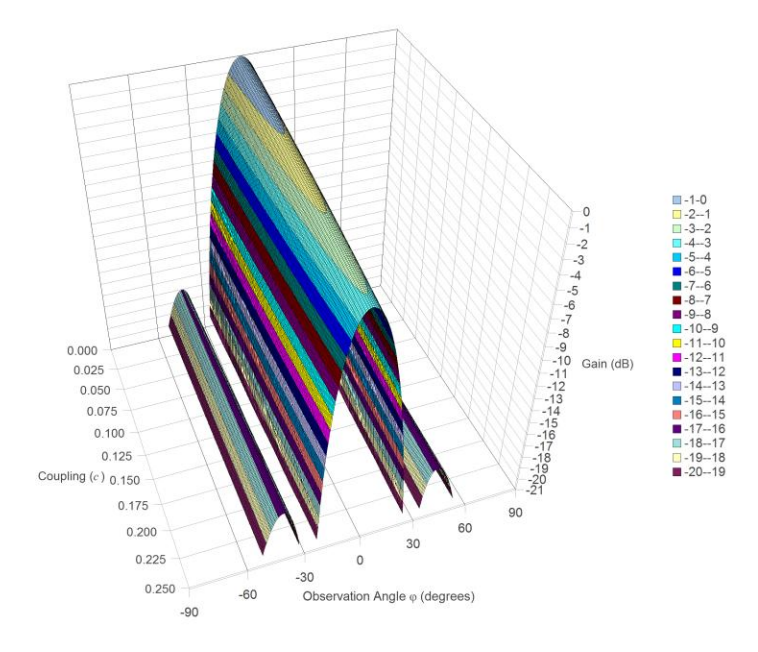


Figure C.3.1-3, Coupling impact on Composite Pattern (phase progression of 0 degrees).

Figure C.3.1-4 represents the coupling impact on the composite horizontal pattern with equal magnitude we ighting and a phase progression of 90 degrees.

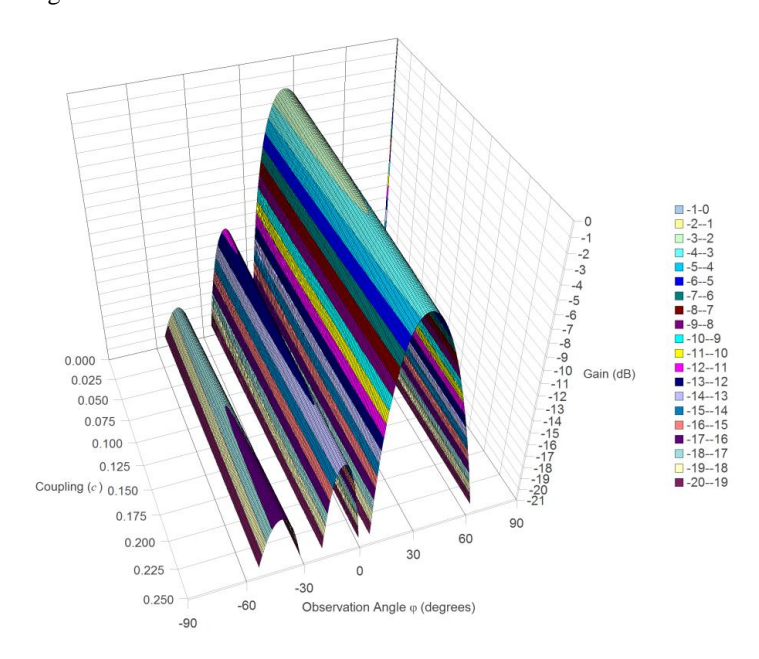


Figure C.3.1-4, Coupling impact on Composite Pattern (phase progression of 90 degrees).

As expected, the coupling between sub-arrays has an impact on individual sub-arrays as well as the composite pattern for the example antenna. The impact would certainly vary depending on the implementation. In AAS BS systems involving sub-arrays, it may be necessary to consider the coupling impact to define the AAS requirements. It should be noted that coupling and its impact on composite beam for an AAS antenna can not be captured by performing conducted test.

C.4 Spatial EVM characteristics

In existing BS specifications, the EVM consist of both linear and non-linear distortion. Group delay variation in the filters is a kind of linear distortion while phase noise and peak reduction algorithms induced distortion is categorized as non-linear distortion. The EVM requirements for E-UTRA are defined in such a manner that the test equipment should contain an equalizer to remove the linear contributions to EVM while for UTRA such equalization is not allowed.

EVM in active antenna arrays will give rise to unwanted in-band emissions that in general do not follow the beam forming or beam shaping that one might anticipate. This is due to the fact that the individual EVM contributions from the different radios supporting each element array separately will in general not be identical but rather in some cases actually being uncorrelated.

The relation between correlated and uncorrelated contributions where peak reduction distortion can possibly be assumed as correlated in some cases but depending on implementation, this contribution could vary significantly and consequently the portion of correlated versus uncorrelated contributions affecting the EVM in particularly side-lobes or nulls.

Considering the peak reduction scheme also called clipping which is one of the main contributing mechanisms to EVM, The spatial distribution of EVM for a 10-element antenna array is further investigated.

As normally only the magnitude of the signal is undergoing the peak reduction process, the phase of the clip distortion is unchanged and follows the carrier phase itself. This means that the clip distortion in this case, follows the beam shaping in the same manner as the carrier itself. The result will be that the same EVM figure will be measured all over the angular sphere as what is measured at each individual antenna port.

A simple simulation is presented below, where a 10-element linear and uniform array antenna is undergoing clipping at a certain magnitude threshold. It is seen that although the phase of the carrier in each branch varies with the port number, the EVM as a function of angle will in fact be constant as shown in figure C.4-1.

The amplitude taper will have a uniform distribution as described below, and the clip threshold is set to 0.5 in relation to normalized amplitude of 1.

A = [1.01.01.01.01.01.01.01.01.01.01]

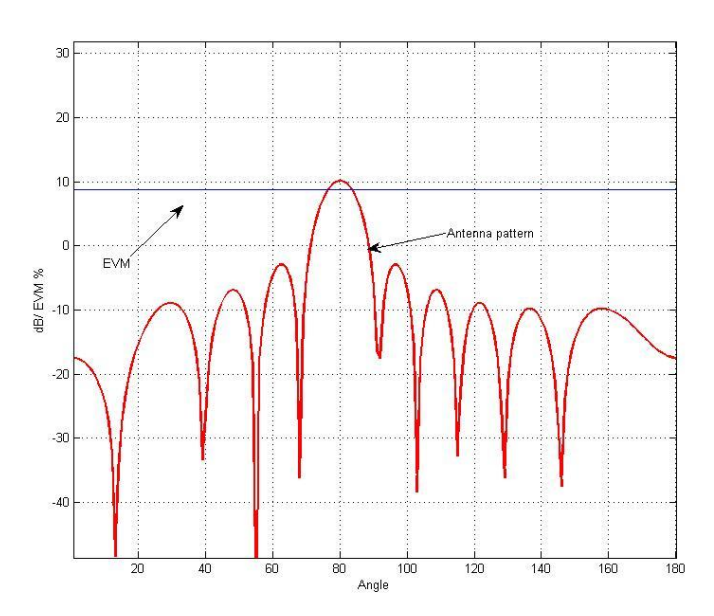


Figure C.4-1, Spatial EVM with uniform amplitude tapering weights.

The outcome would some what be different if the clip contributions are not identical from the different array elements. In this case we have tapered the actual antenna weights instead of having a uniform distribution and the spatial EVM is shown in figure C.4-2. The amplitude taper weights were assumed to be as following:

A = [0.80.91.01.01.01.01.01.00.90.8]

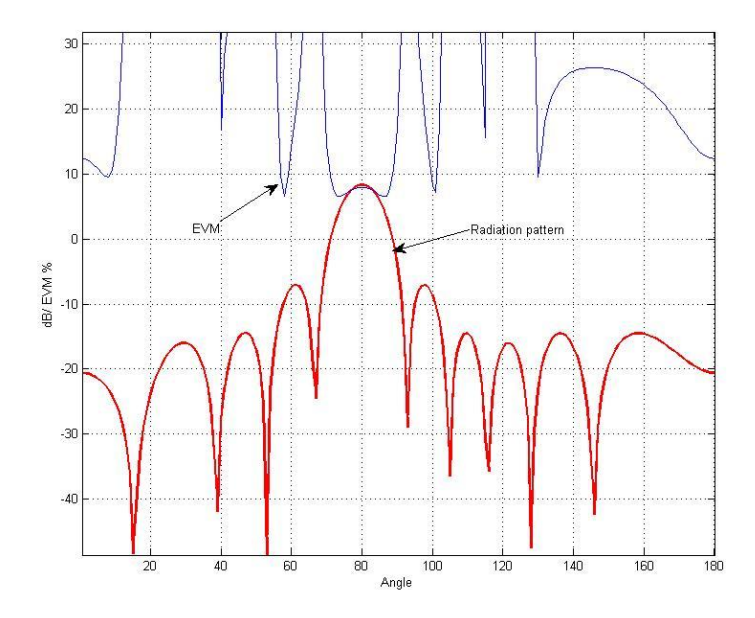


Figure C.4-2, Spatial EVM with non-uniform amplitude tapering weights.

It can be seen that in the null regions in the radiation pattern and side lobes from a linear array antenna with individual array element clipping, the EVM may rise to very high values. The reason is mainly due to the fact that the EVM contributions may not any longer be considered as correlated among array elements and as a result does not give the usual beam forming characteristics as a coherent antenna array system.

We recognize this behaviour regardless of the actual implementation of the peak reduction schemes, and stress the importance to further study this characteristic.

There are however case which we may relax this spatial distribution of EVM behaviour. Viewing a linear uniform array antenna, that is with equal amplitude tapering on all radio branches and given an only down-tilt to the beam by means of applying a progressive phase shift to the carrier, then the clip distortion will in fact be identical from all of the subarrays.

Given the complexity, different level of correlations which would also have tapering weight dependency, the linear and non-linear distortion depending on the RAT as well as implementation specific behaviour, we would propose to further investigate the spatial EVM for AAS.

C.5 Directivity characteristics

The directivity is determined by the electrical far-field pattern generated by an antenna meaning that the directivity will depend on array configuration and excitation.

The maximum directivity is a ratio of the maximum radiation intensity to the radiation intensity averaged over all directions.

The maximum directivity of an antenna is defined as:

$$D_0 = 10 \cdot \log \left(\frac{4\pi \max \left[P(\theta, \varphi)^2 \right]}{\int_{-\pi}^{\pi} \int_{0}^{\pi} \left| P(\theta, \varphi)^2 \sin(\theta) d\theta d\varphi \right|} \right),$$

where $P(\theta, \varphi)$ is the electric far-field pattern of an arbitrary antenna.

C.5.1 Array Element

In section 5.4.4.2 parameters defining the array element characteristics are stated. This section presents an analysis of the directivity of a single array element based on currently defined parameter values.

According to section 5.4.4.2 the radiation pattern for a single antenna element for vertical and horizontal plane is defined as:

Where the composite array element pattern is defined as:

$$A_{E}(\theta,\varphi) = G_{E,\max} - \min \left\{ \min \left[12 \left(\frac{\varphi}{\varphi_{3dB}} \right)^{2}, A_{m} \right] + \min \left[12 \left(\frac{\theta}{\theta_{3dB}} \right)^{2}, SLA_{v} \right] \right\}$$

Since the vertical and horizontal contribution is maximum normalized the composite radiation pattern is adjusted with a gain factor ($G_{E,\max}$).

Together with the parameterized model corresponding parameter values are defined in Table 5.4.4.2.-1. The parameters related to the element characteristics are listed in Table C.5.1-1.

Parameter Symbol Value Unit Horizontal 3dB Beam-width 65 degrees φ_{3dB} Front-to-Back Ratio 30 dB A_m Vertical 3dB Beam-width 65 degrees θ_{3dB} Side Lobe Suppression 30 dB SLA, 8 Array Elemen Gain dBi $G_{E,\max}$

Table C.5.1-1: Array Element Parameters

The maximum gain of an array element is determined by the vertical beam-width, horizontal beam-width, Side-lobe suppression and Front-to-back ratio. It can be noted from Table C.5.1-1 that element gain is specified specifically.

The array element directivity is analysed for given parameters. The electrical far-field pattern generated by a single antenna element can be expressed as:

$$P(\theta,\varphi)=10^{\left(\frac{A_E(\theta,\varphi)}{20}\right)},$$

where $A_{\scriptscriptstyle E}(\theta,\varphi)$ is the far-field pattern in dB.

The directivity is plotted in Figure C.5.1-1 as function of vertical beam-width (θ_{3dB}) and horizontal beam-width (φ_{3dB}). From Figure C.5.1-1 the directivity variation is identified to be in the interval 6-13 dBi depending of element beam-width configuration (θ_{3dB} and φ_{3dB} is swept from 40 to 120 degrees).

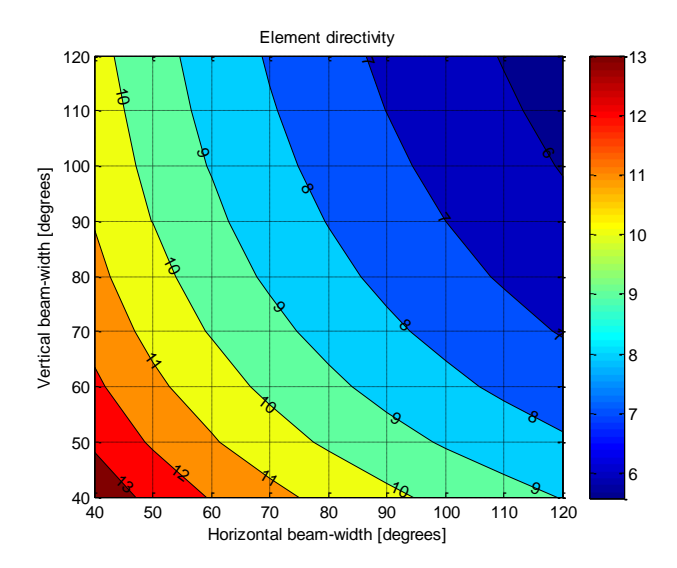


Figure C.5.1-1: Array Element Directivity

For an element configuration with beam-widths of 65 degrees for both horizontal and vertical domain, as assumed for simulations of coexistence in Table 5.4.4.2.-1 the directivity for a single element is 9.8 dBi.

C.5.2 Scan Loss

The spatial characteristics will describe capabilities of enabling spatial filtering and thereby reducing interference and increase the total cell capacity. The directivity is a vital property of an array antenna. The directivity of an array antenna will depend on element separation, element characteristics and applied beam control angles.

Symbol Value Note Parameter Unit Array configuration 10x1 Vertical ULA units $M \times N$ Vertical elements eparation $0.5\lambda, 0.7\lambda,$ m $d_{\cdot \cdot}$ 0.9λ Array Gain dBi $G_{COMP, \max}$ Down-tilt angle 0..50 degrees $heta_{\scriptscriptstyle etilt}$

Table C.5.2-1: Array Parameters

The simulations in this section will analyze radiation pattern and directivity of an array antenna when large tilt angles are applied. The directivity of an antenna is crucial property to capture in link- and system level simulations analyzing receiver in-band blocking or cell capacity.

The electrical far-field pattern generated by an array antenna can be expressed as:

$$P(\theta,\varphi)=10^{\left(\frac{A_A(\theta,\varphi)}{20}\right)},$$

where $A_{\scriptscriptstyle A}(\theta,\varphi)$ is the far-field pattern in dB.

To evaluate the directivity as function of tilt angles a 10 element ULA was configured. The elements were placed along the z-axis with the main beam direction along the x-axis. The main beam is tilted electrically by applying linear phase taper weights as described in Table 5.4.4.2-2. Since the directivity of an array antenna is depended of the element separation distance, the directivity will be calculated for tree different configurations with element separation of 0.5λ , 0.7λ and 0.9λ .

To visualize side lobe and grating lobe response as function of element separation and tilting the radiation pattern is plotted as maximum normalized far-field pattern for 0, 20 and 40 degrees down tilt angles in for array configuration with element separation of 0.5λ and 0.9λ .

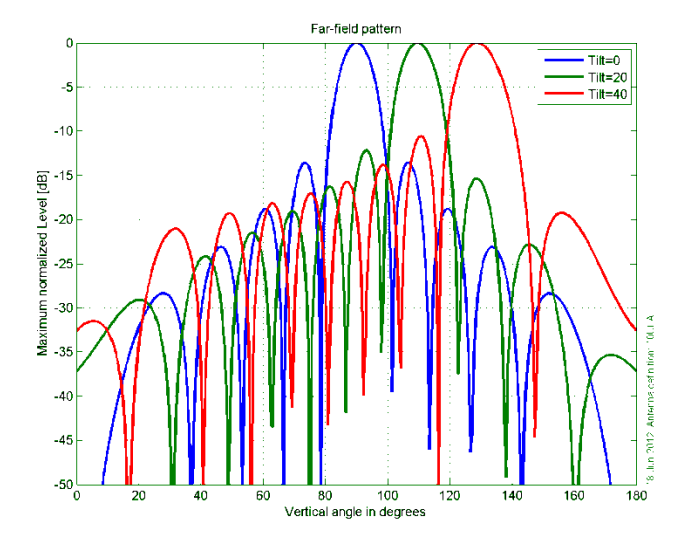


Figure C.5.2-1: Array Antenna Pattern with element separation equal to 0.5λ.

As seen in Figure C.5.2-1 the radiation pattern is dominated by the main beam for array antennas with 0.5λ element separation.

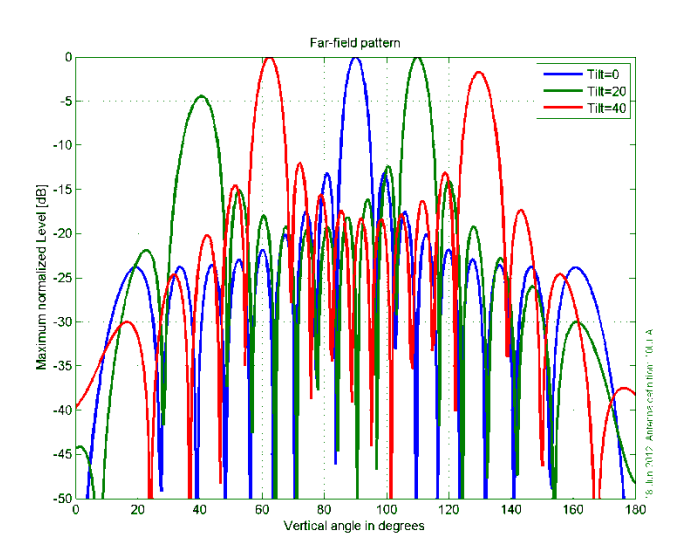


Figure C.5.2-2: Array Antenna Pattern with element separation equal to 0.9λ.

In Figure C.5.2-2 the element separation distance is increased to 0.9λ . It can be noticed that with this configuration the antenna is more susceptible to generate grating lobes when tilt is applied. The grating lobes will impact antenna directivity by radiating energy is unwanted directions.

The directivity of the antenna will depend on the tilt angle and element separation as showed in Figure C.5.2-3.

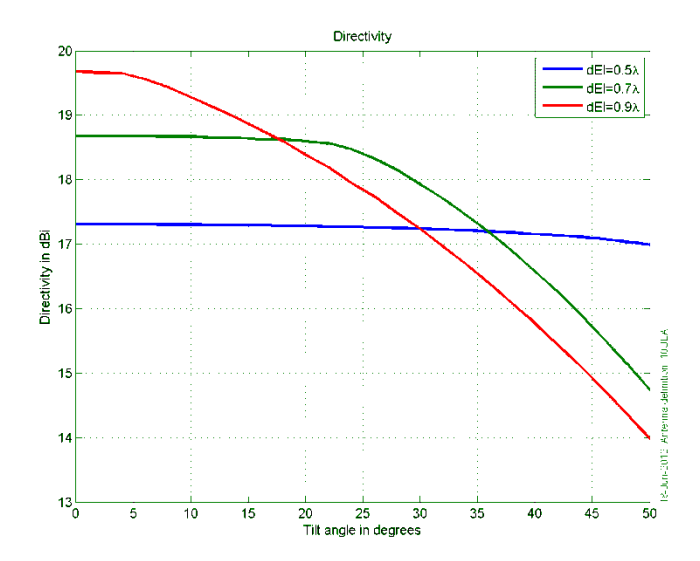


Figure C.5.2-3: Directivity as function of down-tilt angle.

The directivity loss due to large tilt angles is known as scan-loss, Figure C.5.2-3 show scan-loss characteristics for a 10 element ULA antenna different element separations and tilt-angles. Since the gain of an antenna is directly associated to the directivity is it important to capture the scan-loss characteristics in link level and system level simulation studies.

C.5.3 Array Gain

The gain, G of an array antenna can be calculated by subtracting the loss es from the directivity. In practice, gain is often a more interesting performance measure than directivity.

The array antenna gain as function of θ and φ is the directivity minus dissipative losses according to:

$$G(\theta,\varphi) = D(\theta,\varphi) - L_{dis}$$

, where L_{dis} is the dissipative loss of the AAS excluding loss associated with impedance matching and polarization loss.

When referring to directivity and gain without specifying the direction explicitly, one usually refers to maximum directivity D_0 and maximum gain G_0 .

C.5.4 Relation between transceiver boundary and far-field

This sub-section presents an example of relations between transceiver boundary and far-field for transmitter and receiver characteristics.

In the far-field EIRP is defined in a given direction, as the gain of a transmitting antenna multiplied by the net power accepted by the antenna from the connected transmitter as:

$$EIRP(\theta,\varphi) = P_{tx} \cdot G_{tx}(\theta,\varphi) \cdot \varepsilon_{tx}$$

where, P_{tx} is the total output power summed over all TX connectors, $G_{tx}(\theta, \varphi)$ is the DL array antenna gain as function of θ and φ and \mathcal{E}_{tx} is a matching efficiency factor.

If EIRP is noted without angular information it's normal to assume maximum gain in the main beam direction giving $EIRP_{max}$.

In the far-field region the EIRS is defined in a given direction, as the total received power by a receiving antenna divided by the gain of the antenna as:

$$EIRS(\theta,\varphi) = \frac{P_{rx}}{G_{rx}(\theta,\varphi)} \cdot \varepsilon_{rx}$$

where, P_{rx} is the total received power at the detector, $G_{rx}(\theta, \varphi)$ is the UL array antenna gain as function of θ and φ and ε_{rx} is a matching efficiency factor.

If EIRS is noted without angular information it's normal to assume maximum gain in the main beam direction giving $EIRS_{min}$.

C.6 Non core requirement

NOTE: The scope of this SI is limited to core RF and EMC requirements and tests. Non core requirements (e.g. demodulation) and others (e.g. RRM) have not been treated in the Study Item but may need to be considered further.

Annex D: (Informative) Change history

	1	1			Change history	1	
Date	TSG #	TSG Doc.	CR	Rev	Subject/Comment	Old	New
2011-11 2012-03	RAN4#61 RAN4#62bis	R4-116015 R4-121625			Skeleton The text proposals approved in the following documents are	N/A 0.0.1	0.0.1
2012-03	IVAINHIPOZDIS	1023			included: R4-120195, TP subclause 5.2 Deployment scenarios R4-120210, TP subclause Annex A: The SI progress and work plan R4-120988, TP for Overview of international regulation related to AAS	0.0.1	0.1.0
					R4-120990, Radio Reference Architecture for BS with AAS R4-120992, TP subclause 4.1 SI Objective and methodologies R4-121094, Harmonized AAS Nomenclature, Nokia Siemens Networks		
2012-05	RAN4 #63	R4-122525			The text proposal approved in the following documents are implemented: R4-122100, AAS applications R4-122101, TP for TR37840 AAS applications and coexistence scenarios R4-122103, Text proposal for simulation objective for AAS R4-122197, Text Proposal for AAS Definition R4-122198, AAS Reference Structure Update	0.1.0	0.2.0
2012-08	RAN4 #64bis	R4-125456			R4-124886 Text Proposal: 3D antenna modelling R4-124887 Text Proposal: 3D coexistence scenarios and simulation assumptions R4-124890 Text Proposal: Receive Blocking R4-124891 AAS example applications R4-124978 Way forward on AAS test methodology	0.2.0	0.3.0
2012-11	RAN4 #65	R4-126323			R4-125475 TPw ith editorial corrections to TR 37.840 R4-125978 TP on modeling AAS with multiple-column array antenna R4-125981 TP on ACLR simulation results summary R4-125982 TP on in-band blocking simulation results summary R4-125980 TP on BS dow n-tilt angle R4-125983 Text Proposal to clause 8: AAS Testing R4-125985 TP for 8.2.1 Conducted Test R4-125984 TP for 8.2.3 Coupling Test R4-125967 Text Proposal on Far field OTA Test R4-125987 Test methodologies of Far field OTA testwith reverberation chamber for AAS R4-125986 Combined Test Methodology	0.3.0	0.4.0
2012-11	RAN4 #65	R4-127000			R4-126115 TP on improved diagram of the coupling test R4-126334 TP on reverberation chamber OTA test for AAS R4-126883 Update of the SI plan R4-126885 AAS classification R4-126887 TP: Adding directivity and gain to definitions in section 3 of 37.840. R4-126888 TP: TP on spatial domain impacts of AAS R4-126889 TP: Adding directivity analysis to Annex C or TR 37.840 R4-126891 AAS test methods comparison R4-126892 Combined OTA-Conducted Test R4-126893 TP: Adding Near-Field Probe Scanner Test method to section 8. R4-126896 TP for AAS ACLR R4-126897 In-band blocking requirements for AAS R4-126898 TP: Way forward for output power requirement R4-126899 TP: Way forward for reference sensitivity requirement R4-126917 Summary of the methodologies for AAS study R4-126977 TP on Section 5.4.4.2. for general parameters on the AAS antenna model	0.4.0	0.5.0
2012-12	RAN #58	RP-121761			Presentation of TR 37.840 v1.0.0: Study of AAS Base Station; for information	0.5.0	1.0.0
2013-02	RAN4 #66	R4-130984			R4-130145 TP: Aligning section 3 with version 1.0.0 of TR 37.840. R4-130524 Corrections for Deployment Scenarios section R4-130904 TP for receiver reference point Nokia Siemens R4-130905 Text proposal for TR37.840 Clause 9: Conclusion R4-130906 TP for capturing non-core requirements	1.0.0	1.1.0

			R4-130908 AAS reference structure R4-130909 TP: Editorial corrections for TR 37.840 version 1.0.0 R4-130910 TP: Editorial corrections of TR 37.840 section 5.4.4 R4-130911 Text Proposal on remaining sections in TR37.840 R4-130977 Relation between transceiver boundary and far-field R4-130978 TP defining Far field and transceiver boundary requirement definitions		
2013-02	RAN #59	RP-130302	Presentation of TR 37.840 v2.0.0: Study of AAS Base Station; for approval	1.1.0	2.0.0